

Relaying Strategies for Cooperative Systems

Xuehua Zhang

A Thesis

in

The Department

of

Electrical and Computer Engineering

Presented in Partial Fulfillment of the Requirements

for the Degree of Doctor of Philosophy at

Concordia University

Montréal, Québec, Canada

July, 2014

© Xuehua Zhang, 2014

**CONCORDIA UNIVERSITY
SCHOOL OF GRADUATE STUDIES**

This is to certify that the thesis prepared

By: Xuehua Zhang

Entitled: Relaying Strategies for Cooperative Systems

and submitted in partial fulfillment of the requirements for the degree of

Doctor of Philosophy (Electrical Engineering)

complies with the regulations of the University and meets the accepted standards with respect to originality and quality.

Signed by the final examining committee:

_____	Chair
Dr. B. Jaumard	
_____	External Examiner
Dr. F. Labeau	
_____	External to Program
Dr. N. Bouguila	
_____	Examiner
Dr. Y.R. Shayan	
_____	Examiner
Dr. M. Reza Soleymani	
_____	Thesis Co-Supervisor
Dr. A. Ghrayeb	
_____	Thesis Co-Supervisor
Dr. M. Hasna	

Approved by: _____
Dr. F. Haghghat , Graduate Program Director

July 22, 2014 _____
Dr. C. Trueman, Interim Dean
Faculty of Engineering and Computer Science

Abstract

Relaying Strategies for Cooperative Systems

Xuehua Zhang, PhD.

Concordia University, 2014

In this thesis, we investigate several relaying strategies for cooperative networks with the aim of finding techniques to improve the performance of such networks. The objective here is to increase the spectral efficiency while achieving full diversity. Therefore, we focus on two-way relaying and relay assignment since they are both efficient ways in improving the spectral efficiency of cooperative networks. Specifically, we propose efficient relay strategies to cope with the asymmetric data rates in two-way relay channels and address practical issues in relay assignment.

In the first part of the thesis, we consider two decode-and-forward (DF) relaying schemes for two-way relaying channels where the two sources may have different rate requirements. One scheme combines hierarchical zero padding and network coding (HZPNC) at the relay. The novelty of this scheme lies in the way the two signals (that have different lengths) are network-coded at the relay. The other scheme is referred to as opportunistic user selection (OUS) where the user with a better end-to-end channel quality is given priority for transmission. We analyze both schemes where we derive closed form expressions for the end-to-end (E2E) bit error rate (BER). Since the two schemes offer a trade-off between performance and throughput, we analyze and compare both schemes in terms of channel access probability and average throughput. We show that HZPNC offers better throughput and fairness for both users, whereas OUS offers better performance. We also compare the performance of HZPNC with existing schemes including the original zero padding, nesting constellation modulation and superposition modulation. We demonstrate through examples the superiority of the proposed HZPNC scheme in terms of performance and/or reduced complexity.

In the second part of the thesis, we consider a hybrid relaying scheme for two-way relay channels. As per the proposed scheme, if the E2E signal-to-noise ratio (SNR) of both

users is above a specified threshold, both sources transmit over orthogonal channels and the relay node uses hierarchical modulation and network coding to relay the combined signals to both sources in the third time slot. Otherwise, the user with the better E2E SNR transmits, while the other user remains silent. The advantage of the proposed scheme is that it compromises between throughput and reliability. That is, when both users transmit, the throughput improves. Whereas when the better user transmits, multiuser diversity is achieved. Assuming asymmetric channels, we derive exact closed-form expressions for the E2E BER, access probability and throughput for this scheme and compare its performance to that of existing schemes. We also investigate the asymptotic performance of the proposed scheme at high SNRs where we derive the achievable diversity order of both users. We show through analytical and simulation results that the proposed scheme improves 1) the overall system throughput, 2) fairness between the two users, and 3) the transmission reliability. This all comes while achieving diversity two for both users, which is the maximal diversity.

In the third part of the thesis, we study relay assignment with limited feedback. In networks with many multiple source-destination pairs, it is normally difficult for destinations to acquire the channel state information (CSI) of the entire network without feedback. To this end, we design a practical limited feedback strategy in conjunction with two relay assignment schemes, i.e., fullset selection and subset selection, which are based on maximizing the minimum E2E SNR among all pairs. In this strategy, each destination acquires its SNR, quantizes it, and feeds it back to the relays. The relays then construct the E2E SNR table and select the relay assignment permutation from all possible relay assignment permutations or only a subset of these permutations. We analyze the performance of these schemes over independent Rayleigh fading channels in terms of the worst E2E SNR. We derive closed-form expressions for the E2E BER and investigate the asymptotic performance at high SNR. We show that relay assignment with quantized CSI can achieve the same first-order diversity as that of the full CSI case, but there is a second-order diversity loss. We also demonstrate that increasing the quantization levels yields performance that is close to that of having full knowledge of the CSI.

Acknowledgments

I would like to express my deep gratitude to my supervisor Prof. Ali Ghrayeb for his guidance during this thesis. I am grateful for his patience and kindness in answering my questions and revising my submitted reports. I have also benefited tremendously from his enthusiasm, understanding, and patience.

I would also like to express sincere appreciation to my co-supervisor Prof. Mazen Hasna for his guidance during this thesis. I appreciate all his help during my visits to Qatar.

I would like to thank Prof. Hamid Jafarkhani for his great help in finishing the work in Chapter 5.

I would like to thank the committee members: Dr. M. R. Soleymani, Dr. Yousef R. Shayan, Dr. N. Bouguila and Dr. F. Labeau for spending a lot of time in reviewing my thesis. Their comments have improved the presentation of the thesis.

Finally, I would like to thank my families for their love, trust and encouragement.

Contents

List of Figures	ix
List of Tables	xi
List of Symbols	xii
List of Acronyms	xiv
1 Introduction	1
1.1 Cooperative Communication	1
1.2 Two-way Relaying	3
1.3 Relay Selection	5
1.4 Problem Statement and Motivation	6
1.4.1 Relaying Strategies for Two Way Relaying with Asymmetric Data Rates	6
1.4.2 Relay Assignment in Multiple Source-Destination Cooperative Networks with Limited Feedback	6
1.5 Thesis Contributions	7
1.5.1 Relaying Strategies for Two Way Relaying with Asymmetric Data Rates	7
1.5.2 Relay Assignment in Multiple Source-Destination Cooperative Networks with Limited Feedback	8
1.6 Thesis outline	9
2 Background and Literature Review	10
2.1 Existing Techniques for Two-way DF Relaying with Asymmetric Data Rates	10
2.2 Hierarchical Modulation in Cooperative Systems	11
2.3 Multiuser Diversity in Cooperative Systems	13
2.4 Relay Assignment in Cooperative Systems	15
2.5 Quantized CSI Strategies in Cooperative Systems	16
2.6 Conclusions	17
3 Hierarchical Zero Padding Network Coding (HZPNC) and Opportunistic User Selection (OUS)	18
3.1 Introduction	18
3.2 System Model	21

3.3	Proposed Schemes	22
3.3.1	Hierarchical Zero Padding/Network Coding (HZPNC)	22
3.3.2	Opportunistic User Selection (OUS)	24
3.4	Bit Error Rate Performance Analysis	25
3.4.1	HZPNC Scheme	25
3.4.2	Original Zero Padding	28
3.4.3	OUS Scheme	29
3.5	Access Probability and Throughput Analysis	31
3.5.1	Access Probability	31
3.5.2	Throughput	32
3.6	Simulation Results	33
3.7	Conclusions	41
4	Hybrid Network Coding and Opportunistic User Selection (HNCOUS)	43
4.1	Introduction	43
4.2	System Model	45
4.3	Proposed HNCOUS Scheme	46
4.3.1	Description of the HZPNC Scheme	46
4.3.2	Description of the OUS Scheme	47
4.3.3	On the Optimal Threshold	47
4.4	End-to-End BER Performance Analysis	48
4.5	Achievable Diversity Order	53
4.6	Access Probability and Throughput	56
4.6.1	Access Probability	56
4.6.2	Throughput	57
4.7	Simulation Results	58
4.8	Concluding Remarks	64
5	Relay Assignment in Multiple Source–Destination Cooperative Networks with Limited feedback	66
5.1	Introduction	66
5.2	System Model	68
5.3	Relay Assignment with Limited Feedback	69
5.4	The End-to-End Bit Error Rate	72
5.4.1	Preliminaries	72
5.4.2	Subset Selection	73
5.4.3	Fullset Selection	74
5.5	Asymptotic E2E BER Performance	75
5.5.1	Asymptotic E2E BER	75
5.5.2	The Asymptotic Optimal Threshold	75
5.5.3	Achievable Diversity	76
5.6	Simulation Results	79
5.7	Conclusions	81

6	Conclusions and Future Work	84
6.1	Conclusions	84
6.2	Future Work	86
6.2.1	Extending the Performance Analysis of Our Proposed Schemes to Other Scenarios	86
6.2.2	Investigation of the Proposed Schemes in the Context of Variable Rate Transmission	87
6.2.3	Design Spatial Modulation (SM)-based Asymmetric Two-way Relaying Schemes	87
	Appendix A Derivations for Chapter 3	88
A.1	Proof of Equation (3.24)	89
	Appendix B Derivations for Chapter 4	91
B.1	Proof of Lemma 4.1	91
B.2	Proof of Lemma 4.2	92
B.3	Proof of Lemma 4.3	93
B.4	Proof of Lemma 4.4	94
B.5	Proof of Lemma 4.5	94
	Appendix C Derivations for Chapter 5	98
C.1	Proof of Lemma 5.1	98
C.2	Proof of Lemma 5.2	100
C.3	Proof of Lemma 5.3	102
	Bibliography	104

List of Figures

1.1	Cooperative diversity relaying and the corresponding time-division protocol.	1
1.2	Traditional cooperative communications.	4
1.3	Three time slot NC scheme.	4
1.4	Two time slot NC scheme.	5
2.1	4/16-QAM hierarchical modulation.	12
2.2	Downlink of a multiuser wireless system.	13
3.1	E2E BER performance of the original zero padding and HZPNC schemes (for S_1).	34
3.2	E2E BER performance of the original zero padding and HZPNC schemes (for S_2).	35
3.3	Effect of variation of d on the E2E BER performance for two users.	36
3.4	Comparison of E2E BER performance of Nesting constellation modulation and HZPNC.	37
3.5	Comparison of E2E BER performance of Nesting constellation modulation and HZPNC.	38
3.6	Comparison of the sum BER performance of Superposition modulation and HZPNC.	38
3.7	Bit error rate performance (simulated and theoretical) of HZPNC and OUS for S_1	39
3.8	Bit error rate performance (simulated and theoretical) of HZPNC and OUS for S_2	39
3.9	Access probability for HZPNC and OUS.	40
3.10	Throughput for HZPNC and OUS.	40
4.1	E2E BER performance (simulated and theoretical) of our proposed adaptive transmission scheme over symmetric channels.	58
4.2	E2E BER performance (simulated and theoretical) of our proposed adaptive transmission scheme over symmetric channels.	59
4.3	Access probability of HZPNC, OUS and our proposed adaptive transmission scheme corresponding to Figs. 4.1 and 4.2.	60
4.4	Throughput of HZPNC, OUS and our proposed adaptive transmission scheme corresponding to Figs. 4.1 and 4.2.	61
4.5	E2E BER performance (simulated and theoretical) of our proposed adaptive transmission scheme over asymmetric channels.	62
4.6	Access probability of HZPNC, OUS and our proposed adaptive transmission scheme for asymmetric channels.	62

4.7	Throughput of HZPNC, OUS and our proposed adaptive transmission scheme corresponding to Fig. 4.5.	63
4.8	The optimal threshold values as a function of ρ for Figs. 4.1 and 4.5.	63
5.1	A cooperative network with m communication pairs and n relays.	68
5.2	Bit error rate performance (theory and simulation) of subset selection with different number of thresholds.	80
5.3	Bit error rate performance (theory and simulation) of fullset selection with different number of thresholds.	80
5.4	Theoretical bit error rate performance comparison between the fullset selection and subset selection.	81
5.5	The optimal threshold values (exact and asymptotic) as a function of ρ for subset selection.	82
5.6	Comparison of the optimal threshold values as a function of ρ for subset selection and fullset selection.	82

List of Tables

- 5.1 Possible relay assignments based on the full CSI. 70
- 5.2 Quantized CSI based E2E SNR matrix for all possible relay assignments. 70

List of Symbols

S_i	user i
h_{ir}	fading coefficient for link between user i and relay
γ_{ir}	instantaneous SNR for link between user i and relay
γ_{im}	instantaneous SNR for different links
ρ	received SNR per bit
γ_i	E2E SNR of user i
$2d_1$	distance between two fictitious QPSK symbol points
$2d_2$	distance between the actual transmitted 16-QAM constellation points
d	constellation priority parameter
\oplus	exclusive or
y_{ir}	signals received at the relay i
$P_{e,i}$	E2E BER for user i
$P_{e,ir}$	E2E BER over the link between user i and relay
$P_{e,ri}$	E2E BER over the link between relay and user i
$P_{e,im}^{hp}$	BER of HP bits over different links
$P_{e,im}^{lp}$	BER of LP bits over different links
$P_{e,ri}^{hp}$	BER of HP bits over the link between relay and user i
$P_{e,ri}^{lp}$	BER of LP bits over the link between relay and user i
$P_{e,ir}^{hp}$	BER of HP bits over the link between user i and relay
$P_{e,ir}^{lp}$	BER of LP bits over the link between user i and relay
$\text{erfc}\{\cdot\}$	complementary error function
\hat{b}_i	detected bit sequence from user i
\hat{b}_r	network coded bit sequence at relay

γ_{th} threshold
 $E\{\cdot\}$ expectation operation

List of Acronyms

AF	Amplify-and-Forward
ANC	Analog Network Coding
AWGN	Additive White Gaussian Noise
BER	Bit Error Rate
CSI	Channel State Information
CDF	Cumulative Distribution Function
DF	Decode-and-Forward
E2E	End to End
FDMA	Frequency Division Multiple Access
HNCOUS	Hybrid Network Coding and Opportunistic User Selection
HP	High Priority
HZPNC	Hierarchical Zero Padding Network Coding
LP	Low Priority
MIMO	Multiple-input Multiple-output
ML	Maximum Likelihood
MRC	Maximum Ratio Combining

NC	Network Coding
OUS	Opportunistic User Selection
PDF	Probability Density Function
PNC	Physical-layer Network Coding
QAM	Quadrature Amplitude Modulation
QoS	Quality of Service
QPSK	Quadrature Phase Shift keying
SM	Spatial Modulation
SNR	Signal-to-Noise Ratio
XOR	Exclusive-OR

Chapter 1

Introduction

1.1 Cooperative Communication

It is well known that diversity is a powerful technique in combating channel fading. Cooperative diversity is a kind of spatial diversity that can be obtained by exploiting the distributed antennas belonging to each node in a wireless network [1]-[3]. A typical three node cooperative diversity relaying model comprising a source node S , a destination node D , and a relay node R (where R helps the communication between S and D) and the corresponding time division protocol are illustrated in Fig. 1.1.

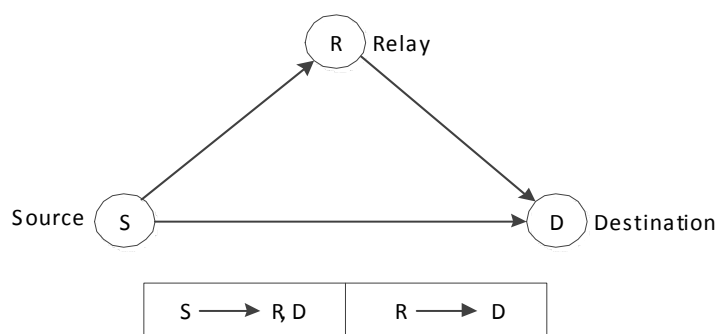


Figure 1.1: Cooperative diversity relaying and the corresponding time-division protocol.

Due to the half-duplex constraint, the relay can not transmit and receive at the same time. Therefore, the relay normally uses different time slots for transmission and reception as shown in Fig. 1.1. In the first time slot, the source transmits to the destination. Owing to the broadcast nature of wireless communications, the relay can also overhear the transmission. Then in the second time slot, the relay forwards the received signal to the destination. After the two time slots, the destination obtains two copies of the same signal sent over two independent channels. By employing appropriate detection schemes such as maximum likelihood (ML), maximum ratio combining (MRC) or selection combining, diversity can be achieved.

The relaying schemes are normally classified as amplify-and-forward (AF), in which the relay can simply retransmit, or forward, the noisy analog signal received from the source, and decode-and-forward (DF), in which the relay decodes each symbol transmitted by the source, and then forwards its encoded symbol to the destination. The capacity of AF relaying is given as [4]

$$C_{AF} = \frac{W}{2} \log_2 \left(1 + \gamma_{SD} + \frac{\gamma_{SR}\gamma_{RD}}{\gamma_{SR} + \gamma_{RD} + 1} \right), \quad (1.1)$$

where W is the bandwidth and γ_{SR} , γ_{RD} , and γ_{SD} are the instantaneous signal-to-noise ratio (SNR) for the links $S \rightarrow R$, $R \rightarrow D$ and $S \rightarrow D$, respectively. While for DF, the capacity is given as [5]

$$C_{DF} = \frac{W}{2} \min \{ \log_2(1 + \gamma_{SR}), \log_2(1 + \gamma_{RD} + \gamma_{SD}) \}. \quad (1.2)$$

If only the direct path is used, the capacity of direct transmission is given as

$$C_D = W \log_2(1 + \gamma_{SD}). \quad (1.3)$$

Comparing (1.1) and (1.2) with (1.3), it is observed that the capacity of cooperative communications is not always greater than that of direct transmission. This is attributed to the fact that cooperative communications needs two time slots to complete one transmission, whereas direct transmission only needs one time slot. Thus, one of the challenges in cooperative communications

is to reduce the spectral loss caused by this half-duplex constraint. Various solutions have been proposed to solve this problem. One of them is relay selection where only one of the best relays or a subset of the relays are selected to transmit. Recently, a significant attention has been given to network coding (NC) (see [6], [7]) since it can also reduce the required time slots for transmission by allowing the relay to help multiple transmissions at the same time.

1.2 Two-way Relaying

The concept of NC was first proposed by Ahlswede, *et. al.* in [8] as a routing method in lossless wireline networks. The key idea of NC is that the relay linearly combines the received data from different sources instead of sending them individually, resulting in an improved bandwidth efficiency. In wireless communications, NC comes naturally due to the broadcast nature of wireless medium where multiple destinations can receive the same signal at the same time. The authors in [9] adapt NC to relay networks.

A variety of NC schemes have been proposed and studied in the literature for different network settings [10]-[26]. Among all the works in this field, much attention has been given to half-duplex two-way relaying [13]-[26], in which two users communicate with each other through one relay, as it is a basic building block in most wireless networks. The first version of two-way relay channels is introduced by Shannon in [13] in an information theoretical context and recently investigated extensively in the context of wireless relaying networks. For traditional cooperative communications, users transmit to each other one at a time as shown in Fig. 1.2. Therefore, four time slots are required to complete a new transmission.

If NC is used, the relay applies NC to the signals received from the two users and broadcasts the resulted signal to both nodes. As a consequence, one time slot is saved. Various NC protocols have been proposed for this two-way relay channel. All proposed protocols can be classified into

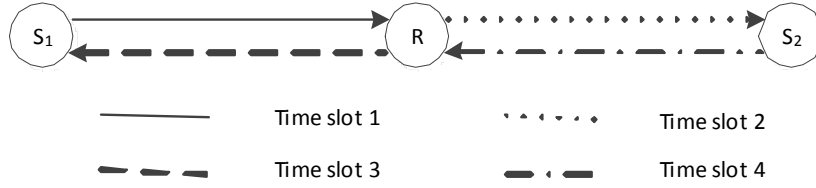


Figure 1.2: Traditional cooperative communications.

two types: three time slot schemes [9] and two time slot schemes (i.e., analog network coding [14]-[16] and physical-layer network coding [17]-[20]) which are illustrated in Figs. 1.3 and 1.4, respectively. The difference between two time slot schemes and three time slot schemes comes from whether or not the two users transmit simultaneously.

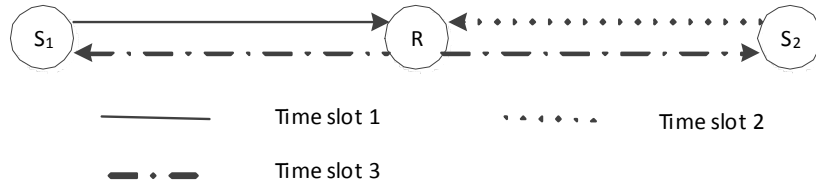


Figure 1.3: Three time slot NC scheme.

Three-time-slot NC combined with threshold-based relaying to control error propagation with MRC and ML are studied in [21], [22] and [23], respectively. In [24], the authors address the problem of relay assignment for cooperative networks comprising multiple bidirectional transmitting pairs. The problem of relay selection is addressed in [25].

While for two-time-slot NC schemes, the two users transmit simultaneously in the first time slot as shown in Fig. 1.4. A two-time-slot DF NC scheme is proposed in [17] and [26] as physical-layer network coding (PNC) where the additive nature of simultaneously arriving electromagnetic waves is exploited and the relay only decodes the received sum of the signals and maps it to a corresponding zero or one. Analog network coding (ANC), which is another two-time-slot NC

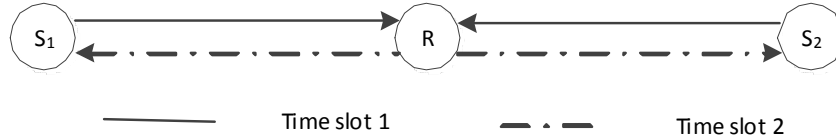


Figure 1.4: Two time slot NC scheme.

scheme, is proposed in [14]. Unlike PNC, the relays in this scheme just amplify and forward the mixed signal to the destination without decoding it.

1.3 Relay Selection

An active research area in cooperative communications is *selection diversity*, which aims at utilizing the system/network resources in a more efficient way [27]-[36]. Specifically, in the presence of multiple relays, only one or a subset of the relays are selected to cooperate, while maintaining full diversity.

Relay selection based on the exact end-to-end (E2E) SNR is studied in [27] and it is shown that this scheme achieves full diversity. A relay selection scheme based on the max-min criterion for both AF and DF is proposed in [28] and [29]. The diversity-multiplexing trade-off is shown to be the same as that of the space-time coding scheme proposed in [30]. According to whether relay selection is performed before or after actual data transmission, this selection scheme can be classified into two main relay selection methods: proactive and reactive opportunistic relaying. In proactive opportunistic relaying, relay selection is based solely on the quality of the subchannels, which takes place before the source actually transmits its signal. Specifically, the relays are ordered according to their respective weakest subchannels, i.e., bottlenecks, and the one exhibiting the best bottleneck is chosen. In reactive opportunistic relaying, on the other hand, relay selection is performed after the source transmission over the first hop. That is, the selected relay is the one

that has successfully decoded the source's message and whose relay-destination subchannel is the strongest. Both proactive and reactive opportunistic relaying are extensively studied in [31]-[36].

1.4 Problem Statement and Motivation

It is shown in the previous sections that one of the challenges in cooperative communications is how to reduce the spectral loss caused by half-duplex relaying. To remedy this, two-way relaying and relay selection/assignment have been introduced where the former attempts to improve the spectral efficiency and the latter aims at improving the reliability. In this thesis, we focus on these two aspects and aim at developing efficient ways of combining these two techniques, particularly for sources that have different data rate requirements.

1.4.1 Relaying Strategies for Two Way Relaying with Asymmetric Data Rates

In most of the work mentioned in Section 1.2 that deals with bidirectional transmission, it is normally assumed that the two transmitting nodes (or users) have the same rate. In many practical scenarios, however (such as having different quality of service (QoS) requirements, different available traffic and so on), the two users may not have the same transmission rate. In light of this, the immediate question that comes to mind is how the relay nodes can cope with this data rate asymmetry without sacrificing the bandwidth efficiency. This is one of the problems that we address in this thesis.

1.4.2 Relay Assignment in Multiple Source-Destination Cooperative Networks with Limited Feedback

It is shown in Section 1.3 that relay selection for one pair and multiple relays has been extensively studied. Recently, relay assignment where multiple simultaneously transmitting pairs

compete for the same pool of relays has also attracted much attention. Most of the existing works on relay assignment assume that there is a central controller in the network that knows the channel state information (CSI) of all the links. However, for a network with multiple source-destination pairs, from a practical point of view, none of the nodes can acquire the CSI of the entire network without feedback. Therefore, it is crucial to design a practical limited feedback strategy in conjunction with relay assignment, which is considered in this thesis.

1.5 Thesis Contributions

The main contributions of the thesis are summarized as follows.

1.5.1 Relaying Strategies for Two Way Relaying with Asymmetric Data Rates

- We propose a hierarchical zero padding network coding (HZPNC) scheme in [37] to cope with the data rate mismatch problem at the relay. This involves employing hierarchical modulation by the user with the higher data rate and at the relay, while padding zeros at specific positions of the shorter bit sequence at the relay. The proposed scheme outperforms other existing schemes such as the original zero padding scheme, nesting constellation modulation and superposition modulation in terms of the bit error rate (BER) performance and/or complexity.
- We analyze the opportunistic user selection (OUS) scheme in [37] with DF relaying, assuming asymmetric data rates, and compare its performance to that of the HZPNC scheme in terms of BER performance, access probability and throughput.
- We derive the probability density function (PDF) of the SNR for each hop with asymmetric channels for the OUS scheme. We derive closed-form expressions for the E2E BER perfor-

mance for HZPNC, OUS, and the original zero padding. We also derive expressions for the access probability and throughput for the HZPNC and OUS schemes.

- We propose hybrid network coding and opportunistic user selection (HNCOUS) scheme in [38] which offers a better performance compared to that of OUS in terms of E2E BER, access probability and throughput. In addition, our proposed HNCOUS scheme has almost the same access probability and throughput as that of HZPNC at high SNR.
- We derive the PDF of the instantaneous SNR for OUS and HZPNC. These PDFs are needed to derive the E2E BER performance of the proposed HNCOUS scheme.
- We derive exact closed-form expressions for the E2E BER performance for our proposed HNCOUS scheme over *asymmetric* channels for *asymmetric* data rates. We also derive expressions for the access probability and throughput for this scheme.
- We examine the asymptotic E2E BER performance of HNCOUS at high SNR for both users and determine the achievable diversity gain. It is shown that the proposed scheme achieves full diversity, which is the number of available users.

1.5.2 Relay Assignment in Multiple Source-Destination Cooperative Networks with Limited Feedback

- We present a limited feedback quantization strategy and investigate two relay assignment schemes that are based on the quantized CSI in [39] and [40]. That is, the relay assignment is performed based on quantized CSI instead of full CSI, which is a practical scenario.
- For both subset and fullset selection, we derive exact E2E BER expressions in terms of the worst E2E SNR among all pairs.

- We examine the asymptotic performance at high SNR in terms of the worst E2E SNR among all pairs. The optimal threshold function is identified and confirmed by simulation results.
- We adopt a generalized diversity measure to determine the achievable diversity gain. It is shown that the presented relay assignment schemes can achieve diversity $(n, -(n-1))$ with quantized CSI and $(n, 0)$ with full CSI, where n is the number of relays. So even with only quantized CSI, our relay assignment schemes achieve the first-order full diversity. However, we show that there is a second-order diversity loss.

1.6 Thesis outline

The remainder of this thesis is organized as follows.

Chapter 2 provides some relevant background and literature review on the topics pertaining to our proposed research.

In Chapter 3, we focus on proposing efficient relaying strategies at the relay nodes to cope with asymmetric data rates in two-way relay channels. In particular, we propose two DF relaying schemes. One scheme combines HZPNC at the relay. The other scheme is referred to as OUS where the user with a better E2E channel quality is given priority for transmission.

Based on the results obtained in Chapter 3, in Chapter 4, we propose an HNCOUS scheme that aims at taking advantage of both OUS and HZPNC.

Chapter 5 is concerned with practical issues in relay assignment. In particular, we design a practical limited feedback quantization strategy in conjunction with relay assignment schemes.

In Chapter 6, we summarize the thesis and present some potential future works.

Chapter 2

Background and Literature Review

2.1 Existing Techniques for Two-way DF Relaying with Asymmetric Data Rates

When one user uses a higher modulation scheme than that of the other one in two-way relaying, the data sequence lengths received at the relay will be different. Since the data bit sequence lengths received at the relay are different, we cannot apply XOR network coding directly. Some approaches have been proposed to tackle this issue. They are listed as follows.

- Original zero padding: The simplest way to cope with this unmatched data sequence length problem at the relay nodes is zero padding whereby we append zeros to the end of the shorter data sequence to make the two data sequences have the same length. This zero padding process suggests that both users need to operate at the higher modulation scheme which will deteriorate the performance of the system.
- Nesting constellation modulation: The nesting constellation modulation scheme is proposed in [41], in which NC is reinterpreted as a mapping of modulation constellation. Then both

users only need to deal with their original intended modulation scheme. But this joint modulation/NC approach requires considerable changes to the de(modulator) design and increases the detection and demodulation complexity, making it unfavorable in practical implementation.

- Superposition modulation: Besides the above mentioned bit level NC schemes, i.e., original zero padding and nesting constellation modulation, rate mismatch can also be solved by symbol level network coding scheme, i.e. superposition modulation [42], in which the relay divides its power between the two decoded symbols and broadcasts the sum of the two symbols to the destinations. Since the power at the relay is not shared by the two symbols as the case of bit level network coding schemes, it will have a worse BER performance compared to that of bit level NC.

2.2 Hierarchical Modulation in Cooperative Systems

Hierarchical modulation offers different degrees of protection to the transmitted bits according to their relative importance. In [43], the authors derive an exact recursive BER expression for hierarchical M-ary quadrature amplitude modulation (M-QAM). Most of the work on hierarchical modulation focuses on point to point communication. However, with the development of cooperative communication techniques, some efforts have been made to study hierarchical modulation in the context of cooperative communications.

In [44], the authors first study hierarchical modulation combined with cooperative communications, in which a multi-tier cooperative broadcasting strategy is presented and efficient detection schemes are designed. A simple cooperative communication system model which consists of one source, one relay and one destination is considered in [45]. The authors focus on building up an analyzing model which is used to derive the exact closed form BER expression for this cooperative

communication system with hierarchical modulation. In [46], hierarchical modulation is used to at the source to improve the throughput of cooperative systems with distributed channel coding. Hierarchical modulation is employed at the relay in a multiuser cooperative system to improve the network throughput in [47].

In Fig. 2.1 below, we illustrate the 4/16 hierarchical constellation, which we use in Chapters 3 and 4. The filled circles represent the fictitious quadrature phase shift keying (QPSK) symbols and the blank circles represent the actual transmitted 16-QAM symbols. The transmitted bit sequence consists of two subsequences, high priority (HP) bits and low priority (LP) bits. The HP bits are assigned to the positions of the fictitious QPSK symbols, while the LP bits are assigned to the remaining positions. In the figure, $2d_1$ is the distance between two fictitious QPSK symbol points and $2d_2$ is the distance between the actual transmitted 16-QAM constellation points within one quadrant. The constellation priority parameter is denoted by $d = d_1/d_2$.

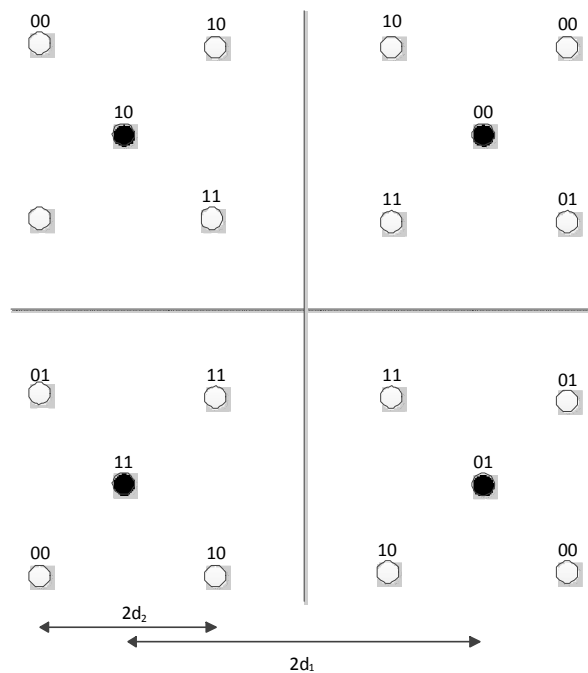


Figure 2.1: 4/16-QAM hierarchical modulation.

2.3 Multiuser Diversity in Cooperative Systems

Multiuser diversity exists when there are multiple users that want to communicate and they experience independent fading. Thus, similar to other classical diversity techniques, multiuser diversity is also obtained by exploiting the multiple independent faded paths. The idea is to let the user with the best instantaneous SNR transmit.

To elaborate, we plot a downlink of a multiuser wireless system in Fig. 2.2, where a base station transmits to multiple users.

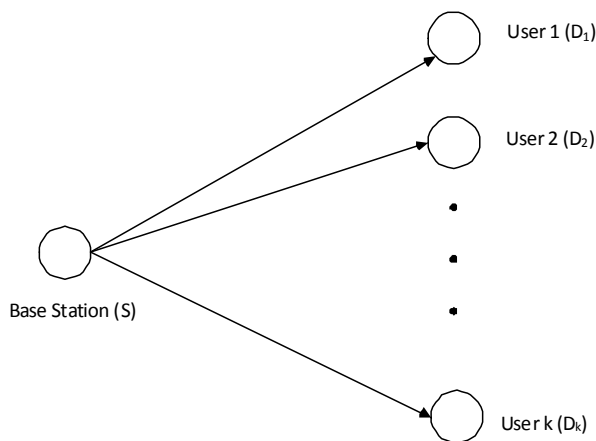


Figure 2.2: Downlink of a multiuser wireless system.

Let S and D_k ($k = 1, 2, \dots, K$) denote the base station and k th user, respectively. Thus

$$k^* = \arg \max_k \{ \gamma_{SD_k}, k = 1, 2, \dots, K \}, \quad (2.1)$$

where k^* represents the index of the selected user and γ_{SD_k} is the instantaneous SNR from the base station to the k th user. It is clear from (2.1) that multiuser diversity is proportional to the number of

users. This is attributed to the fact that the more users available, the more chance to have a better channel quality for the best user.

Since the total uplink or downlink capacity can be maximized by selecting the user with the best E2E instantaneous SNR to transmit, multiuser diversity has been extensively studied for traditional networks [48], [49]. Although higher throughput can be achieved by picking the user with the best E2E instantaneous SNR to transmit, the performance improvement comes at the expense of failing to achieve fairness among users. That is, the users with the strongest channels on average will occupy the channel most of the time. In order to cope with the fairness issue, proportional fair scheduling is proposed and studied in [50]-[52]. The best user is selected as the one which has the best E2E instantaneous SNR compared to its own average SNR.

Recently, multiuser diversity has also been studied in conjunction with cooperative communication in order to improve the reliability of networks. Zhang *et al.* studied a multiuser diversity based cooperative network with one relay and multiple users in [53] which is extended to a general multiuser diversity based cooperative network with multiple users and multiple relays in [54] and [55]. It is shown that both cooperative and multiuser diversity can be achieved. By considering the correlation of effective SNRs of different source-relay pairs, Kim *et al* [56] investigate the effective diversity order of a downlink of N users with M relays. The authors show that the maximum diversity order of $MN + N$ can be only achieved under certain conditions.

Since bidirectional communication can also be viewed as a multiuser system where two users communicate with each other, the authors in [4] study the scheme that supports two sources opportunistically based on the E2E instantaneous SNR for AF relaying. In particular, only the source with the better E2E instantaneous SNR transmits at a time and the other one remains silent. Joint source and relay selection for this scheme is considered in [57]. It is shown that better reliability can be achieved.

2.4 Relay Assignment in Cooperative Systems

Most of the works in relay selection consider selecting the best relay, according to a certain criterion, to serve a pair of nodes in a network. Recently, relay assignment in a network setting where multiple simultaneously transmitting pairs compete for the same pool of relays has attracted a lot of attention [24], [58]-[64]. Some existing schemes are listed as follows.

- **Random Selection:** Relay assignment choice is randomly selected from all the assignment permutations. It is shown in [24] and [58] that the performance of this scheme is the same as the case of one pair with one relay. That is, the diversity of this scheme is one.
- **Sequential Selection [24]:** We first pick one relay and one pair which have the largest value of E2E SNR, then we remove this pair and this relay. The same thing repeats until all pairs have their corresponding selected relays. As such, all pairs have an equal opportunity to be served by the best relay, the second best relay, etc., leading to equivalent performances among all of them. Furthermore, since the performance is dominated by the case when the pair is assigned last in the process, the overall diversity of this scheme is $n - m + 1$, where n is the number of the relays and m is the number of pairs. That is, when the last pair is assigned a relay, only $n - m + 1$ relays are left for assignment, hence the relays contribute only $n - m + 1$ to the diversity.
- **Max-min Capacity:** In [62], the authors propose an assignment scheme, which is based on maximizing the minimum capacity among all pairs. The authors focus on reducing the complexity by developing a polynomial time algorithm, which has a linear complexity for each iteration.
- **Max-min E2E SNR:** In [24] and [60], we consider two relay assignment schemes, fullset and subset selection, which are based on maximizing the minimum E2E SNR among all

pairs. They are extended to the case of one relay helping multiple pairs in [61]. These two schemes can be viewed as an extension of the opportunistic proactive relaying scheme proposed in [28] and [29] to the case of multiple pairs. Fullset selection is also investigated in [62] and [63] with an effort to reduce the search complexity and investigate the performance analytically. Compared to fullset selection, subset selection significantly reduces the search complexity while achieving the same diversity order, which is the number of relays.

- **Selection Cooperation:** In [32], the authors extend the opportunistic reactive relaying scheme to a network setting. In this scheme, the relays are selected from the relays that have decoded the message correctly. Each destination picks the relay with the highest instantaneous relay-destination SNR independently. If one relay is selected by more than one destination, it divides its power among the pairs that it helps.
- **Maximize Sum Rate:** In [65], the authors examine the diversity of an assignment scheme, which is based on maximizing the sum rate among all pairs and show that the sum-rate scheme achieves full diversity if all of the E2E channels are independent.

2.5 Quantized CSI Strategies in Cooperative Systems

Most of the current work on cooperative communications assume that some central node has exact knowledge of the network-wide CSI. In many practical scenarios, however, only a quantized version of the CSI may be available via feedback. Therefore, it becomes essential to investigate the performance of cooperative networks under the assumption of quantized CSI.

The performance of cooperative networks with quantized CSI has been studied for several scenarios. As a general result, it is shown that the performance of cooperative communication with limited feedback is close to that of having full knowledge of the CSI with even a few number of feedback bits [66]-[71].

In [66], the authors investigate power control in a cooperative network with different forms of feedback and show that only a few bits of feedback can achieve most of the gains of full CSI. The authors in [67] study DF relaying with quantized feedback in terms of the outage exponent and show that significant performance gains can be achieved with even one bit of feedback. The performance of relay selection in dual-hop AF systems with full CSI and quantized CSI is studied in [68]. It is shown that the performance of relay selection with quantized CSI approaches that of perfect CSI with only a few feedback bits.

Beamforming with quantized feedback for one transmitting pair is investigated in [70] and [69]. It is shown that both maximal diversity and high array gain can be achieved with only a few feedback bits. It is generalized to interference networks with multiple transmitting pairs in [71].

2.6 Conclusions

In this chapter, we reviewed existing techniques for two-way DF relaying with asymmetric data rates and relay assignment. We have seen that some challenges still remain untackled, including the absence of efficient techniques coping with two-way DF relaying with asymmetric data rates, and some issues facing the implementation of relay assignment schemes. This motivates us to propose efficient relaying strategies in the following chapters to tackle these issues. We have also reviewed hierarchical modulation and multiuser diversity that are related to the work done in this thesis.

Chapter 3

Hierarchical Zero Padding Network Coding (HZPNC) and Opportunistic User Selection (OUS)

3.1 Introduction

In this chapter, we consider a cooperative network comprising two users and an intermediate relay node. The users are assumed to have different data rates. Without loss of generality, and for ease of presentation, we assume that one user uses 4-QAM and the other uses 16-QAM (we also consider 64-QAM later on.). The relay receives and decodes the bits received from both users in the first two time-slots.¹ In the third time-slot, the relay applies exclusive-or (XOR) to both bit streams and broadcasts the resulting bit stream to both nodes. Since the data sequence lengths received at the relay are different, we can not apply XOR network coding directly. In [41], the author try to solve the rate mismatch by reinterpreting network coding as a mapping of modulation constellation. However, this joint modulation/NC approach requires considerable changes to the

¹A time-slot in this context implies the time required to transmit an entire frame.

de(modulator) design and increases the detection and demodulation complexity. In contrast, one simple way, without increasing the complexity of demodulation, is to append zeros to the end of the shorter bit sequence to make the two bit sequences have the same length. This zero padding process suggests that both users need to operate at 16-QAM which will deteriorate the performance of the system.

To remedy the rate mismatch challenge without much performance degradation, we propose to use 4/16-QAM hierarchical modulation at both the source and relay. The 4/16-QAM hierarchical modulation consists of two different transmission priorities for the data stream, HP bits and LP bits. Specifically, the bit stream corresponding to the user using 16-QAM is divided into two substreams, high and low priority. At the relay, the HP substream is XORed with the 4-QAM stream coming from the second user, and the LP substream is unchanged. Therefore, the proposed NC scheme can be viewed as modified zero padding. The difference between the original zero padding and the proposed one is that the zeros are added at specific positions in the latter case. At the destination of the user employing 4-QAM, it only needs to decode the high priority bits which corresponds to a fictitious 4-QAM constellation instead of 16-QAM constellation. Compared to the original zero padding scheme, the complexity of the proposed scheme remains unchanged while the performance is improved. In addition, employing hierarchical modulation gives more freedom to adjust the E2E performance of the two users by adjusting the relative distances between the constellation points. We hereafter refer to the proposed scheme as HZPNC.

We point out that we are not the first to relate hierarchical modulation to network coding. In fact, the authors in [72] propose to use 4/16-QAM hierarchical modulation at the source to cope with the performance degradation caused by asymmetric relay channels. Comparing our work with [72], there are three main differences. Firstly, the problem we address here is how to cope with the data rate mismatch at the relay, while in [72], the authors address the problem of how to avoid performance degradation caused by asymmetric relay channels. Secondly, the scheme proposed

in [72] relies on the direct path to alleviate the problem of asymmetric relay channels, rendering that scheme inapplicable in the absence of the direct path. There is no such constraint for our scheme. Finally, since the direct path can not be utilized for MRC detection at the destination for the scheme proposed in [72], one user will only have diversity order one although the direct path is available. For our scheme, however, both users are expected to achieve diversity order two in case the direct path is available.

On another relevant aspect, two-way relay channels have been studied in the context of multi-user systems. Specifically, in the presence of multiple users, only the user with the best E2E instantaneous SNR transmits and the rest remain silent until their channels improve. In [4] and [57], the authors study the performance of this scheme for AF relaying. It is shown that higher reliability is achieved. In this chapter, we extend this scheme to the DF relaying case, and we refer to it as OUS. The reason for considering OUS here is that it provides another solution to the data rate mismatch problem, which renders itself a competitor for the proposed HZPNC scheme. Obviously there is a sharp contrast between the two schemes. For instance, OUS is expected to achieve better performance compared to the HZPNC scheme due to the multiuser diversity. However, the performance improvement comes at the expense of using more time slots as compared to HZPNC, as well as failing to achieve fairness among users. We study the performance of both schemes over independent Rayleigh fading channels. We derive closed-form expressions for the exact E2E BER performance. We also study the access probability of OUS since it lacks fairness among users. A performance comparison between HZPNC and existing schemes such as zero padding, nesting constellation modulation [41] and superposition modulation [42] is given to demonstrate the superiority of the HZPNC scheme. We present several examples through which we validate the theoretical results.

The remainder of this chapter is organized as follows. The system model is presented in Section 3.2. In Section 3.3, the proposed HZPNC and OUS schemes are presented. We analyze the E2E

BER performance of the two proposed schemes in Section 3.4. We compare the HZPNC and OUS schemes in terms of access probability and throughput in Section 3.5. We present several numerical examples in Section 3.6, and Section 3.7 concludes this chapter.

3.2 System Model

We consider a bidirectional cooperative network with two users denoted by S_1 and S_2 , and one relay denoted by R , where the users communicate with each other via the relay node over orthogonal subchannels. For simplicity, we assume that there is no direct path between the two users. Both users and the relay are equipped with a single antenna and operate in a half-duplex mode. The two users have different data rates. In particular, we assume that one user uses 4-QAM and the other uses 16-QAM. (We also give results for the case when the second user uses 64-QAM.)

The network subchannels are assumed to experience independent slow and frequency non-selective Rayleigh fading. Let h_{1r} , h_{2r} , h_{r1} and h_{r2} denote the fading coefficients for the following hops $S_1 \rightarrow R$, $S_2 \rightarrow R$, $R \rightarrow S_1$ and $R \rightarrow S_2$, respectively. Similarly, let γ_{1r} , γ_{2r} , γ_{r1} and γ_{r2} denote the instantaneous SNRs for the links $S_1 \rightarrow R$, $S_2 \rightarrow R$, $R \rightarrow S_1$ and $R \rightarrow S_2$, respectively. To make the presentation simpler, we denote the instantaneous SNRs over different links by γ_{im} for $i = 1, 2$ and $m = 1, 2$ where $\gamma_{11} = \gamma_{1r}$, $\gamma_{12} = \gamma_{r2}$, $\gamma_{21} = \gamma_{2r}$ and $\gamma_{22} = \gamma_{r1}$, i.e., index i refers to the user and m refers to which hop of that user. To this end, the pdf of γ_{im} is given as

$$f_{\gamma_{im}}(\gamma_{im}) = \frac{1}{\bar{\gamma}_{im}} e^{-\frac{1}{\bar{\gamma}_{im}} \gamma_{im}}, \quad (3.1)$$

where $\bar{\gamma}_{im} = \rho E[|h_{im}|^2]$ is the average SNR for different links and $\rho = \frac{E_b}{N_0}$. For DF relaying, the E2E SNR of user i is approximated as $\gamma_i = \min(\gamma_{i1}, \gamma_{i2})$ [73], and its pdf is expressed as

$$f_{\gamma_i}(\gamma_i) = \frac{1}{\bar{\gamma}_i} e^{-\frac{1}{\bar{\gamma}_i} \gamma_i}, \quad (3.2)$$

where $\bar{\gamma}_i = \frac{\bar{\gamma}_{i1} \bar{\gamma}_{i2}}{\bar{\gamma}_{i1} + \bar{\gamma}_{i2}}$. Thus the E2E SNR of S_i in this part refers to $\gamma_i = \min(\gamma_{i1}, \gamma_{i2})$.

3.3 Proposed Schemes

3.3.1 Hierarchical Zero Padding/Network Coding (HZPNC)

As mentioned above, this scheme involves using a 4/16-QAM hierarchical modulation, where one user uses 4-QAM and the other uses 16-QAM. Since the two user sequences received at the relay have different lengths, we use hierarchical zero padding with network coding. In the following subsections, we elaborate on how this scheme works.

Hierarchical Zero Padding

Since we assume that the two users have different data rates, the length of the bit sequences received from the two users at the relay will be different. In order to clearly illustrate the network coding schemes at the relay, we assume that the detected bit sequences from S_1 and S_2 at the relay are $\hat{b}_1 = 1101$ and $\hat{b}_2 = 11101011$, respectively. Conventional zero padding involves appending zeros to the end of \hat{b}_1 to make it have the same length as that of \hat{b}_2 . Thus, $\hat{b}_1 = 11010000$. Consequently, $\hat{b}_r = \hat{b}_1 \oplus \hat{b}_2 = 00111011$, which will then be modulated into a 16-QAM sequence and broadcasted to both users. In order to get their desired received data, both users need to decode these 16-QAM symbols.

For hierarchical zero padding, instead of adding zeros to the end of \hat{b}_1 , we append zeros to particular positions of \hat{b}_1 . Since 4/16-QAM hierarchical modulation is used at S_2 , \hat{b}_2 consists of HP bits ($\hat{b}_2^h = 1110$) and LP bits ($\hat{b}_2^l = 1011$). Note that the first two bits of every symbol are HP bits. At the relay, \hat{b}_1 is XORed with \hat{b}_2^h and the resulting bits are placed on the position of HP bits

again. Then we get $\hat{b}_r^h = 0011$. The LP bits ($\hat{b}_2^l = 1011$) remain unchanged and placed on the LP bit positions, that is, $\hat{b}_r^l = 1011$. Then $\hat{b}_r = \underline{00}101\underline{11}1$ (the HP bits are underlined.) We can also understand this process in the following way. We treat the original bits of \hat{b}_1 as HP bits, that is, $\hat{b}_1^h = 1101$. We put zeros on the position of LP bits of \hat{b}_1 , that is, $\hat{b}_1^l = 0000$. Then we get the new \hat{b}_1 which is 11000100. Then $\hat{b}_r = \hat{b}_1 \oplus \hat{b}_2 = 00101111$. \hat{b}_r is then modulated by the 4/16-QAM modulation and broadcasted to the two users. We can see that we put zeros on specific positions of \hat{b}_1 to make it have the same length as \hat{b}_2 , hence the name hierarchical zero padding/network coding.

From the above description, the advantages of our proposed HZPNC scheme over original zero padding can be summarized as follows: 1) S_2 needs to only decode the fictitious 4-QAM symbols instead of decoding the 16-QAM symbols; 2) the E2E BER performance of S_1 is only influenced by the BER of the HP bits from S_2 , which has better BER than that of the LP bits; and 3) According to 1) and 2), our proposed HZPNC scheme will have better E2E BER performance than that of the original zero padding for S_1 , and this comes at no additional complexity.

Three time-slot DF Network Coding

Let y_{1r} and y_{2r} denote the signals received at the relay from S_1 and S_2 , respectively (over two time-slots). These signals can be expressed as $y_{1r} = \sqrt{2\rho}h_{1r}x_1 + n_{1r}$ and $y_{2r} = \sqrt{4\rho}h_{2r}x_2 + n_{2r}$, where x_i ($i = 1, 2$) denotes the transmitted signal from user i , and n_{ir} are additive white complex Gaussian noise (AWGN) samples with zero mean and unit variance. The relay then uses ML detection to detect the two signals (arriving from the two users over two time-slots). That is,

$$\begin{aligned}\hat{x}_1 &= \arg \min_{x_1 \in 4\text{-QAM}} \left| y_{1r} - \sqrt{2\rho}h_{1r}x_1 \right| \\ \hat{x}_2 &= \arg \min_{x_2 \in 4/16\text{-QAM}} \left| y_{2r} - \sqrt{4\rho}h_{2r}x_2 \right|.\end{aligned}$$

The resulting sequences are network-coded and modulated by 4/16-QAM modulation. The modulated signal x_r is broadcasted to both users in the third time-slot. The signals received at the two

users are expressed as $y_{ri} = \sqrt{4\rho}h_{ri}x_r + n_{ri}$ ($i = 1, 2$). Then the received signals can be decoded at the destination using ML as

$$\hat{x}_{r1} = \arg \min_{x_r \in 16\text{-QAM}} \left| y_{r1} - \sqrt{4\rho}h_{r1}x_r \right|,$$

and

$$\hat{x}_{r2} = \arg \min_{x_r \in \text{fictitious } 4\text{-QAM}} \left| y_{r2} - \sqrt{4\rho}h_{r2}x_r \right|,$$

respectively. Note that the data of S_1 is embedded within the HP bits of x_r . As such, S_2 needs to only decode the HP bits which comprise the fictitious 4-QAM. Since each user knows its own transmitted signal, it can decode the desired signal according to the network coding scheme used at the relay.

3.3.2 Opportunistic User Selection (OUS)

For this scheme, only one user with the best E2E instantaneous SNR transmits at a time. That is, if $\gamma_i > \gamma_j$ ($i = 1, 2; j = 1, 2$, s.t. $i \neq j$), only user i transmits to user j with the help of the relay. Let us assume user 1 is selected as an example. So in the first time slot, the selected user 1 transmits to the relay, the received signal at the relay is $y_r = \sqrt{2\rho}h_{1r}x_1 + n_{1r}$. Then the relay decodes the received signal as

$$\hat{x}_1 = \arg \min_{x_1 \in 4\text{-QAM}} \left| y_r - \sqrt{2\rho}h_{1r}x_1 \right|$$

The resulting sequence is modulated by 4-QAM modulation. The modulated signal x_r is transmitted to the user 2. The signal received by the user is $y_2 = \sqrt{2\rho}h_{r2}x_r + n_{r2}$. Then the user can decode the received signal as

$$\hat{x}_r = \arg \min_{x_r \in 4\text{-QAM}} \left| y_2 - \sqrt{2\rho}h_{r2}x_r \right|.$$

3.4 Bit Error Rate Performance Analysis

In this section, we derive closed-form expressions for E2E BER for the two relaying schemes, namely, HZPNC and OUS. For both schemes, we assume that S_1 employs 4-QAM and S_2 employs 4/16-QAM. However, the proposed schemes and performance analysis of these schemes can be extended to other hierarchical modulation schemes following the results of [43].

3.4.1 HZPNC Scheme

According to the proposed HZPNC, the bits from S_1 are XORed with the HP bits from S_2 . Consequently, S_2 decodes only the fictitious 4-QAM constellation of the 4/16 hierarchical constellation. The E2E BER at S_2 is given as [24]

$$P_{e,1} = \left(1 - P_{e,r2}^{hp}\right) \left[\begin{array}{c} P_{e,1r} \left(1 - P_{e,2r}^{hp}\right) \\ + P_{e,2r}^{hp} \left(1 - P_{e,1r}\right) \end{array} \right] + \left(1 - \left[\begin{array}{c} P_{e,1r} \left(1 - P_{e,2r}^{hp}\right) \\ + P_{e,2r}^{hp} \left(1 - P_{e,1r}\right) \end{array} \right]\right) P_{e,r2}^{hp} \quad (3.3)$$

where $P_{e,2r}^{hp}$ and $P_{e,r2}^{hp}$ are the probabilities of making an error over the $S_2 \rightarrow R$ and $R \rightarrow S_2$ links, respectively, for the HP bits from S_2 ; $P_{e,1r}$ is the BER over the $S_1 \rightarrow R$ link for the bits from S_1 .

For the 4-QAM modulation, the BER over any of the links can be expressed as

$$P_{e,im} = \int_0^{\infty} P_e^{4QAM}(\gamma_{im}) f_{\gamma_{im}}(\gamma_{im}) d\gamma_{im}, \quad (3.4)$$

where $P_e^{4QAM}(\gamma_{im})$ is the exact conditional BER, conditioned on the instantaneous SNR, and is given by

$$P_e^{4QAM}(\gamma_{im}) = \frac{1}{2} \operatorname{erfc} \sqrt{\gamma_{im}}, \quad (3.5)$$

and $f_{\gamma_{im}}(\gamma_{im})$ is expressed by (3.1).

Plugging (3.1) and (3.5) into (3.4) and carrying out the integration, we obtain

$$P_{e,im} = I_1(1, \bar{\gamma}_{im}), \quad (3.6)$$

where [74]

$$I_1(a, b) = \int_0^{\infty} \frac{1}{2} \operatorname{erfc} \sqrt{a\gamma_{im}} \frac{1}{b} e^{-\frac{1}{b}\gamma_{im}} d\gamma_{im} = \frac{1}{2} \left(1 - \sqrt{\frac{ab}{1+ab}} \right). \quad (3.7)$$

Consequently, $P_{e,im}$ for the case $i = 1, m = 1$ ($S_1 \rightarrow R$ link) is given as $P_{e,1r} = I_1(1, \bar{\gamma}_{1r})$.

In order to get the BER expression for S_2 , we still need the BER expression for the HP bits for 4/16-QAM, which can be expressed as

$$P_{e,im}^{hp} = \int_0^{\infty} P_{e,hp}^{4/16QAM}(\gamma_{im}) f_{\gamma_{im}}(\gamma_{im}) d\gamma_{im}, \quad (3.8)$$

where $P_{e,hp}^{4/16QAM}(\gamma_{im})$ is the exact conditional BER for the HP bits, conditioned on instantaneous SNR for the 4/16-QAM modulation, and is given by [43]

$$P_{e,hp}^{4/16QAM}(\gamma_{im}) = \frac{1}{2} \left[\frac{1}{2} \operatorname{erfc} \sqrt{\frac{2(d^2 - 2d + 1)}{1 + d^2} \gamma_{im}} + \frac{1}{2} \operatorname{erfc} \sqrt{\frac{2(d^2 + 2d + 1)}{1 + d^2} \gamma_{im}} \right], \quad (3.9)$$

where $d = d_1/d_2$ is the constellation priority parameter defined in Chapter 2. Plugging (3.1) and (3.9) into (3.8) and carrying out the integration, we obtain

$$P_{e,im}^{hp} = \frac{1}{2} \left[I_1 \left(\frac{2(d^2 - 2d + 1)}{1 + d^2}, \bar{\gamma}_{im} \right) + I_1 \left(\frac{2(d^2 + 2d + 1)}{1 + d^2}, \bar{\gamma}_{im} \right) \right]. \quad (3.10)$$

Note that $P_{e,2r}^{hp} = P_{e,2l}^{hp}$ and $P_{e,r2}^{hp} = P_{e,l2}^{hp}$. Plugging these expressions as well as that of $P_{e,1r}$ into (3.3) yields a closed-form expression for $P_{e,1}$.

Now for the BER at S_1 , recall that the bits coming from S_2 consist of HP and LP bits. The HP bits are XORed with the bits from S_1 and the LP bits are relayed without network coding. As such, the E2E BER at S_1 is obtained as

$$P_{e,2} = \frac{1}{2} \left(P_{e,2}^{hp} + P_{e,2}^{lp} \right), \quad (3.11)$$

where $P_{e,2}^{hp}$ and $P_{e,2}^{lp}$ represent the E2E BER of the HP and LP bits, respectively. Now $P_{e,2}^{hp}$ can be expressed as [24]

$$P_{e,2}^{hp} = \left(1 - P_{e,r1}^{hp}\right) \left[\begin{array}{c} P_{e,1r} \left(1 - P_{e,2r}^{hp}\right) \\ + P_{e,2r}^{hp} \left(1 - P_{e,1r}\right) \end{array} \right] + \left(1 - \left[\begin{array}{c} P_{e,1r} \left(1 - P_{e,2r}^{hp}\right) \\ + P_{e,2r}^{hp} \left(1 - P_{e,1r}\right) \end{array} \right]\right) P_{e,r1}^{hp}, \quad (3.12)$$

where $P_{e,1r}$ and $P_{e,2r}^{hp}$ are defined above. When $i = 2, m = 2$, we have $P_{e,r1}^{hp} = P_{e,22}^{hp}$. Having found expressions for all the terms in (3.12), we can easily find a closed-form expression for $P_{e,2}^{hp}$.

Concerning the LP bits, since they are relayed without network coding, the corresponding E2E BER is given by

$$P_{e,2}^{lp} = P_{e,2r}^{lp} (1 - P_{e,r1}^{lp}) + (1 - P_{e,2r}^{lp}) P_{e,r1}^{lp}, \quad (3.13)$$

where

$$P_{e,im}^{lp} = \int_0^{\infty} P_{e,lp}^{4/16QAM}(\gamma_{im}) f_{\gamma_{im}}(\gamma_{im}) d\gamma_{im}, \quad (3.14)$$

and $P_{e,lp}^{4/16QAM}(\gamma_{im})$ is the exact conditional BER for the LP bits, conditioned on the instantaneous SNR, for the 4/16QAM modulation and is given by [43]

$$P_{e,lp}^{4/16QAM}(\gamma_{im}) = \frac{1}{2} \left[\begin{array}{c} \operatorname{erfc} \sqrt{\frac{2}{1+d^2} \gamma_{im}} + \frac{1}{2} \operatorname{erfc} \sqrt{\frac{2(4d^2-4d+1)}{1+d^2} \gamma_{im}} \\ - \frac{1}{2} \operatorname{erfc} \sqrt{\frac{2(4d^2+4d+1)}{1+d^2} \gamma_{im}} \end{array} \right]. \quad (3.15)$$

Plugging (3.1) and (3.15) into (3.14) and carrying out the integration, we obtain

$$P_{e,im}^{lp} = I_1 \left(\frac{2}{1+d^2}, \bar{\gamma}_{im} \right) + \frac{1}{2} \left[I_1 \left(\frac{2(4d^2-4d+1)}{1+d^2}, \bar{\gamma}_{im} \right) - I_1 \left(\frac{2(4d^2+4d+1)}{1+d^2}, \bar{\gamma}_{im} \right) \right]. \quad (3.16)$$

By setting $i = 2, m = 2$ in (3.16), we obtain $P_{e,r1}^{lp} = P_{e,22}^{lp}$. We can similarly obtain $P_{e,1r}^{lp} = P_{e,11}^{lp}$.

These expressions lead to a closed-form expression for $P_{e,2}^{lp}$. Having obtained expressions for $P_{e,2}^{hp}$ and $P_{e,2}^{lp}$, $P_{e,2}$ is obtained by plugging $P_{e,2}^{hp}$ and $P_{e,2}^{lp}$ into (3.11).

3.4.2 Original Zero Padding

We derive in this section the E2E BER performance of the original zero padding scheme, whereby the zeros are just added at the end of the shorter bit sequence. Recall that the bits from S_1 are XORed with the bits from S_2 . Therefore, the E2E BER at S_2 can be expressed as

$$P_{e,1} = (1 - P_{e,r2}) \left[\begin{array}{c} P_{e,1r} (1 - P_{e,2r}) \\ + P_{e,2r} (1 - P_{e,1r}) \end{array} \right] + \left(1 - \left[\begin{array}{c} P_{e,1r} (1 - P_{e,2r}) \\ + P_{e,2r} (1 - P_{e,1r}) \end{array} \right] \right) P_{e,r2}, \quad (3.17)$$

where $P_{e,1r}$ is derived above. Since we do not distinguish HP and LP bit in the original zero padding scheme, the BER over different links is the same and can be expressed as

$$P_{e,im} = \frac{1}{2} (P_{e,im}^{hp} + P_{e,im}^{lp}), \quad (3.18)$$

where $P_{e,im}^{hp}$ and $P_{e,im}^{lp}$ are given in (3.10) and (3.16), respectively. Therefore, we have $P_{e,2r}^{hp} = P_{e,21}^{hp}$, $P_{e,r2}^{hp} = P_{e,22}^{hp}$, $P_{e,2r}^{lp} = P_{e,21}^{lp}$ and $P_{e,r2}^{lp} = P_{e,22}^{lp}$. Plugging the expressions for $P_{e,2r}^{hp}$ and $P_{e,2r}^{lp}$ into (3.18) yields an expression for $P_{e,2r}$. An expression for $P_{e,r2}$ can be obtained the same way. Plugging the expressions of $P_{e,1r}$, $P_{e,2r}$ and $P_{e,r2}$ into (3.17) yields an expression for $P_{e,1}$.

Now we derive an expression for $P_{e,2}$. Note that half of the bits from S_2 are XORed with the bits coming from S_1 , while the remaining bits are forwarded to the destination without network coding. Consequently, the E2E BER at S_1 can be expressed as

$$P_{e,2} = \frac{1}{2} (P_{e,2}^{NC} + P_{e,2}^{noNC}), \quad (3.19)$$

where

$$P_{e,2}^{NC} = (1 - P_{e,r1}) \left[\begin{array}{c} P_{e,1r} (1 - P_{e,2r}) \\ + P_{e,2r} (1 - P_{e,1r}) \end{array} \right] + \left(1 - \left[\begin{array}{c} P_{e,1r} (1 - P_{e,2r}) \\ + P_{e,2r} (1 - P_{e,1r}) \end{array} \right] \right) P_{e,r1} \quad (3.20)$$

and

$$P_{e,2}^{noNC} = P_{e,2r} (1 - P_{e,r1}) + (1 - P_{e,2r}) P_{e,r1}. \quad (3.21)$$

From (3.18), we can obtain an expression for $P_{e,r1}$. By plugging the expression of $P_{e,r1}$, $P_{e,2r}$ and $P_{e,1r}$ into (3.20) and (3.21), we can get expressions for $P_{e,2}^{NC}$ and $P_{e,2}^{noNC}$.

3.4.3 OUS Scheme

For this scheme, if the instantaneous E2E SNR of S_i is greater than that of S_j , only S_i transmits to S_j . Thus, when either the $S_i \rightarrow R$ or $R \rightarrow S_j$ link is in error, the received signal at S_j will be in error. Therefore, the E2E BER of S_i can be expressed as

$$P(\varepsilon_i | \gamma_i > \gamma_j) = P(\varepsilon_{im} | \gamma_i > \gamma_j)(1 - P(\varepsilon_{in} | \gamma_i > \gamma_j)) + P(\varepsilon_{in} | \gamma_i > \gamma_j)(1 - P(\varepsilon_{im} | \gamma_i > \gamma_j)), \quad (3.22)$$

where $i, j = 1, 2$, where $i \neq j$, and $m, n = 1, 2$, where $m \neq n$. The indices have the same definition as that of γ_{im} in Section 3.2, that is, $P(\varepsilon_{11} | \gamma_1 > \gamma_2)$ refers to $P(\varepsilon_{1r} | \gamma_1 > \gamma_2)$, which represents the BER over the $S_1 \rightarrow R$ link given that $\gamma_1 > \gamma_2$. Since S_1 employs 4-QAM, the BER over different links can be expressed as

$$P(\varepsilon_{1m} | \gamma_1 > \gamma_2) = \int_0^{\infty} P_e^{4QAM}(\gamma_{1m}) f_{\gamma_{1m} | \gamma_1 > \gamma_2}(\gamma_{1m}) d\gamma_{1m} \quad (3.23)$$

The pdf of γ_{im} conditioned on $\gamma_i > \gamma_j$ is derived as (see Appendix A. 1)

$$f_{\gamma_{im} | \gamma_i > \gamma_j}(\gamma_{im}) = \frac{\bar{\gamma}_{in}(\bar{\gamma}_i + \bar{\gamma}_j)}{\bar{\gamma}_{im}\bar{\gamma}_i(\bar{\gamma}_{in} + \bar{\gamma}_j)} \left(e^{-\frac{1}{\bar{\gamma}_{im}}\gamma_{im}} - e^{-(\frac{1}{\bar{\gamma}_i} + \frac{1}{\bar{\gamma}_j})\gamma_{im}} \right). \quad (3.24)$$

Plugging (3.5) and (3.24) into (3.23) and carrying out the integration, we obtain

$$P(\varepsilon_{1m} | \gamma_1 > \gamma_2) = \frac{\bar{\gamma}_{1n}(\bar{\gamma}_1 + \bar{\gamma}_2)}{\bar{\gamma}_{1m}\bar{\gamma}_1(\bar{\gamma}_{1n} + \bar{\gamma}_2)} \left[\bar{\gamma}_{1m} I_1(1, \bar{\gamma}_{1m}) - \frac{\bar{\gamma}_1\bar{\gamma}_2}{\bar{\gamma}_1 + \bar{\gamma}_2} I_1\left(1, \frac{\bar{\gamma}_1\bar{\gamma}_2}{\bar{\gamma}_1 + \bar{\gamma}_2}\right) \right]. \quad (3.25)$$

Note that $P(\varepsilon_{1r} | \gamma_1 > \gamma_2) = P(\varepsilon_{22} | \gamma_1 > \gamma_2)$ and $P(\varepsilon_{r2} | \gamma_1 > \gamma_2) = P(\varepsilon_{12} | \gamma_1 > \gamma_2)$. Plugging these expressions into (3.22) yields a closed form expression for $P(\varepsilon_1 | \gamma_1 > \gamma_2)$.

Since S_2 uses hierarchical 4/16-QAM modulation and we do not distinguish between the HP and LP bits, $P(\varepsilon_{2m} | \gamma_2 > \gamma_1)$ is given by

$$P(\varepsilon_{2m} | \gamma_2 > \gamma_1) = \frac{1}{2}(P(\varepsilon_{2m}^{hp} | \gamma_2 > \gamma_1) + P(\varepsilon_{2m}^{lp} | \gamma_2 > \gamma_1)), \quad (3.26)$$

where $P(\varepsilon_{2m}^{hp} | \gamma_2 > \gamma_1)$ represents the BER of the HP bits given that $\gamma_2 > \gamma_1$, and $P(\varepsilon_{2m}^{lp} | \gamma_2 > \gamma_1)$ represents the BER of the LP bits given that $\gamma_2 > \gamma_1$. The BER of the HP bits can be expressed as

$$P(\varepsilon_{2m}^{hp} | \gamma_2 > \gamma_1) = \int_0^{\infty} P_{e, hp}^{4/16QAM}(\gamma_{2m}) f_{\gamma_{2m} | \gamma_2 > \gamma_1}(\gamma_{2m}) d\gamma_{2m}. \quad (3.27)$$

Plugging (3.9) and (3.24) into (3.27) and carrying out the integration, we obtain

$$P(\varepsilon_{2m}^{hp} | \gamma_2 > \gamma_1) = \frac{1}{2} \frac{\bar{\gamma}_{2n}(\bar{\gamma}_1 + \bar{\gamma}_2)}{\bar{\gamma}_{2m}\bar{\gamma}_2(\bar{\gamma}_{2n} + \bar{\gamma}_1)} \left\{ \begin{array}{l} \bar{\gamma}_{2m} \left[\begin{array}{l} I_1 \left(\frac{2(d^2-2d+1)}{1+d^2}, \bar{\gamma}_{2m} \right) \\ + I_1 \left(\frac{2(d^2+2d+1)}{1+d^2}, \bar{\gamma}_{2m} \right) \end{array} \right] \\ - \frac{\bar{\gamma}_1\bar{\gamma}_2}{\bar{\gamma}_1+\bar{\gamma}_2} \left[\begin{array}{l} I_1 \left(\frac{2(d^2-2d+1)}{1+d^2}, \frac{\bar{\gamma}_1\bar{\gamma}_2}{\bar{\gamma}_1+\bar{\gamma}_2} \right) \\ + I_1 \left(\frac{2(d^2+2d+1)}{1+d^2}, \frac{\bar{\gamma}_1\bar{\gamma}_2}{\bar{\gamma}_1+\bar{\gamma}_2} \right) \end{array} \right] \end{array} \right\}. \quad (3.28)$$

Note that $P(\varepsilon_{2r}^{hp} | \gamma_2 > \gamma_1) = P(\varepsilon_{22}^{hp} | \gamma_2 > \gamma_1)$ and $P(\varepsilon_{r1}^{hp} | \gamma_2 > \gamma_1) = P(\varepsilon_{21}^{hp} | \gamma_2 > \gamma_1)$.

Similarly, the BER of the LP bits can be expressed as

$$P(\varepsilon_{2m}^{lp} | \gamma_2 > \gamma_1) = \int_0^{\infty} P_{e, lp}^{4/16QAM}(\gamma_{2m}) f_{\gamma_{2m} | \gamma_2 > \gamma_1}(\gamma_{2m}) d\gamma_{2m} \quad (3.29)$$

Then plugging (3.15) and (3.24) into (3.29) and carrying out the integration, we obtain

$$P(\varepsilon_{2m}^{lp} | \gamma_2 > \gamma_1) = \frac{\bar{\gamma}_{2n}(\bar{\gamma}_2 + \bar{\gamma}_1)}{\bar{\gamma}_{2m}\bar{\gamma}_2(\bar{\gamma}_{2n} + \bar{\gamma}_1)} \left\{ \begin{array}{l} \bar{\gamma}_{2m} \left[\begin{array}{l} I_1 \left(\frac{2}{1+d^2}, \bar{\gamma}_{2m} \right) \\ + \frac{1}{2} I_1 \left(\frac{2(4d^2-4d+1)}{1+d^2}, \bar{\gamma}_{2m} \right) \\ - \frac{1}{2} I_1 \left(\frac{2(4d^2+4d+1)}{1+d^2}, \bar{\gamma}_{2m} \right) \end{array} \right] \\ - \frac{\bar{\gamma}_1\bar{\gamma}_2}{\bar{\gamma}_1+\bar{\gamma}_2} \left[\begin{array}{l} I_1 \left(\frac{2}{1+d^2}, \frac{\bar{\gamma}_1\bar{\gamma}_2}{\bar{\gamma}_1+\bar{\gamma}_2} \right) \\ + \frac{1}{2} I_1 \left(\frac{2(4d^2-4d+1)}{1+d^2}, \frac{\bar{\gamma}_1\bar{\gamma}_2}{\bar{\gamma}_1+\bar{\gamma}_2} \right) \\ - \frac{1}{2} I_1 \left(\frac{2(4d^2+4d+1)}{1+d^2}, \frac{\bar{\gamma}_1\bar{\gamma}_2}{\bar{\gamma}_1+\bar{\gamma}_2} \right) \end{array} \right] \end{array} \right\}. \quad (3.30)$$

Note that $P(\varepsilon_{2r}^{lp} | \gamma_2 > \gamma_1) = P(\varepsilon_{21}^{lp} | \gamma_2 > \gamma_1)$ and $P(\varepsilon_{r1}^{lp} | \gamma_2 > \gamma_1) = P(\varepsilon_{22}^{lp} | \gamma_2 > \gamma_1)$.

Having obtained the expressions for $P(\varepsilon_{2m}^{hp} | \gamma_2 > \gamma_1)$ and $P(\varepsilon_{2m}^{lp} | \gamma_2 > \gamma_1)$, $P(\varepsilon_{2r} | \gamma_2 > \gamma_1)$ is obtained by plugging $P(\varepsilon_{2r}^{hp} | \gamma_2 > \gamma_1)$ and $P(\varepsilon_{2r}^{lp} | \gamma_2 > \gamma_1)$ into (3.26) and $P(\varepsilon_{r1} | \gamma_2 > \gamma_1)$ is

obtained by plugging $P(\varepsilon_{r1}^{hp} | \gamma_2 > \gamma_1)$ and $P(\varepsilon_{r1}^{lp} | \gamma_2 > \gamma_1)$ into (3.26). Plugging the derived expressions $P(\varepsilon_{2r} | \gamma_2 > \gamma_1)$ and $P(\varepsilon_{r1} | \gamma_2 > \gamma_1)$ into (3.22), we obtain a closed form expression for $P(\varepsilon_2 | \gamma_2 > \gamma_1)$, as desired.

3.5 Access Probability and Throughput Analysis

In this section, we compare the HZPNC and OUS schemes in terms of access probability and throughput.

3.5.1 Access Probability

According to the HZPNC scheme, both users transmit via channel sharing. The two users communicate with each other over three time-slots. During the three time-slots, each user occupies two time-slots with one time-slot overlapping. Therefore, the access probability for both users is

$$P_i^{HZPNC} = \frac{2}{3}. \quad (3.31)$$

As for the OUS scheme, a user transmits once its instantaneous E2E SNR is greater than that of the other one, resulting in an access probability of

$$\begin{aligned} P_i^{OUS} &= P_r(\gamma_i > \gamma_j) \\ &= \int_0^\infty \frac{1}{\bar{\gamma}_j} e^{-\frac{\gamma_j}{\bar{\gamma}_j}} dz_j \int_{\gamma_j}^\infty \frac{1}{\bar{\gamma}_i} e^{-\frac{\gamma_i}{\bar{\gamma}_i}} d\gamma_1 \\ &= \frac{\bar{\gamma}_i}{\bar{\gamma}_i + \bar{\gamma}_j} \end{aligned} \quad (3.32)$$

$$\triangleq \frac{k_i}{k_i + 1}, \quad (3.33)$$

where $k_i \triangleq \bar{\gamma}_i / \bar{\gamma}_j$. From (3.33), we observe that P_i^{OUS} only depends on the value of k_i . For symmetric channels, for example, the average E2E SNRs are the same, i.e., $k_i = 1$, suggesting

that both users will have the same access probability, which is $P_i^{OUS} = 0.5$. In this case, the OUS scheme has a lower access probability compared to that of the HZPNC scheme for each user by $\frac{1}{6}$.

Now define ΔP_i as

$$\Delta P_i \triangleq P_i^{HZPNC} - P_i^{OUS} = \frac{2}{3} - \frac{k_i}{k_i + 1}, \quad (3.34)$$

which represents the access probability difference between the two schemes. Solving $\frac{2}{3} - \frac{k_i}{k_i + 1} > 0$, we obtain $\frac{1}{2} < k_i < 2$, which is the range of k_i for which the HZPNC scheme has a higher access probability than that of the OUS scheme for both users. Beyond this range, one user of OUS scheme will have a higher access probability than those of HZPNC scheme, whereas the other one will have a lower access probability.

3.5.2 Throughput

We do the throughput analysis for the general case where it is assumed that S_1 uses 2^{2s} -QAM and S_2 uses $2^{2s}/2^{2r}$ -QAM hierarchical modulation for $s = 1, 2, \dots, r - 1$, and $r = 2, 3, \dots, R$. Since three time-slots are used for HZPNC, the corresponding throughput can be expressed as

$$T^{HZPNC} = \frac{2(s+r)}{3} \text{ bits/time slot}, \quad (3.35)$$

whereas for OUS, when a user transmits, it needs two time-slots to finish its transmission, thus the corresponding throughput is expressed as

$$T^{OUS} = \frac{2s \times P_r(\gamma_1 > \gamma_2) + 2r \times P_r(\gamma_2 > \gamma_1)}{2}. \quad (3.36)$$

Plugging (3.32) into (3.36), we obtain

$$T^{OUS} = \frac{s\bar{\gamma}_1 + r\bar{\gamma}_2}{\bar{\gamma}_1 + \bar{\gamma}_2} = \frac{sk_1 + r}{k_1 + 1} \text{ bits/time slot}, \quad (3.37)$$

where k_1 is defined above. Now define ΔT as

$$\Delta T \triangleq T^{HZPNC} - T^{OUS} = \frac{2(s+r)}{3} - \frac{sk_1 + r}{k_1 + 1}, \quad (3.38)$$

which is the throughput difference between the two schemes.

For symmetric channels, i.e., $k_1 = 1$, we have $\Delta T = \frac{s+r}{6}$, suggesting that HZPNC achieves a higher throughput, as expected. However, it is not straightforward to say which scheme has a higher throughput for asymmetric channels, that is, when $k_1 \neq 1$. For fixed values of s and r , ΔT is only a function of k_1 . We can consider two cases as examples. One is the example used throughout this chapter where $s = 1$ and $r = 2$. Plugging $s = 1$ and $r = 2$ into (3.38), we obtain $\Delta T = \frac{k_1}{k_1+1}$, suggesting that T^{HZPNC} is greater than T^{OUS} by $\frac{k_1}{k_1+1}$.

Another example is when $s = 1$ and $r = 4$, which corresponds to S_1 using 4-QAM and S_2 using 4/256-QAM hierarchical modulation. Plugging $s = 1$ and $r = 4$ into (3.38), we obtain $\Delta T = \frac{7k_1-2}{3(k_1+1)}$. By solving $\frac{7k_1-2}{3(k_1+1)} > 0$, we find that $\Delta T > 0$ when $k_1 > \frac{2}{7}$, meaning that T^{HZPNC} is greater than T^{OUS} by $\frac{7k_1-2}{3(k_1+1)}$ for $k_1 > \frac{2}{7}$. On the other hand, $T^{NC} < T^{OUS}$ by $\frac{7k_1-2}{3(k_1+1)}$ when $k_1 < \frac{2}{7}$. Nonetheless, the probability that T^{NC} is less than T^{OUS} is very small, and it happens only when one user has a much higher modulation and access probability than those of the other user.

3.6 Simulation Results

We present in this section numerical examples that aim at validating the E2E BER expressions derived for HZPNC and OUS. We also study the impact of varying the priority parameter d on the BER performance of HZPNC. In addition, we compare the two schemes in terms of E2E BER, access probability and throughput. Throughout the simulations, we assume that S_1 uses 4-QAM and S_2 uses 4/16-QAM hierarchical modulation, $d = 2$ and all channel variances are set to one, unless mentioned otherwise.

In Fig. 3.1, we compare the simulated E2E BER and the theoretical one based on the expressions derived in Section 3.4 for the original zero padding and HZPNC schemes (for S_1). We also plot the simulation results for the case when S_1 uses 4-QAM and S_2 uses 4/64-QAM. As shown in

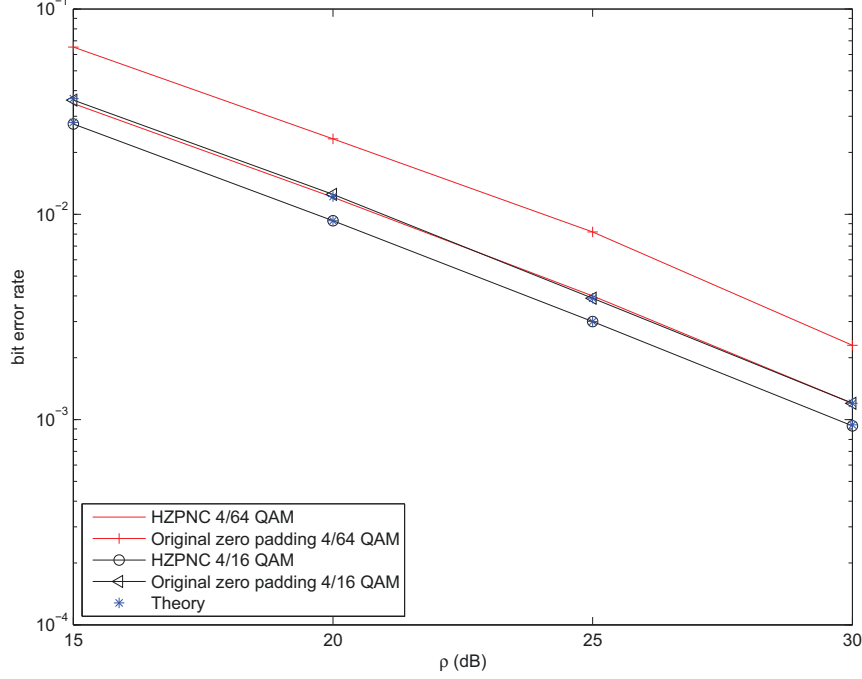


Figure 3.1: E2E BER performance of the original zero padding and HZPNC schemes (for S_1).

In the figure, the simulation results agree with the theoretical results. We also observe the superiority of HZPNC over the original zero padding scheme for S_1 , which is about 1 dB for 4/16-QAM and 3 dB for 4/64-QAM, and this comes at no additional complexity. This improvement is attributed to the fact that S_2 needs only to decode the fictitious 4-QAM instead of 16-QAM, and the E2E BER performance is only influenced by the BER of the HP bits from S_2 , which have a lower BER than that of the LP bits. The results for S_2 are reported in Fig. 3.2. We also observe from the figure the perfect match between theory and simulations. In addition, our proposed HZPNC scheme achieves the same performance as the original zero padding for S_2 .

In Fig. 3.3, we examine the influence of the value of d on the BER performance of the two users. We consider two values of d , namely 1.5 and 2. We observe from the figure that the performance of S_1 improves as d decreases from 2 to 1.5, whereas the performance of S_2 deteriorates. The improvement in the performance of S_1 is due to the fact that the BER of the HP bits is improved as

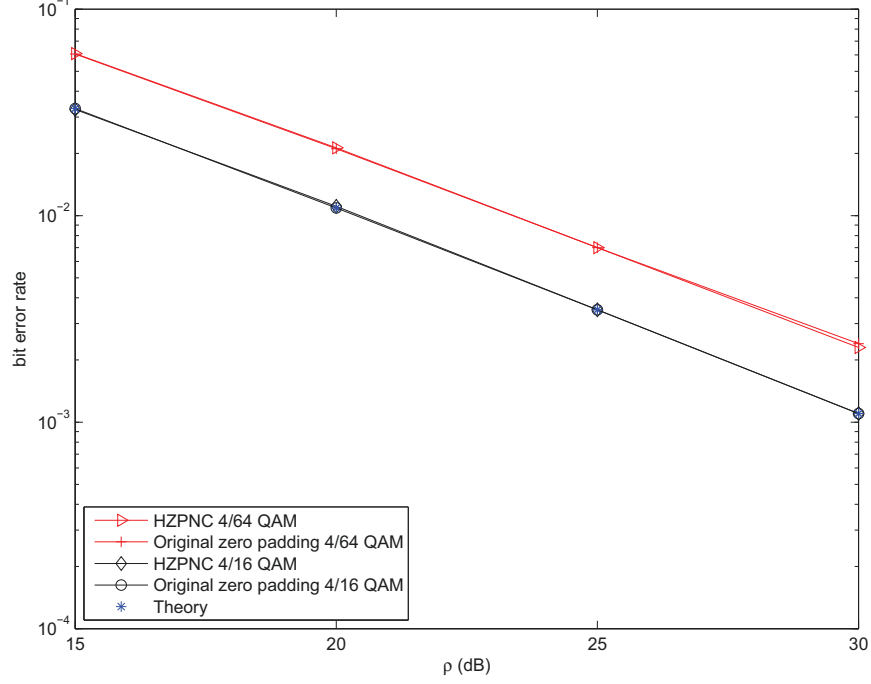


Figure 3.2: E2E BER performance of the original zero padding and HZPNC schemes (for S_2).

d decreases, and this comes at the expense deteriorating the BER of the LP bits. The consequence of this is a deterioration of the BER performance S_2 since it depends on the LP bits. So the conclusion here is that changing the value of d improves the performance of one user while it deteriorates the performance of the other.

In Fig. 3.5, we compare the E2E BER performance of HZPNC against that of the nesting constellation modulation proposed in [41]. For nesting constellation modulation, the sequence length mismatch at the relay is taken care of by using repetition coding. For example, let $\hat{b}_1 = 1101$. Then it is encoded into $\hat{b}_1 = 11110011$, which now has the same length as that of $\hat{b}_2 = 11101011$. Then $\hat{b}_r = \hat{b}_1 \oplus \hat{b}_2 = 00101111$ is modulated as 16-QAM and broadcasted to the destinations. For S_2 to recover the signal of interest, it needs to do a constellation conversion from 16-QAM to 4-QAM according to Table I in [41]. As shown in the figure, the performance of S_1 is slightly better than that of HZPNC and the performance of S_2 is the opposite. As a whole, both schemes

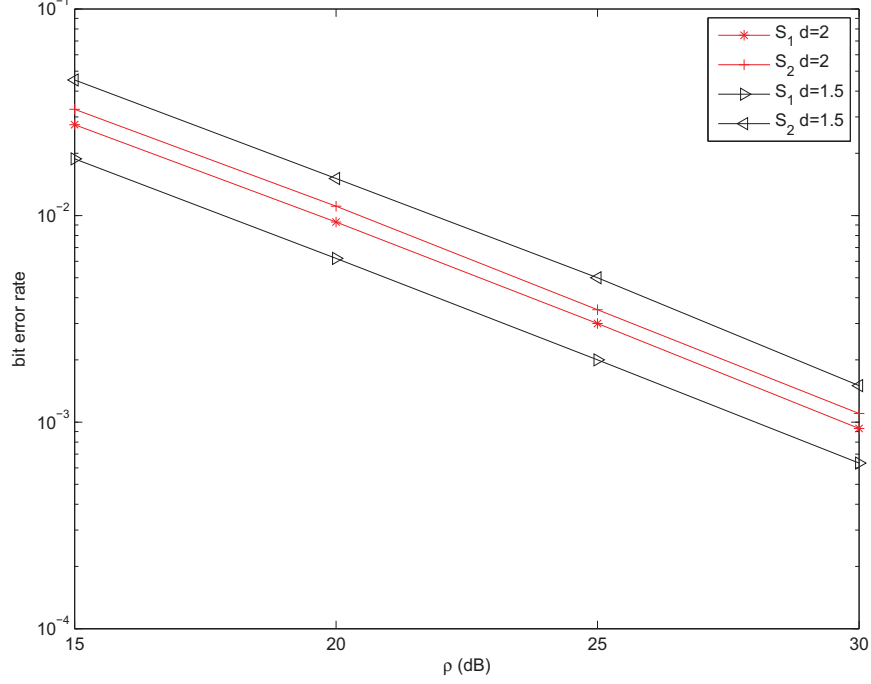


Figure 3.3: Effect of variation of d on the E2E BER performance for two users.

almost have similar sum BER performance (the average performance of both users), except that the nesting constellation modulation is more complex.

In Fig. 3.6, we compare the E2E BER performance of HZPNC with that of superposition modulation [42]. For the latter scheme, after the relay decodes the 4-QAM symbol \hat{x}_1 from S_1 and the 16-QAM symbol \hat{x}_2 from S_2 , it divides its power between these two symbols and transmits $\hat{x}_r = \sqrt{1 - \gamma^2}\hat{x}_1 + \sqrt{\gamma^2}\hat{x}_2$ to the destinations. Then a destination subtracts its own symbol and decodes the desired signal. In the simulations, we set $\gamma = 0.8$, $\gamma = 0.5$ and $\gamma = 0.2$. It is shown in the figure that the performance of HZPNC is better than that of superposition modulation, and the gap increases as γ decreases. We remark that the plotted performance is the average of the performance of the two users.

We compare in Fig. 3.7 the BER performance of HZPNC and OUS for S_1 . For presentation convenience, we let the set $\{E[|h_{1r}|^2], E[|h_{2r}|^2], E[|h_{r2}|^2], E[|h_{r1}|^2]\}$ denote the variances

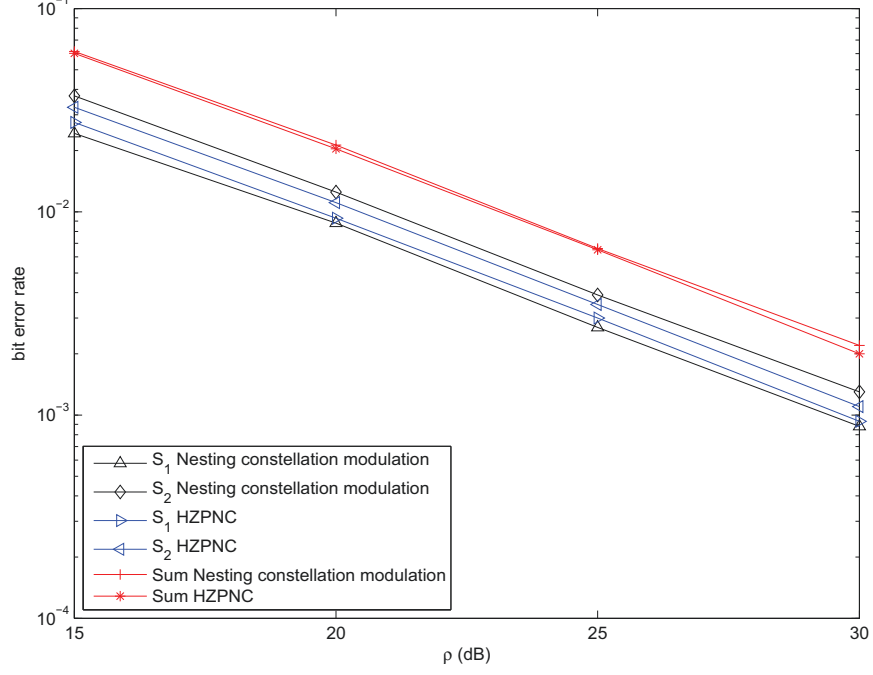


Figure 3.4: Comparison of E2E BER performance of Nesting constellation modulation and HZPNC.

of the four subchannels. In the simulations, for both schemes, we randomly set channel 1 as $(\frac{1}{4}, \frac{1}{4}, \frac{1}{4}, \frac{1}{4})$, channel 2 as $(\frac{1}{2}, 1, \frac{1}{2}, \frac{1}{5})$, and channel 3 as $(1, 1, 1, \frac{1}{5})$. From the figure, we observe the following. First, there is a perfect match between simulations and theory, which validates our analysis. Second, it is shown that HZPNC achieves diversity order one, while OUS achieves diversity order two, which is expected since OUS benefits from the multiuser diversity gain. Finally, it is shown that OUS has a better E2E BER performance than that of HZPNC for all channels. The E2E BER performance for S_2 is shown in Fig. 3.8, with similar observations. However, the performance superiority of OUS over HZPNC comes at the expense of much reduced throughput, as will be demonstrated below.

In Fig. 3.9, we show the access probability for different values of k_1 for HZPNC and OUS. The access probability of HZPNC remains unchanged during all the range, which is $\frac{2}{3}$. Whereas, for OUS, when $\bar{\gamma}_1 < \bar{\gamma}_2$, S_1 has a lower access probability than S_2 . The opposite is true when $\bar{\gamma}_1 > \bar{\gamma}_2$,

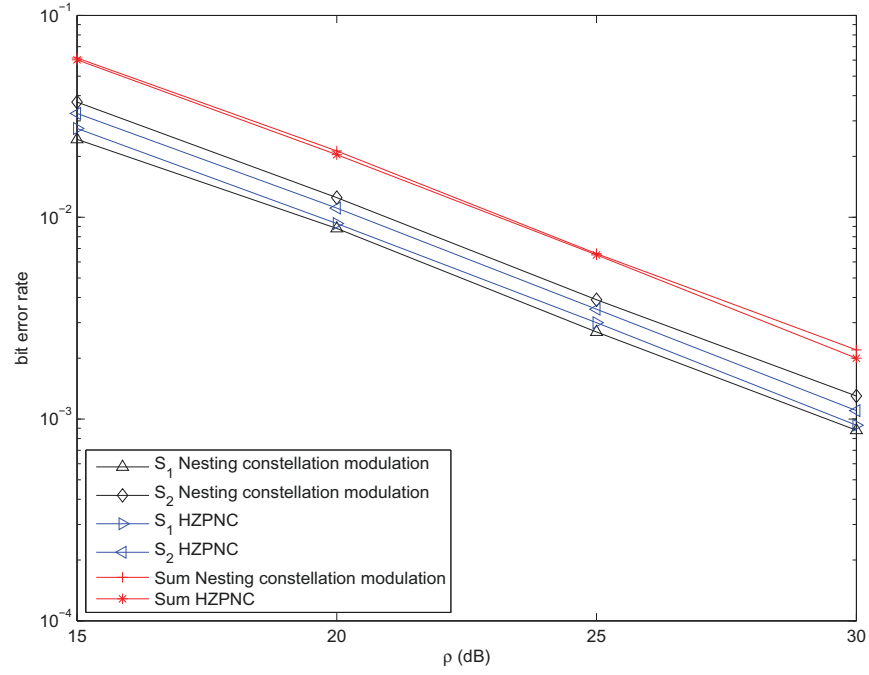


Figure 3.5: Comparison of E2E BER performance of Nesting constellation modulation and HZPNC.

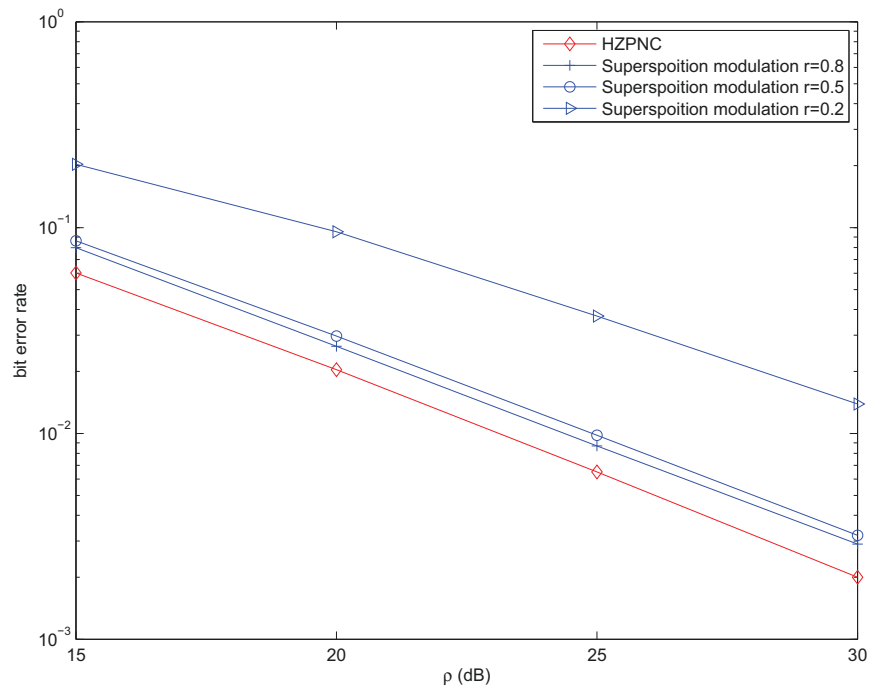


Figure 3.6: Comparison of the sum BER performance of Superposition modulation and HZPNC.

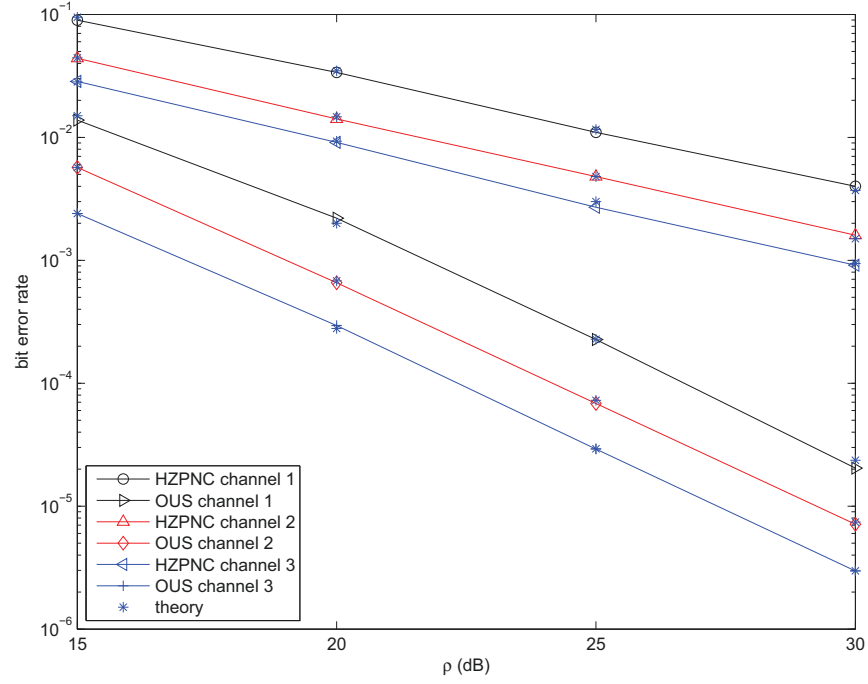


Figure 3.7: Bit error rate performance (simulated and theoretical) of HZPNC and OUS for S_1 .

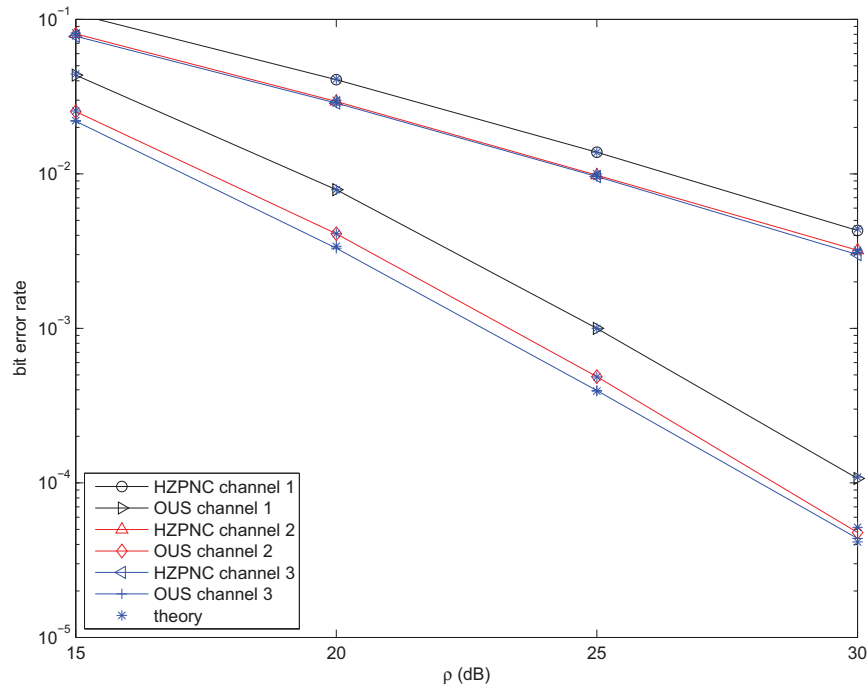


Figure 3.8: Bit error rate performance (simulated and theoretical) of HZPNC and OUS for S_2 .

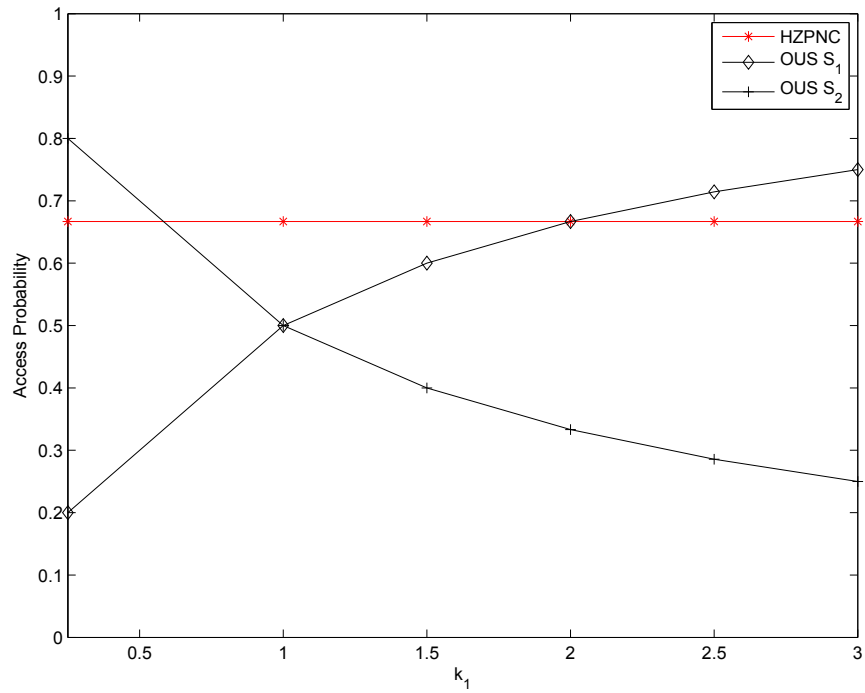


Figure 3.9: Access probability for HZPNC and OUS.

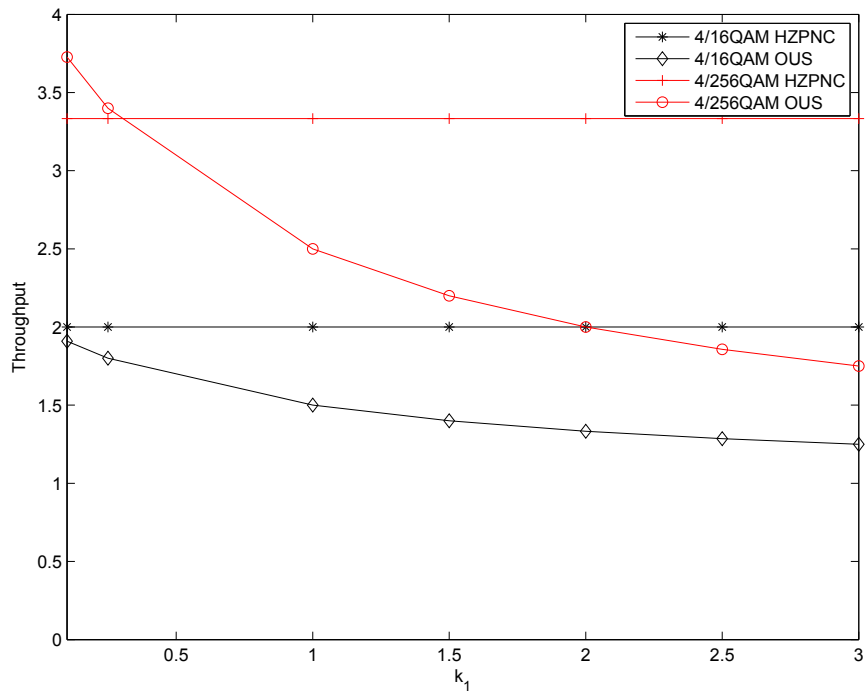


Figure 3.10: Throughput for HZPNC and OUS.

which is expected. It is also shown that both OUS users have a lower access probability than the HZPNC users for the range $\frac{1}{2} < k_1 < 2$. While for the range $k_1 > 2$, S_1 has a higher access probability and S_2 has a lower access probability than those for HZPNC. However, for $k_1 < \frac{1}{2}$, the two OUS users exchange roles. For $k_1 = 1$, both users have the same chance to access the channel. For this case, the access probability is $\frac{1}{2}$ for both users which is $\frac{1}{6}$ less than that of the HZPNC scheme.

In Fig. 3.10, we show the throughput for different values of k_1 for both HZPNC and OUS. We consider two cases. In both cases, S_1 uses 4-QAM, whereas S_2 uses 4/16-QAM or 4/256-QAM. For all scenarios, we find that the throughput of OUS decreases with increasing k_1 . This is expected since S_1 uses a lower order modulation scheme than that of S_2 . Obviously if S_1 has a better chance to transmit, the average throughput will decrease. In addition, if S_2 employs 4/16-QAM, the throughput of HZPNC will always be higher than that of OUS. However, if S_2 uses a much higher modulation scheme such as 4/256-QAM and this user also has a much higher access probability, the throughput of OUS will be higher than that of HZPNC, which is illustrated in the figure.

3.7 Conclusions

We have studied in this chapter two DF relaying schemes for two-way relay channels with asymmetric data rates, namely HZPNC and OUS. We analyzed both schemes where we derived closed-form expressions for the E2E BER performance. We also studied both schemes in terms of the access probability and throughput. We showed that each scheme offers certain advantages over the other. For instance, the HZPNC scheme offers better throughput, but this comes at the expense of degraded E2E BER performance as compared to that of OUS. On the other hand, the OUS scheme achieves better E2E BER performance, taking advantage of the multiuser diversity.

The pitfall of OUS, however, is the lack of fairness between the communicating users. That is, depending on the individual channel quality, one user may enjoy better access probability than the other. We also compared the performance of HZPNC with existing schemes, including the original zero padding, nesting constellation modulation and superposition modulation. We demonstrated the efficacy of the HZPNC scheme over all schemes in terms of the BER performance and/or complexity. Since these two schemes offer different advantages, it is natural to devise a hybrid scheme that combines these two schemes. This will be considered in next chapter.

Chapter 4

Hybrid Network Coding and Opportunistic User Selection (HNCOUS)

4.1 Introduction

To remedy the rate mismatch challenge without increasing the complexity or deteriorating the performance, we have proposed a HZPNC scheme in Chapter 3, which involves employing hierarchical modulation by the user with the higher data rate, while padding zeros at specific positions of the shorter bit sequence at the relay. We also considered another scheme which is referred to as OUS where the user with the better E2E channel quality is given priority for transmission. The OUS scheme improves E2E BER performance, taking advantage of the available multiuser diversity. The pitfall of OUS, however, is the lack of fairness between the communicating users. That is, depending on the individual channel quality, one user may enjoy better access probability than the other. This motivates us to design a new relaying strategy, which can improve fairness, while still exploiting multiuser diversity.

In this chapter, we propose an HNCOUS scheme that aims at taking advantage of both OUS and HZPNC. Specifically, the proposed scheme captures the multiuser diversity offered by OUS and

improves the throughput through HZPNC. For simplicity, we consider a relay network comprising two users and one relay. The two users are assumed to transmit at different data rates. To achieve fairness, the proposed scheme allows not only the user with the better E2E SNR to transmit but also the other user if the channel quality of this user is above a predetermined threshold. In addition, to improve the throughput, HZPNC is employed at the relay when both users transmit. Thus, when both users transmit, the relay XORs the signals received from the two users (over two time-slots) and forwards the resulting signal in the third time-slot. Since the two received sequences have different lengths, i.e., users have different rates, a certain form of zero padding is done at the relay to make the two sequences suitable for XORing.

We examine the performance of the proposed HNCOUS scheme on asymmetric independent Rayleigh fading channels. We derive closed form expressions for the E2E BER, access probability and throughput and compare it with HZPNC and OUS scheme. We also derive the asymptotic BER expression at high SNR and show that the maximum diversity order is achieved, which is the number of users. We also present several examples through which we validate the theoretical results.

The remainder of the chapter is organized as follows. The system model is presented in Section 4.2. In Section 4.3, the proposed HNCOUS scheme is presented. We analyze the E2E BER performance of the proposed scheme in Section 4.4. The diversity order of the proposed scheme is derived in Section 4.5, and we examine its performance in terms of access probability and throughput in Section 4.6. We present several numerical examples in Section 4.7, and conclude the chapter in Section 4.8.

4.2 System Model

We consider a bidirectional cooperative network with two users denoted by S_1 and S_2 , and one relay denoted by R , where the users communicate with each other via the relay node over orthogonal subchannels. For simplicity, we assume that there is no direct path between the two users. Both users and the relay are equipped with a single antenna and operate in a half-duplex mode. The two users have different data rates. In particular, we assume that one user uses 4-QAM and the other uses 16-QAM, but the scheme and analytical approach can be extended to other modulation schemes.¹

The network subchannels are assumed to experience independent slow and frequency non-selective Rayleigh fading. Let h_{ir}, h_{rj} for $i, j = 1, 2$ denote the fading coefficients for the following hops $S_i \rightarrow R, R \rightarrow S_j$, respectively. The subchannels are assumed to be independent and asymmetric, i.e., all the subchannels have different average SNRs, which is the most general case. Let γ_{ir}, γ_{rj} denote the instantaneous SNRs for the links $S_i \rightarrow R, R \rightarrow S_j$, respectively. To make the presentation simpler, we denote the instantaneous SNRs over different links by γ_{im} for $i, m = 1, 2$ where $\gamma_{11} = \gamma_{1r}, \gamma_{12} = \gamma_{r2}, \gamma_{21} = \gamma_{2r}$ and $\gamma_{22} = \gamma_{r1}$, i.e., index i refers to the user and m refers to the m th hop of that user. The pdf of γ_{im} is given as

$$f_{\gamma_{im}}(\gamma_{im}) = \frac{1}{\bar{\gamma}_{im}} e^{-\frac{1}{\bar{\gamma}_{im}} \gamma_{im}}, \quad (4.1)$$

where $\bar{\gamma}_{im} = \rho E[|h_{im}|^2]$ is the average SNR for the pertaining link and $\rho = \frac{E_b}{N_0}$. For DF relaying, the exact E2E instantaneous SNR of S_i is well approximated as $\gamma_i = \min(\gamma_{i1}, \gamma_{i2})$, and its pdf is expressed as

$$f_{\gamma_i}(\gamma_i) = \frac{1}{\bar{\gamma}_i} e^{-\frac{1}{\bar{\gamma}_i} \gamma_i}, \quad (4.2)$$

where $\bar{\gamma}_i = \frac{\bar{\gamma}_{i1}\bar{\gamma}_{i2}}{\bar{\gamma}_{i1} + \bar{\gamma}_{i2}}$. Thus, the E2E instantaneous SNR of S_i in this paper refers to $\gamma_i = \min(\gamma_{i1}, \gamma_{i2})$.

¹We merely use specific modulations in the development of the proposed adaptive scheme just for ease of presentation. The results obtained in this chapter are in fact independent of the modulation schemes employed.

4.3 Proposed HNCOUS Scheme

As mentioned above, the proposed HNCOUS scheme aims at improving the fairness by opportunistically allowing the second user to transmit although it has a worse channel. In particular, for a given threshold γ_{th} , if both instantaneous E2E SNRs are above γ_{th} , both users transmit and HZPNC is used; otherwise, the user with the better E2E SNR transmits while the other user remains silent. In this section, we describe the mode of operation in each case. Note that when $\gamma_{th} = 0$, the proposed adaptive transmission scheme reduces to the case when both users always transmit, i.e., HZPNC, whereas when $\gamma_{th} = \infty$, the proposed scheme reduces to the case when only the best user transmits, i.e., OUS.

4.3.1 Description of the HZPNC Scheme

When HZPNC is used, in the first two time-slots, the two sources transmit their signals in succession. The relay node decodes the two received signals, applies HZPNC to the decoded signals (after applying some form of zero padding if needed), and broadcasts the resulting signal to all nodes.

We assume that S_1 uses 4-QAM modulation and S_2 uses 16-QAM hierarchical modulation. The received bit sequences \hat{b}_i ($i = 1, 2$) corresponding to one symbol at the relay will not be equal in length. Since S_2 employs 4/16-QAM hierarchical modulation, \hat{b}_2 consists of 2 HP bits and 2 LP bits. Then the 2 bits of \hat{b}_1 are XORed with the 2 HP bits of \hat{b}_2 and the 2 LP bits of S_2 remain unchanged. The resulting bit sequence is then modulated by 4/16-QAM hierarchical modulation with the NC bits as HP bits and the unchanged bits as LP bits. The modulated signal x_r is then broadcasted to all nodes in the third time-slot. The signals received at the two users are expressed as $y_{ri} = \sqrt{4\rho}h_{ri}x_r + n_{ri}$ for $i = 1, 2$. These received signals can be decoded at their respective

destination using ML as

$$\hat{x}_r = \arg \min_{x_r \in \text{fictitious 4-QAM}} \left| y_{r2} - \sqrt{4\rho} h_{r2} x_r \right|,$$

and

$$\hat{x}_r = \arg \min_{x_r \in 4/16\text{-QAM}} \left| y_{r1} - \sqrt{4\rho} h_{r1} x_r \right|,$$

respectively. As shown above, since the data of S_1 at the relay is only involved with the HP bits of x_r , S_2 only needs to decode the HP bits, which correspond to a fictitious 4-QAM. Since each user knows its own transmitted signal, it can decode the desired signal according to the NC scheme used at the relay.

4.3.2 Description of the OUS Scheme

For this scheme, only the user with the better instantaneous E2E SNR transmits at a time. That is, if $\gamma_i > \gamma_j$ ($i, j = 1, 2$, s.t. $i \neq j$), only S_i transmits to S_j with the help of the relay. Let us assume that S_1 is selected as an example. So in the first time-slot, S_1 transmits to the relay. The received signal at the relay is $y_r = \sqrt{2\rho} h_{1r} x_1 + n_{1r}$. Then the relay decodes the received signal as

$$\hat{x}_1 = \arg \min_{x_1 \in 4\text{-QAM}} \left| y_r - \sqrt{2\rho} h_{1r} x_1 \right|.$$

The resulting sequence is then remodulated by the 4-QAM modulator. The modulated signal, denoted by x_r , is transmitted to S_2 in the second time-slot. The signal received by S_2 is $y_2 = \sqrt{2\rho} h_{r2} x_r + n_{r2}$. Then S_2 can decode the received signal as

$$\hat{x}_r = \arg \min_{x_r \in 4\text{-QAM}} \left| y_2 - \sqrt{2\rho} h_{r2} x_r \right|.$$

4.3.3 On the Optimal Threshold

As mentioned above, the threshold γ_{th} is employed to decide whether to allow both users or the user with the better E2E SNR to transmit. The criterion used to derive γ_{opt} , which is the optimal

threshold, is to minimize the worst E2E BER of the two users. For instance, the optimal threshold for S_i , denoted by γ_{opt} , can be obtained as

$$\gamma_{opt} = \arg \min_{\bar{\gamma}_{im}, \gamma_{th}} (P_i),$$

where the E2E BER of S_i , denoted by P_i , is a function of the average SNR and γ_{th} . Since the E2E BER expression for S_i is not invertible, the exact optimal thresholds can only be obtained by numerically minimizing the E2E BER with an exhaustive grid search [75], and this is the approach followed in this chapter. However, in Section 4.5, we give the optimal threshold function and verify it via simulations in Section 4.7. As far as implementation is concerned, we assume that a central controller in the network has the CSI of all links. It calculates the optimal thresholds and decides which transmission mode to use.

4.4 End-to-End BER Performance Analysis

In this section, we derive a closed-form expression for the E2E BER for the proposed HNCOUS scheme. We assume that S_1 employs 4-QAM and S_2 employs 4/16-QAM. However, the performance analysis can be extended to other hierarchical modulation schemes following the results of [43].

Lemma 4.1 *The E2E BER corresponding to user S_i can be expressed as*

$$P_i = \frac{2e^{-(\frac{1}{\bar{\gamma}_i} + \frac{1}{\bar{\gamma}_j})\gamma_{th}} P(\varepsilon_i | \min(\gamma_i, \gamma_j) > \gamma_{th})}{2e^{-(\frac{1}{\bar{\gamma}_i} + \frac{1}{\bar{\gamma}_j})\gamma_{th}} + 3\frac{\bar{\gamma}_i}{\bar{\gamma}_i + \bar{\gamma}_j} \left(1 - e^{-(\frac{1}{\bar{\gamma}_i} + \frac{1}{\bar{\gamma}_j})\gamma_{th}}\right)} + \frac{3\frac{\bar{\gamma}_i}{\bar{\gamma}_i + \bar{\gamma}_j} \left(1 - e^{-(\frac{1}{\bar{\gamma}_i} + \frac{1}{\bar{\gamma}_j})\gamma_{th}}\right) P(\varepsilon_i | \gamma_i > \gamma_j, \gamma_j < \gamma_{th})}{2e^{-(\frac{1}{\bar{\gamma}_i} + \frac{1}{\bar{\gamma}_j})\gamma_{th}} + 3\frac{\bar{\gamma}_i}{\bar{\gamma}_i + \bar{\gamma}_j} \left(1 - e^{-(\frac{1}{\bar{\gamma}_i} + \frac{1}{\bar{\gamma}_j})\gamma_{th}}\right)}, \quad (4.3)$$

where $P(\varepsilon_i | \min(\gamma_i, \gamma_j) > \gamma_{th})$ represents the E2E BER of S_i conditioned on $\min(\gamma_i, \gamma_j) > \gamma_{th}$, which is the E2E BER for S_i when using HZPNC, and $P(\varepsilon_i | \gamma_i > \gamma_j, \gamma_j < \gamma_{th})$ denotes the E2E BER of S_i conditioned on $\gamma_i > \gamma_j, \gamma_j < \gamma_{th}$, which is the E2E BER for S_i when using OUS.

Proof. See Appendix B. 1. ■

In what follows, we derive closed-form expressions for these probabilities. We will start with the expression $P(\varepsilon_i | \min(\gamma_i, \gamma_j) > \gamma_{th})$. According to the HZPNC scheme proposed in [1], the bits from S_1 are XORed with the HP bits from S_2 (assuming that S_1 uses 4-QAM and S_2 uses hierarchical 4/16-QAM). Consequently, S_2 decodes only the fictitious 4-QAM constellation of the hierarchical 4/16-QAM constellation. The E2E BER at S_2 conditioned on $\min(\gamma_i, \gamma_j) > \gamma_{th}$ is given as

$$\begin{aligned}
P(\varepsilon_1 | \min(\gamma_1, \gamma_2) > \gamma_{th}) &= \left(1 - P(\varepsilon_{r2}^{hp} | \gamma_{r2} > \gamma_{th})\right) \left[P(\varepsilon_{1r} | \gamma_{1r} > \gamma_{th}) \left(1 - P(\varepsilon_{2r}^{hp} | \gamma_{2r} > \gamma_{th})\right) \right. \\
&\quad \left. + P(\varepsilon_{2r}^{hp} | \gamma_{2r} > \gamma_{th}) (1 - P(\varepsilon_{1r} | \gamma_{1r} > \gamma_{th})) \right] \\
&\quad + P(\varepsilon_{r2}^{hp} | \gamma_{r2} > \gamma_{th}) \\
&\quad \cdot \left\{ 1 - \left[P(\varepsilon_{1r} | \gamma_{1r} > \gamma_{th}) \left(1 - P(\varepsilon_{2r}^{hp} | \gamma_{2r} > \gamma_{th})\right) \right. \right. \\
&\quad \left. \left. + P(\varepsilon_{2r}^{hp} | \gamma_{2r} > \gamma_{th}) (1 - P(\varepsilon_{1r} | \gamma_{1r} > \gamma_{th})) \right] \right\}, \tag{4.4}
\end{aligned}$$

where $P(\varepsilon_{2r}^{hp} | \gamma_{2r} > \gamma_{th})$ and $P(\varepsilon_{r2}^{hp} | \gamma_{r2} > \gamma_{th})$ are the probabilities of making an error over the $S_2 \rightarrow R$ and $R \rightarrow S_2$ links, conditioned on $\gamma_{2r} > \gamma_{th}$ and $\gamma_{r2} > \gamma_{th}$, respectively, for the HP bits from S_2 ; $P(\varepsilon_{1r} | \gamma_{1r} > \gamma_{th})$ is the BER over the $S_1 \rightarrow R$ link, conditioned on $\gamma_{1r} > \gamma_{th}$, for the bits from S_1 . Since $\gamma_i = \min(\gamma_{i1}, \gamma_{i2})$, $\min(\gamma_i, \gamma_j) > \gamma_{th}$ is equivalent to $\gamma_{i1} > \gamma_{th}$, $\gamma_{i2} > \gamma_{th}$, $\gamma_{j1} > \gamma_{th}$, $\gamma_{j2} > \gamma_{th}$. The instantaneous SNRs of different links are independent, therefore the BERs over different links are only related to the instantaneous SNR of their respective links. Thus, we only remain the effective items in the condition of (4.4).

Lemma 4.2 *The BER over any of the links employing 4-QAM modulation and for the HP bits from S_2 conditioned on $\gamma_{im} > \gamma_{th}$ can be expressed as*

$$P(\varepsilon_{im} | \gamma_{im} > \gamma_{th}) = e^{\frac{1}{\bar{\gamma}_{im}} \gamma_{th}} I(1, \bar{\gamma}_{im}, \gamma_{th}, \infty), \tag{4.5}$$

and

$$P(\varepsilon_{im}^{hp} | \gamma_{im} > \gamma_{th}) = \frac{1}{2} e^{\frac{1}{\bar{\gamma}_{im}} \gamma_{th}} \left[I\left(\frac{2(d^2 - 2d + 1)}{1 + d^2}, \bar{\gamma}_{im}, \gamma_{th}, \infty\right) + I\left(\frac{2(d^2 + 2d + 1)}{1 + d^2}, \bar{\gamma}_{im}, \gamma_{th}, \infty\right) \right], \quad (4.6)$$

where [76]

$$\begin{aligned} I(a, b, \gamma_{thl}, \gamma_{th(l+1)}) &= \int_{\gamma_{thl}}^{\gamma_{th(l+1)}} \frac{1}{2} \operatorname{erfc} \sqrt{a\gamma} \frac{1}{b} e^{-\frac{1}{b}\gamma} d\gamma \\ &= \frac{1}{2} e^{-\frac{1}{b}\gamma_{thl}} \operatorname{erfc} \sqrt{a\gamma_{thl}} - \frac{1}{2} \sqrt{\frac{ab}{1+ab}} \operatorname{erfc} \sqrt{\gamma_{thl} \left(a + \frac{1}{b}\right)} \\ &\quad - \frac{1}{2} e^{-\frac{1}{b}\gamma_{th(l+1)}} \operatorname{erfc} \sqrt{a\gamma_{th(l+1)}} + \frac{1}{2} \sqrt{\frac{ab}{1+ab}} \operatorname{erfc} \sqrt{\gamma_{th(l+1)} \left(a + \frac{1}{b}\right)}. \end{aligned}$$

Proof. See Appendix B. 2. ■

Note that $P(\varepsilon_{1r} | \gamma_{1r} > \gamma_{th}) = P(\varepsilon_{11} | \gamma_{11} > \gamma_{th})$, $P(\varepsilon_{2r}^{hp} | \gamma_{2r} > \gamma_{th}) = P(\varepsilon_{21}^{hp} | \gamma_{21} > \gamma_{th})$ and $P(\varepsilon_{r2}^{hp} | \gamma_{r2} > \gamma_{th}) = P(\varepsilon_{12}^{hp} | \gamma_{12} > \gamma_{th})$. Plugging these expressions into (4.4) yields a closed-form expression for $P(\varepsilon_1 | \min(\gamma_1, \gamma_2) > \gamma_{th})$.

Now for the BER at S_1 , recall that the bits coming from S_2 consist of HP and LP bits. The HP bits are XORed with the bits from S_1 and the LP bits are relayed without NC. As such, the E2E BER at S_1 is obtained as

$$P(\varepsilon_2 | \min(\gamma_1, \gamma_2) > \gamma_{th}) = \frac{1}{2} (P(\varepsilon_2^{hp} | \min(\gamma_1, \gamma_2) > \gamma_{th}) + P(\varepsilon_2^{lp} | \min(\gamma_1, \gamma_2) > \gamma_{th})), \quad (4.7)$$

where $P(\varepsilon_2^{hp} | \min(\gamma_1, \gamma_2) > \gamma_{th})$ and $P(\varepsilon_2^{lp} | \min(\gamma_1, \gamma_2) > \gamma_{th})$ represent the E2E BER of the HP and LP bits conditioned on $\min(\gamma_1, \gamma_2) > \gamma_{th}$, respectively. Now $P(\varepsilon_2^{hp} | \min(\gamma_1, \gamma_2) > \gamma_{th})$ can

be expressed as

$$\begin{aligned}
P(\varepsilon_2^{hp} | \min(\gamma_1, \gamma_2) > \gamma_{th}) &= \left(1 - P(\varepsilon_{r1}^{hp} | \gamma_{r1} > \gamma_{th}) \right) \\
&\cdot \left[P(\varepsilon_{1r} | \gamma_{1r} > \gamma_{th}) \left(1 - P(\varepsilon_{2r}^{hp} | \gamma_{2r} > \gamma_{th}) \right) \right. \\
&+ \left. P(\varepsilon_{2r}^{hp} | \gamma_{2r} > \gamma_{th}) \left(1 - P(\varepsilon_{1r} | \gamma_{1r} > \gamma_{th}) \right) \right] \\
&+ P(\varepsilon_{r1}^{hp} | \gamma_{r1} > \gamma_{th}) \\
&\cdot \left\{ 1 - \left[P(\varepsilon_{1r} | \gamma_{1r} > \gamma_{th}) \left(1 - P(\varepsilon_{2r}^{hp} | \gamma_{2r} > \gamma_{th}) \right) \right. \right. \\
&\left. \left. + P(\varepsilon_{2r}^{hp} | \gamma_{2r} > \gamma_{th}) \left(1 - P(\varepsilon_{1r} | \gamma_{1r} > \gamma_{th}) \right) \right] \right\}, \quad (4.8)
\end{aligned}$$

where $P(\varepsilon_{1r} | \gamma_{1r} > \gamma_{th})$ and $P(\varepsilon_{2r}^{hp} | \gamma_{2r} > \gamma_{th})$ are defined above. When $i = m = 2$, we have $P(\varepsilon_{r1}^{hp} | \gamma_{r1} > \gamma_{th}) = P_{22}^{hp}(\gamma_{22} > \gamma_{th})$. Having found expressions for all the terms in (4.8), we can easily find a closed-form expression for $P(\varepsilon_2^{hp} | \min(\gamma_1, \gamma_2) > \gamma_{th})$.

Concerning the LP bits, since they are relayed without NC, the corresponding E2E BER is given by

$$\begin{aligned}
P(\varepsilon_2^{lp} | \min(\gamma_1, \gamma_2) > \gamma_{th}) &= P(\varepsilon_{2r}^{lp} | \gamma_{2r} > \gamma_{th}) (1 - P(\varepsilon_{r1}^{lp} | \gamma_{r1} > \gamma_{th})) \\
&+ P(\varepsilon_{r1}^{lp} | \gamma_{r1} > \gamma_{th}) (1 - P(\varepsilon_{2r}^{lp} | \gamma_{2r} > \gamma_{th})). \quad (4.9)
\end{aligned}$$

Lemma 4.3 *The BER of the LP bits over any of the links conditioned on $\gamma_{im} > \gamma_{th}$ can be expressed as*

$$\begin{aligned}
P(\varepsilon_{im}^{lp} | \gamma_{im} > \gamma_{th}) &= e^{\frac{1}{\bar{\gamma}_{im}} \gamma_{th}} \left[I \left(\frac{2}{1+d^2}, \bar{\gamma}_{im}, \gamma_{th}, \infty \right) + \frac{1}{2} I \left(\frac{2(4d^2 - 4d + 1)}{1+d^2}, \bar{\gamma}_{im}, \gamma_{th}, \infty \right) \right. \\
&\left. - \frac{1}{2} I \left(\frac{2(4d^2 + 4d + 1)}{1+d^2}, \bar{\gamma}_{im}, \gamma_{th}, \infty \right) \right]. \quad (4.10)
\end{aligned}$$

Proof. See Appendix B. 3. ■

By setting $i = m = 2$ in (4.10), we obtain $P_{r1}^{lp}(\gamma_{r1} > \gamma_{th}) = P_{22}^{lp}(\gamma_{22} > \gamma_{th})$. We can similarly obtain $P(\varepsilon_{2r}^{lp} | \gamma_{2r} > \gamma_{th}) = P(\varepsilon_{21}^{lp} | \gamma_{21} > \gamma_{th})$. These expressions lead to a closed-form expression for $P(\varepsilon_2^{lp} | \min(\gamma_1, \gamma_2) > \gamma_{th})$. Having obtained expressions for $P(\varepsilon_2^{hp} | \min(\gamma_1, \gamma_2) > \gamma_{th})$ and

$P(\varepsilon_2^{lp} | \min(\gamma_1, \gamma_2) > \gamma_{th}), P(\varepsilon_2 | \min(\gamma_1, \gamma_2) > \gamma_{th})$ is obtained by plugging $P(\varepsilon_2^{hp} | \min(\gamma_1, \gamma_2) > \gamma_{th})$ and $P(\varepsilon_2^{lp} | \min(\gamma_1, \gamma_2) > \gamma_{th})$ into (4.7).

Now we derive a closed-form expression for $P(\varepsilon_i | \gamma_i > \gamma_j, \gamma_j < \gamma_{th})$ given in (4.3). This corresponds to the OUS scheme, for which if the instantaneous E2E SNR of S_i is greater than that of S_j , where $i \neq j$, only S_i transmits to S_j . Thus, when either the $S_i \rightarrow R$ or $R \rightarrow S_j$ link is in error, the received signal at S_j will be in error. Therefore, the E2E BER of S_i given $\gamma_i > \gamma_j, \gamma_j < \gamma_{th}$ can be expressed as

$$\begin{aligned} & P(\varepsilon_i | \gamma_i > \gamma_j, \gamma_j < \gamma_{th}) \\ &= P(\varepsilon_{im} | \gamma_i > \gamma_j, \gamma_j < \gamma_{th})(1 - P(\varepsilon_{in} | \gamma_i > \gamma_j, \gamma_j < \gamma_{th})) \\ & \quad + P(\varepsilon_{in} | \gamma_i > \gamma_j, \gamma_j < \gamma_{th})(1 - P(\varepsilon_{im} | \gamma_i > \gamma_j, \gamma_j < \gamma_{th})), \end{aligned} \quad (4.11)$$

where $i, j, n, m = 1, 2$, and $i \neq j, m \neq n$.

Lemma 4.4 For M -QAM modulation, the BER over any of the links can be expressed as

$$\begin{aligned} P(\varepsilon_{im} | \gamma_i > \gamma_j, \gamma_j < \gamma_{th}) &= \frac{1}{\sqrt{M} \log_2 \sqrt{M}} \sum_{k=1}^{\log_2 \sqrt{M} (1-2^{-k})\sqrt{M}-1} \sum_{i=0}^{i \cdot 2^{k-1}} \\ & \quad (-1)^{\lfloor \frac{i \cdot 2^{k-1}}{\sqrt{M}} \rfloor} \times \left(2^{k-1} - \left\lfloor \frac{i \cdot 2^{k-1}}{\sqrt{M}} + \frac{1}{2} \right\rfloor \right) \\ & \quad \cdot \left\{ \frac{\bar{\gamma}_{in}(\bar{\gamma}_i + \bar{\gamma}_j)}{\bar{\gamma}_{im}\bar{\gamma}_i(\bar{\gamma}_{in} + \bar{\gamma}_j) \left(1 - e^{-\left(\frac{1}{\bar{\gamma}_i} + \frac{1}{\bar{\gamma}_j}\right)\gamma_{th}} \right)} \right. \\ & \quad \cdot \left[\bar{\gamma}_{im} I_1 \left(\frac{3 \log_2^M (2i+1)^2}{2(M-1)}, \bar{\gamma}_{im}, \gamma_{th} \right) \right. \\ & \quad \left. \left. - \frac{\bar{\gamma}_i \bar{\gamma}_j}{\bar{\gamma}_i + \bar{\gamma}_j} I_1 \left(\frac{3 \log_2^M (2i+1)^2}{2(M-1)}, \frac{\bar{\gamma}_i \bar{\gamma}_j}{\bar{\gamma}_i + \bar{\gamma}_j}, \gamma_{th} \right) \right] \right. \\ & \quad \left. + \left[\frac{\bar{\gamma}_{in}(\bar{\gamma}_i + \bar{\gamma}_j) \left(1 - e^{-\left(\frac{1}{\bar{\gamma}_{in}} + \frac{1}{\bar{\gamma}_j}\right)\gamma_{th}} \right)}{\bar{\gamma}_{im}\bar{\gamma}_i(\bar{\gamma}_{in} + \bar{\gamma}_j) \left(1 - e^{-\left(\frac{1}{\bar{\gamma}_i} + \frac{1}{\bar{\gamma}_j}\right)\gamma_{th}} \right)} \bar{\gamma}_{im} \right. \right. \\ & \quad \left. \left. \cdot I \left(\frac{3 \log_2^M (2i+1)^2}{2(M-1)}, \bar{\gamma}_{im}, \gamma_{th} \right) \right] \right\}, \end{aligned} \quad (4.12)$$

Note that for our case, $M = 4$ for S_1 and 16 for S_2 .

Proof. See Appendix B. 4. ■

Note that $P_{e,1r} = P(\varepsilon_{11} | \gamma_1 > \gamma_2, \gamma_2 < \gamma_{th})$, $P_{e,r2} = P(\varepsilon_{12} | \gamma_1 > \gamma_2, \gamma_2 < \gamma_{th})$, $P_{e,2r} = P(\varepsilon_{21} | \gamma_2 > \gamma_1, \gamma_1 < \gamma_{th})$ and $P_{e,r1} = P(\varepsilon_{22} | \gamma_2 > \gamma_1, \gamma_1 < \gamma_{th})$. Plugging these expressions into (4.11) yields a closed-form expression for $P(\varepsilon_i | \gamma_i > \gamma_j, \gamma_j < \gamma_{th})$.

4.5 Achievable Diversity Order

While the BER performance expressions derived above are exact, they do not yield the diversity order achieved. In this section, we derive the corresponding asymptotic expressions at high SNR to show the achievable diversity order. For simplicity, we assume symmetric channels, i.e., all the channel gains are modeled as zero mean, unit variance complex Gaussian random variables, and $d = 2$ since the diversity order does not change with the channel setting and modulation scheme, as demonstrated in [77].

With the assumption made above, it is easy to obtain that $\bar{\gamma}_i = \bar{\gamma}_j = \frac{1}{2}\rho$. Since S_2 uses a higher modulation scheme than that of S_1 , the E2E BER of S_2 is worse than that of S_1 . Then according to (4.3), we have

$$P_1 \leq P_2 = \frac{P_2^1 + P_2^2}{2e^{-\frac{4}{\rho}\gamma_{th}} + \frac{3}{2}(1 - e^{-\frac{4}{\rho}\gamma_{th}})} \leq \frac{P_2^1 + P_2^2}{2}, \quad (4.13)$$

where $P_2^1 = 2e^{-\frac{4}{\rho}\gamma_{th}}P(\varepsilon_2 | \min(\gamma_1, \gamma_2) > \gamma_{th})$ and $P_2^2 = \frac{3}{2}(1 - e^{-\frac{4}{\rho}\gamma_{th}})P(\varepsilon_2 | \gamma_2 > \gamma_1, \gamma_1 < \gamma_{th})$.

Now we can upper bound P_2^1 as

$$\begin{aligned}
P_2^1 &\leq 2 \left[\frac{1}{2} (P(\varepsilon_2^{hp} | \min(\gamma_1, \gamma_2) > \gamma_{th}) + P(\varepsilon_2^{lp} | \min(\gamma_1, \gamma_2) > \gamma_{th})) \right] \\
&\leq P(\varepsilon_{im} | \gamma_{im} > \gamma_{th}) + 2P(\varepsilon_{im}^{hp} | \gamma_{im} > \gamma_{th}) + 2P(\varepsilon_{im}^{lp} | \gamma_{im} > \gamma_{th}) \\
&\leq e^{\frac{1}{\rho}\gamma_{th}} \int_{\gamma_{th}}^{\infty} \left(\frac{1}{2} \operatorname{erfc} \sqrt{\frac{2}{5}\gamma_{im}} + \operatorname{erfc} \sqrt{\frac{2}{5}\gamma_{im}} + \frac{3}{2} \operatorname{erfc} \sqrt{\frac{2}{5}\gamma_{im}} \right) \frac{1}{\rho} e^{-\frac{1}{\rho}\gamma_{im}} d\gamma_{im} \\
&\leq e^{\frac{1}{\rho}\gamma_{th}} \int_{\gamma_{th}}^{\infty} \frac{3}{2} e^{-\frac{2}{5}\gamma_{im}} \frac{1}{\rho} e^{-\frac{1}{\rho}\gamma_{im}} d\gamma_{im} \tag{4.14}
\end{aligned}$$

$$\leq \frac{15}{4\rho} e^{-\frac{2}{5}\gamma_{th}}, \tag{4.15}$$

where (4.14) follows from $\operatorname{erfc}\sqrt{x} \leq \frac{1}{2}e^{-x}$. Similarly, P_2^2 can be upper bounded as

$$\begin{aligned}
P_2^2 &\leq 3 \left(1 - e^{-\frac{4}{\rho}\gamma_{th}} \right) P(\varepsilon_{im} | \gamma_2 > \gamma_1, \gamma_1 < \gamma_{th}) \\
&\leq \left(1 - e^{-\frac{4}{\rho}\gamma_{th}} \right) \int_0^{\infty} \frac{15}{8} \operatorname{erfc} \sqrt{\frac{2}{5}\gamma_{im}} f_{\gamma_{im} | \gamma_i > \gamma_j, \gamma_j < \gamma_{th}}(\gamma_{im}) d\gamma_{im} \\
&\leq \left(1 - e^{-\frac{4}{\rho}\gamma_{th}} \right) \int_0^{\infty} \frac{15}{16} e^{-\frac{2}{5}\gamma_{im}} f_{\gamma_{im} | \gamma_i > \gamma_j, \gamma_j < \gamma_{th}}(\gamma_{im}) d\gamma_{im} \\
&\leq P_2^{21} + P_2^{22},
\end{aligned}$$

where

$$P_2^{21} = \left(1 - e^{-\frac{4}{\rho}\gamma_{th}} \right) \int_0^{\gamma_{th}} \frac{15}{16} e^{-\frac{2}{5}\gamma_{im}} f_{\gamma_{im} | \gamma_i > \gamma_j, \gamma_j < \gamma_{th}}(\gamma_{im}) d\gamma_{im}, \tag{4.16}$$

and

$$P_2^{22} = \left(1 - e^{-\frac{4}{\rho}\gamma_{th}} \right) \int_{\gamma_{th}}^{\infty} \frac{15}{16} e^{-\frac{2}{5}\gamma_{im}} f_{\gamma_{im} | \gamma_i > \gamma_j, \gamma_j < \gamma_{th}}(\gamma_{im}) d\gamma_{im}. \tag{4.17}$$

Plugging (B.26) into (4.16), we have

$$\begin{aligned}
P_2^{21} &= \int_0^{\gamma_{th}} \frac{15}{16} \frac{4}{3\rho} e^{-\frac{2}{5}\gamma_{im}} \left(e^{-\frac{1}{\rho}\gamma_{im}} - e^{-\frac{4}{\rho}\gamma_{im}} \right) d\gamma_{im} \\
&\leq \int_0^{\infty} \frac{5}{4\rho} e^{-\frac{2}{5}\gamma_{im}} \left(e^{-\frac{1}{\rho}\gamma_{im}} - e^{-\frac{4}{\rho}\gamma_{im}} \right) d\gamma_{im} \\
&= \frac{15}{4\rho^2 \left(\frac{2}{5} + \frac{1}{\rho} \right) \left(\frac{2}{5} + \frac{4}{\rho} \right)} \tag{4.18}
\end{aligned}$$

$$\leq \frac{375}{16\rho^2}, \tag{4.19}$$

where (4.18) follows from Equation B.1 in [43]. Plugging (B.25) into (4.17), we have

$$\begin{aligned}
P_2^{22} &= e^{\frac{1}{\rho}\gamma_{th}} \int_{\gamma_{th}}^{\infty} \frac{15}{16} \frac{4}{3\rho} e^{-\frac{2}{5}\gamma_{im}} \left(1 - e^{-\frac{3}{\rho}\gamma_{th}} \right) e^{-\frac{1}{\rho}\gamma_{th}} e^{-\frac{1}{\rho}\gamma_{im}} d\gamma_{im} \\
&\leq e^{\frac{1}{\rho}\gamma_{th}} \int_{\gamma_{th}}^{\infty} \frac{5}{4\rho} e^{-\frac{2}{5}\gamma_{im}} e^{-\frac{1}{\rho}\gamma_{im}} d\gamma_{im} \\
&\leq \frac{25}{8\rho} e^{-\frac{2}{5}\gamma_{th}}. \tag{4.20}
\end{aligned}$$

Plugging (4.15), (4.19) and (4.20) into (4.13), we have

$$P_1 \leq \frac{15}{4\rho} e^{-\frac{2}{5}\gamma_{th}} + \frac{375}{16\rho^2} + \frac{25}{8\rho} e^{-\frac{2}{5}\gamma_{th}} = \frac{55}{8\rho} e^{-\frac{2}{5}\gamma_{th}} + \frac{375}{16\rho^2}. \tag{4.21}$$

As mentioned before, the threshold γ_{th} is a function of ρ . Based on the insight from the asymptotic BER expression derived above, we plug $\gamma_{th} = n \log(c\rho)$ for some constants n and c into (4.21), which yields

$$P_1 \leq \frac{55}{8\rho} e^{-\frac{2}{5} \times n \log(c\rho)} + \frac{375}{16\rho^2} = \frac{55}{8c^{\frac{2}{5}n} \rho^{\frac{2}{5}n+1}} + \frac{375}{16\rho^2} = O(\rho^{-2}), \tag{4.22}$$

for $n \geq 2.5$. Therefore, we conclude that our proposed scheme achieves full diversity which is the number of available users. It is also confirmed through simulations in Section 4.7 that the exact optimal threshold function for the case when S_1 employs 4-QAM and S_2 employs 4/16-QAM is in fact in the form of $5 \log(c\rho)$, which leads to full diversity according to (4.22).

4.6 Access Probability and Throughput

In this section, we analyze the proposed HNCOUS scheme in terms of the access probability and throughput and compare it with those of the HZPNC and OUS schemes individually.

4.6.1 Access Probability

According to the HZPNC scheme [37], both users transmit via channel sharing. The two users communicate with each other over three time-slots. During the three time-slots, each user occupies two time-slots with one time-slot overlapping. Then the access probability is $\frac{2}{3}$ for the HZPNC case. As for the OUS scheme, a user transmits once its instantaneous E2E SNR is greater than that of the other one, resulting in an access probability of

$$P_i^{OUS} = P_r(\gamma_i > \gamma_j) = \frac{\bar{\gamma}_i}{\bar{\gamma}_i + \bar{\gamma}_j}. \quad (4.23)$$

For symmetric channels, for example, the average E2E SNRs for both users are the same, i.e., $\bar{\gamma}_i = \bar{\gamma}_j$, suggesting that both users will have the same access probability, i.e., $P_i^{OUS} = 0.5$. According to the proposed scheme, a user transmits once its instantaneous E2E SNR is larger than the other one and the instantaneous E2E SNR of the worse user is below a predetermined threshold γ_{th} or both instantaneous E2E SNRs of the two users are above γ_{th} . So the probability that S_i transmits can be expressed as

$$\begin{aligned} P_i^{proposed} &= P_r(\gamma_i > \gamma_j, \gamma_j < \gamma_{th}) \times 1 + P_r(\min(\gamma_i, \gamma_j) > \gamma_{th}) \times \frac{2}{3} \\ &= \frac{\bar{\gamma}_i}{\bar{\gamma}_i + \bar{\gamma}_j} + \left[\frac{2}{3} - \frac{\bar{\gamma}_i}{\bar{\gamma}_i + \bar{\gamma}_j} \right] e^{-(\frac{1}{\bar{\gamma}_i} + \frac{1}{\bar{\gamma}_j})\gamma_{th}}. \end{aligned} \quad (4.24)$$

Now define ΔP_i as

$$\begin{aligned} \Delta P_i &\triangleq P_i^{proposed} - P_i^{OUS} \\ &= \left[\frac{2}{3} - \frac{\bar{\gamma}_i}{\bar{\gamma}_i + \bar{\gamma}_j} \right] e^{-(\frac{1}{\bar{\gamma}_i} + \frac{1}{\bar{\gamma}_j})\gamma_{th}}, \end{aligned} \quad (4.25)$$

which represents the access probability difference between the two schemes. When the channels are symmetric, the average E2E SNRs are the same, i.e., $\bar{\gamma}_i = \bar{\gamma}_j$. Therefore, our proposed scheme offers a higher access probability than that of OUS for each user by $\frac{1}{6}e^{-(\frac{1}{\bar{\gamma}_i} + \frac{1}{\bar{\gamma}_j})\gamma_{th}}$. As for asymmetric channels, solving $\frac{2}{3} - \frac{\bar{\gamma}_i}{\bar{\gamma}_i + \bar{\gamma}_j} > 0$, we obtain $\frac{\bar{\gamma}_i}{\bar{\gamma}_j} < 2$, which is the range for which the proposed scheme has a higher access probability compared to that of the OUS scheme for both users. Beyond this range, one user of the OUS scheme will have a higher access probability than those of our proposed scheme, whereas the other one will have a lower access probability.

4.6.2 Throughput

We do the throughput analysis for the general case where it is assumed that S_1 uses 2^{2s} -QAM and S_2 uses $2^{2s}/2^{2r}$ -QAM hierarchical modulation for $s = 1, 2, \dots, r-1$, and $r = 2, 3, \dots, R$. The throughput of our proposed scheme can be written as

$$\begin{aligned} T^{proposed} &= T^{HZPNC} \times P_r(\min(\gamma_1, \gamma_2) > \gamma_{th}) \\ &\quad + T^{OUS} \times [P_r(\gamma_1 > \gamma_2, \gamma_2 < \gamma_{th}) + P_r(\gamma_2 > \gamma_1, \gamma_1 < \gamma_{th})], \end{aligned} \quad (4.26)$$

where T^{OUS} and T^{HZPNC} are the throughputs of OUS and HZPNC, respectively, which are given as

$$T^{OUS} = \frac{\bar{\gamma}_1}{\bar{\gamma}_1 + \bar{\gamma}_2} s + \frac{\bar{\gamma}_2}{\bar{\gamma}_1 + \bar{\gamma}_2} r \text{ bits/time slot}, \quad (4.27)$$

and

$$T^{HZPNC} = \frac{2s + 2r}{3} \text{ bits/time slot}, \quad (4.28)$$

where we assume that S_1 uses 2^{2s} -QAM modulation and S_2 uses $2^{2s}/2^{2r}$ -QAM hierarchical modulation. Plugging (4.27), (4.28), (B.4) and (B.5) into (4.26), we obtain

$$\begin{aligned} T^{proposed} &= e^{-(\frac{1}{\bar{\gamma}_1} + \frac{1}{\bar{\gamma}_2})\gamma_{th}} \frac{2s + 2r}{3} \\ &\quad + (1 - e^{-(\frac{1}{\bar{\gamma}_1} + \frac{1}{\bar{\gamma}_2})\gamma_{th}}) \left(\frac{\bar{\gamma}_1}{\bar{\gamma}_1 + \bar{\gamma}_2} s + \frac{\bar{\gamma}_2}{\bar{\gamma}_1 + \bar{\gamma}_2} r \right) \text{ bits/time slot}. \end{aligned} \quad (4.29)$$

We know that, in general, HZPNC has a higher throughput than that of OUS [37]. Thus the throughput of the proposed scheme has a higher throughput than that of OUS. However, in the extreme case when one user has a much higher order modulation scheme and a higher access probability than those of the other user, OUS will have a higher throughput than HZPNC. In this unlikely case, OUS will also have a higher throughput than that of our proposed scheme.

4.7 Simulation Results

We present in this section numerical examples that aim at validating the E2E BER expressions derived for the proposed HNCOUS scheme. In addition, we compare our proposed scheme with HZPNC and OUS in terms of the E2E BER, access probability and throughput. Throughout the simulations, we assume that S_1 uses 4-QAM and S_2 uses 4/16-QAM hierarchical modulation, and $d = 2$.

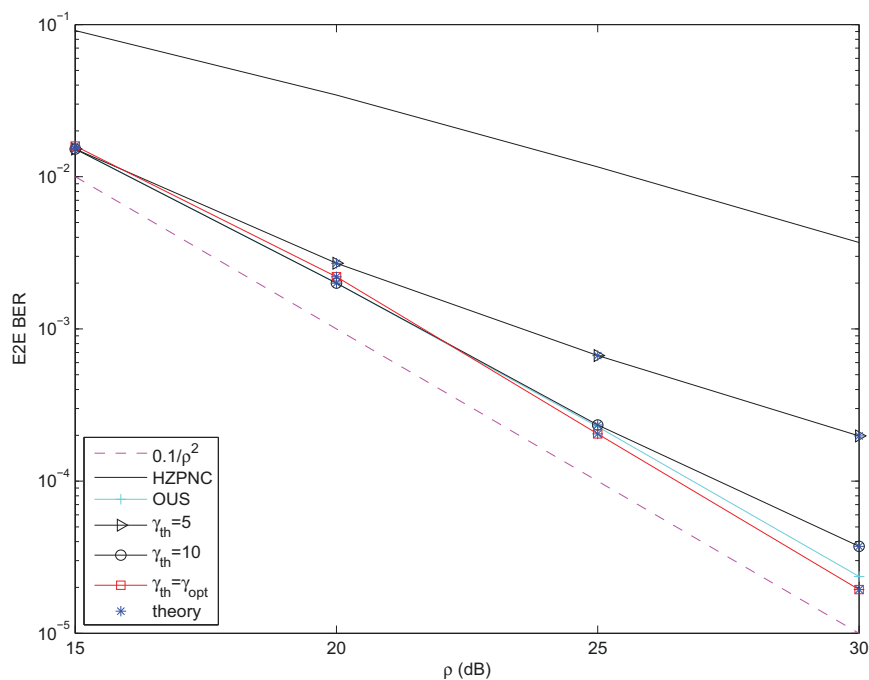


Figure 4.1: E2E BER performance (simulated and theoretical) of our proposed adaptive transmission scheme over symmetric channels.

In Fig. 4.1, we compare the derived theoretical results to the simulation results over symmetric channels with different thresholds for S_1 . In our simulations, we set the variances of the channel coefficients to $\frac{1}{4}$. We consider the cases: $\gamma_{th} = 5, 10$. We also plot three particular cases, namely HZPNC (i.e. $\gamma_{th} = 0$), OUS (i.e. $\gamma_{th} = \infty$) and $\gamma_{th} = \gamma_{opt}$ where $\gamma_{opt} = [4 \ 6.9 \ 13.2 \ 18.5]$ which is obtained numerically by minimizing the worst E2E BER of the two users. We also include the curve obtained by using $\frac{0.1}{\rho^2}$, which is used as a benchmark. We can see from the figure that the performance improves as the threshold increases from 0 to 10. We also see the perfect match between theory and simulations, which validates the derived BER for symmetric channels. Furthermore, we can see that the performance of our proposed HNCOUS scheme with $\gamma_{th} = \gamma_{opt}$ is slightly better than that of OUS. Finally, by comparing the slopes of the curves, we observe that our proposed HNCOUS scheme achieves diversity gain two.

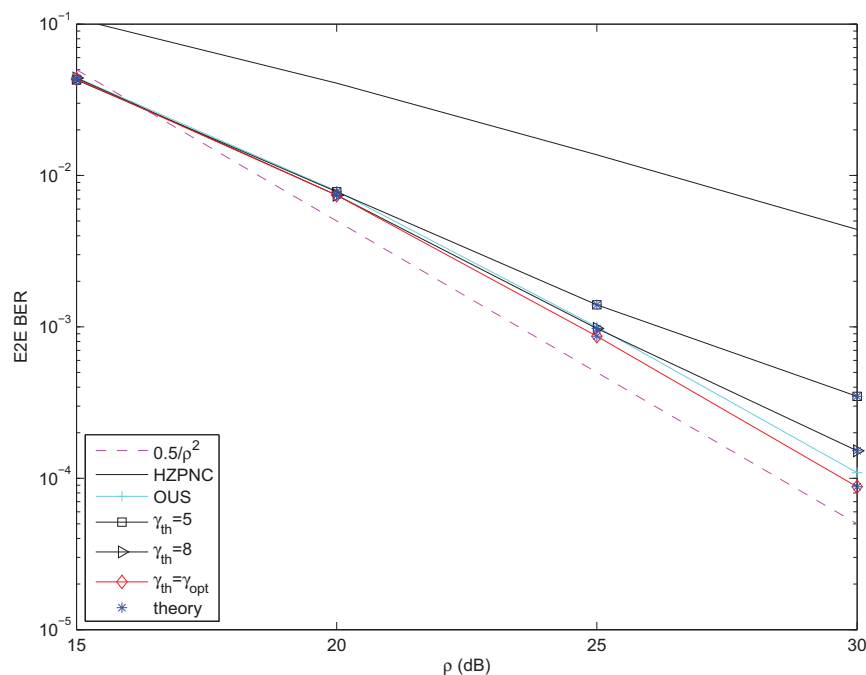


Figure 4.2: E2E BER performance (simulated and theoretical) of our proposed adaptive transmission scheme over symmetric channels.

The E2E BER performance for S_2 is shown in Fig. 4.2, with similar observations. As shown in

the figure, the E2E BER performance for S_2 with γ_{opt} is also slightly better than that of OUS and achieves diversity gain two.

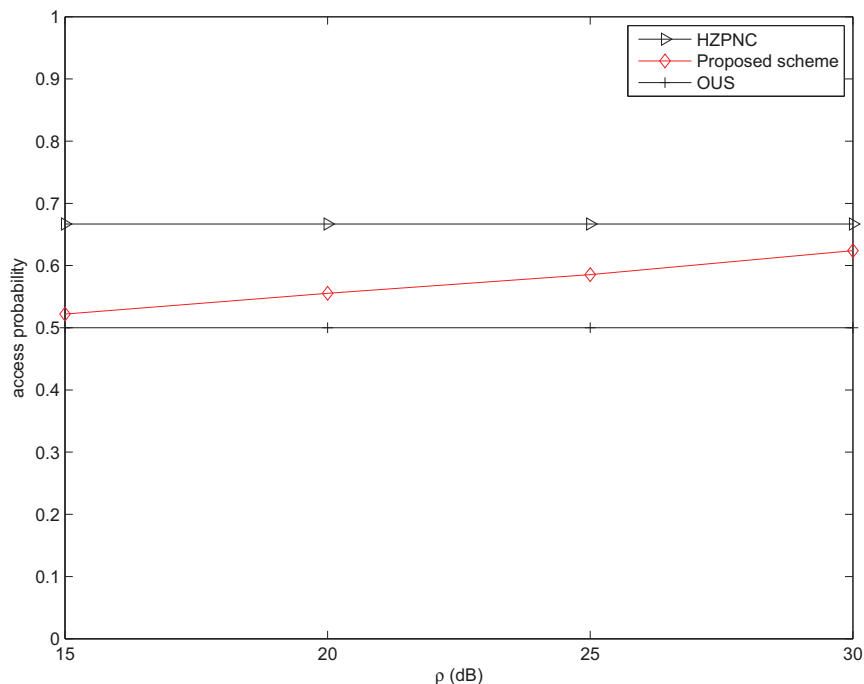


Figure 4.3: Access probability of HZPNC, OUS and our proposed adaptive transmission scheme corresponding to Figs. 4.1 and 4.2.

In Fig. 4.3, we present the access probability for HZPNC, OUS and our proposed HNCOUS scheme with the optimal thresholds corresponding to Figs. 4.1 and 4.2. Since the channels are symmetric, the two users have the same access probability for OUS, which is 0.5. We can see that the access probability of our proposed HNCOUS scheme falls between that of HZPNC and OUS, as expected. It is also shown, however, that the access probability for the proposed scheme is close to that of OUS at low SNRs and approaches that of HZPNC as SNR increases. This is attributed to the fact that, as SNR increases, it is more likely that both channels are in a good state, leading to using HZPNC more often.

In Fig. 4.4, we present the throughput for HZPNC, OUS and our proposed HNCOUS scheme with the optimal thresholds corresponding to Figs. 4.1 and 4.2. It is shown that our proposed

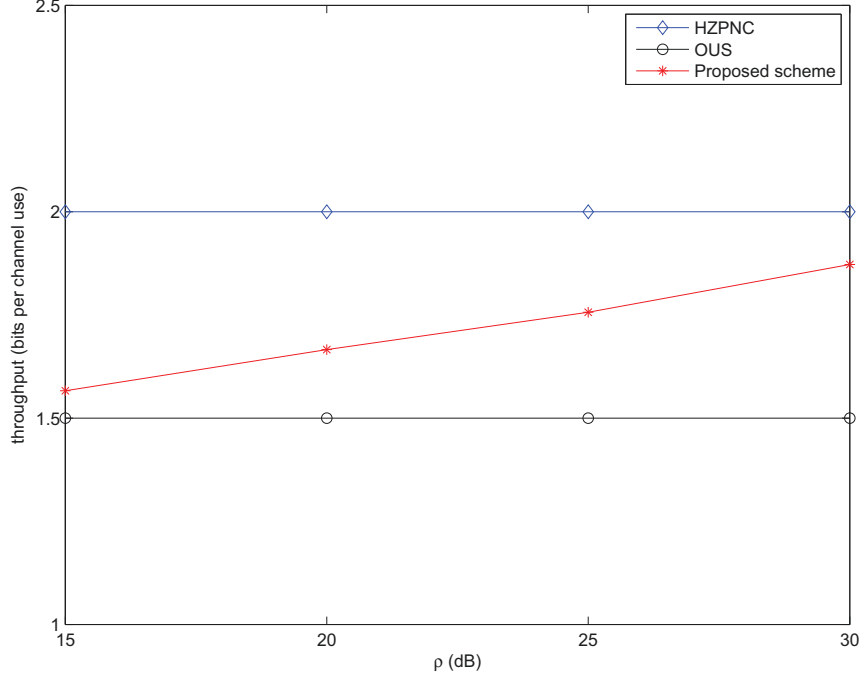


Figure 4.4: Throughput of HZPNC, OUS and our proposed adaptive transmission scheme corresponding to Figs. 4.1 and 4.2.

scheme has a higher throughput than that of OUS, as expected, but this throughput approaches that of HZPNC at high SNRs, which follows the behavior of the access probability reported in Fig. 4.3.

In Fig. 4.5, we compare the performance of our proposed scheme with OUS for asymmetric channels. In our simulations, we set the variances of the channel coefficients for the $S_1 - R$, $R - S_2$, $S_2 - R$ and $R - S_1$ links to $\frac{1}{2}$, $\frac{1}{2}$, $\frac{1}{4}$ and 1, respectively. We numerically obtain the optimal thresholds. The optimal thresholds are $\gamma_{opt} = [6.5 \ 9 \ 15.3 \ 21]$ for $\rho = [15 \ 20 \ 25 \ 30]$. We see the perfect match between theory and simulations, which validates the derived BER for asymmetric channels. In addition, we observe that the performance of our proposed HNCOUS scheme with $\gamma_{th} = \gamma_{opt}$ are slightly better than those of OUS and achieves diversity gain two for both users.

In Fig. 4.6, we plot the access probabilities of HZPNC, OUS and our proposed HNCOUS scheme with the optimal thresholds γ_{opt} corresponding to Fig. 4.5. The access probability of OUS

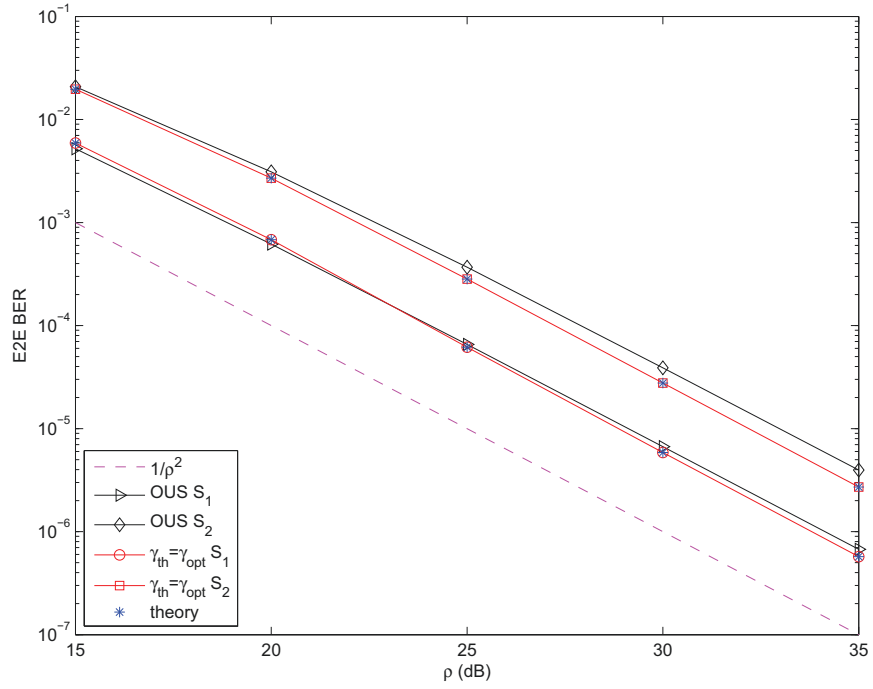


Figure 4.5: E2E BER performance (simulated and theoretical) of our proposed adaptive transmission scheme over asymmetric channels.

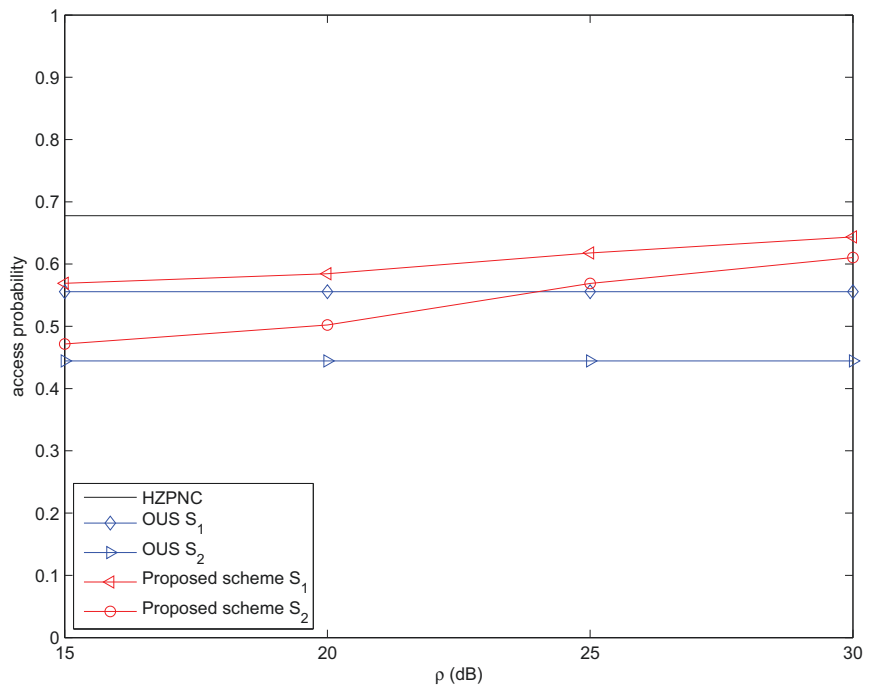


Figure 4.6: Access probability of HZPNC, OUS and our proposed adaptive transmission scheme for asymmetric channels.

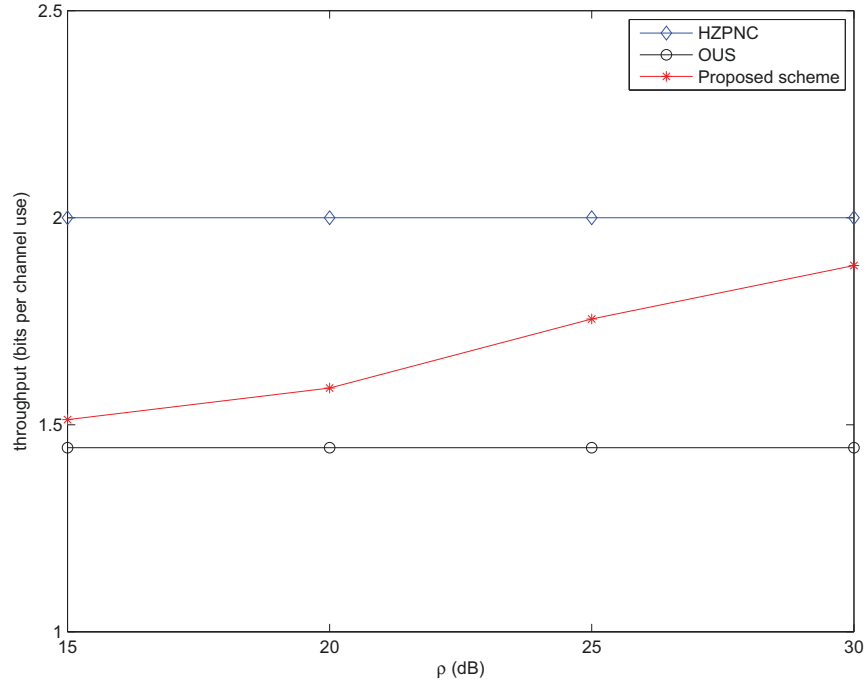


Figure 4.7: Throughput of HZPNC, OUS and our proposed adaptive transmission scheme corresponding to Fig. 4.5.

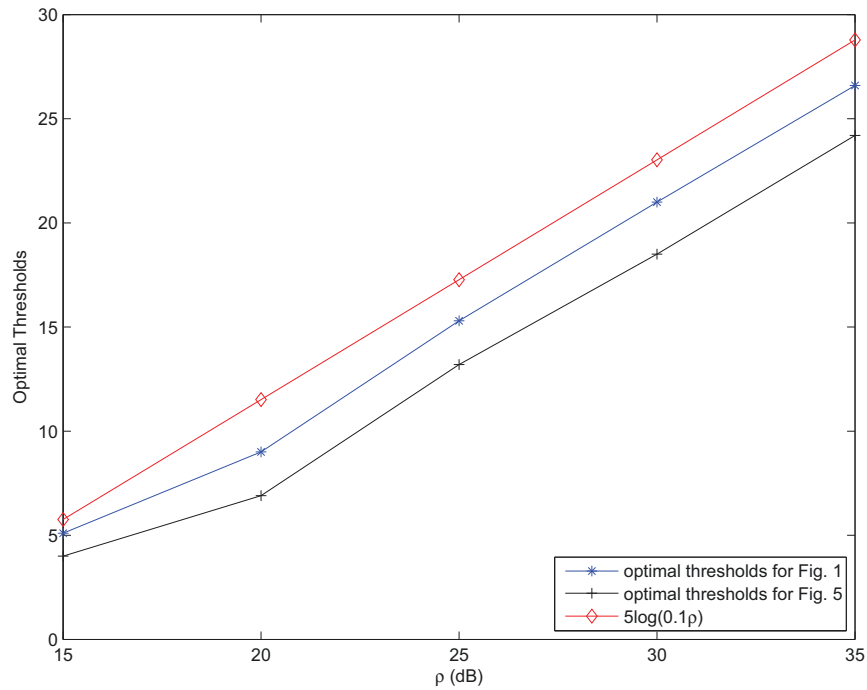


Figure 4.8: The optimal threshold values as a function of ρ for Figs. 4.1 and 4.5.

for S_1 is 0.5556 and 0.4444 for S_2 . It is shown that the access probability of our proposed scheme falls between that of HZPNC and OUS for both users. As the SNR increases, however, the access probability of our proposed scheme for both users increases and approaches that of HZPNC. We can also observe that the gap between the access probability of our proposed scheme for the two users is less than that of OUS and decreases as the SNR increases. This clearly shows how our proposed scheme improves fairness between the users as compared to OUS.

In Fig. 4.7, we illustrate the throughput of HZPNC, OUS and our proposed scheme with the optimal thresholds γ_{opt} corresponding to Fig. 4.5. Similar to the observations of Fig. 4.4, our proposed scheme also achieves a higher throughput than that of OUS in this case.

In Fig. 4.8, we plot the values of γ_{opt} that correspond to Fig. 1 (symmetric channels) and Fig. 5 (asymmetric channels) versus ρ . In the same figure, we plot the function $5\log(0.1\rho)$. We observe from the figure that all curves have the same behavior, suggesting that $\gamma_{opt} = 5\log(c\rho)$, which was assumed in obtaining 4.29.

4.8 Concluding Remarks

We proposed an HNCOUS scheme for two-way communication with asymmetric data rates that aims at improving fairness and still exploiting multiuser diversity gain. The proposed scheme either allows only the best user to transmit or both users transmit using network coding, depending on the user channels quality. If both users have good channels, both users transmit at the same time using network coding; otherwise, the better user transmits while the other user remains silent. We analyzed the proposed adaptive transmission scheme in terms of the E2E BER, access probability and throughput. We examined the performance of the proposed schemes over asymmetric fading channels. We showed that the proposed scheme retains the diversity achieved through multiuser selection, and offers throughput that approaches the best possible throughput at high SNRs. The

implication here is that the two users enjoy better transmission fairness and throughput, while in general achieving better BER performance.

Chapter 5

Relay Assignment in Multiple Source–Destination Cooperative Networks with Limited feedback

5.1 Introduction

As mentioned in Chapter 2, much attention has been given to problems pertaining to relay assignment for cooperative networks. However, in networks with many multiple source-destination pairs, it is normally difficult for destinations to acquire the CSI of the entire network without feedback. To this end, in this chapter, we design a practical limited feedback strategy in conjunction with two relay assignment schemes, i.e., fullset selection and subset selection, which are based on maximizing the minimum E2E SNR among all pairs. In this strategy, each destination acquires its SNR, quantizes it, and feeds it back to the relays. The relays then construct the E2E SNR table and select the relay assignment permutation from all possible relay assignment permutations or only a subset of these permutations. In addition, we study the impact of using quantized CSI

on the performance of relay assignment by deriving the E2E BER expressions and analyzing the achievable diversity order.

Some related work in the field of limited feedback can be found in [78]-[80]. The performance of multiuser diversity with limited feedback is studied in [78]. Limited feedback has also been studied for cooperative networks in [66]-[69]. More references can be found in [79]. In [80], the authors consider several partner selection schemes with limited feedback. However, the schemes in [80] are based on quantized average CSI and no theoretical insight about the impact of limited feedback has been provided. Therefore, to the best of our knowledge, few works have been done to study the impact of using quantized instantaneous CSI on the performance of relay assignment in multiple source–destination cooperative networks. This motivates our work.

We examine the fullset and subset relay assignment schemes with quantized CSI and analyze their performance in terms of the E2E BER. In particular, we derive the exact E2E BER expressions for fullset selection and subset selection in terms of the worst E2E SNR among all pairs over independent Rayleigh fading channels and carry out the asymptotic analysis (i.e., at high SNR) in order to show the form of the optimal thresholds used in the quantization process and the achievable diversity.

The remainder of the chapter is organized as follows. The system model is presented in Section 5.2. In Section 5.3, the proposed limited feedback quantization strategy and the corresponding relay assignment schemes are presented. We analyze the E2E BER performance for both subset and fullset selection in Section 5.4, and examine its asymptotic performance at high SNR in Section 5.5. We present several numerical examples in Section 5.6, and conclude the chapter in Section 5.7.

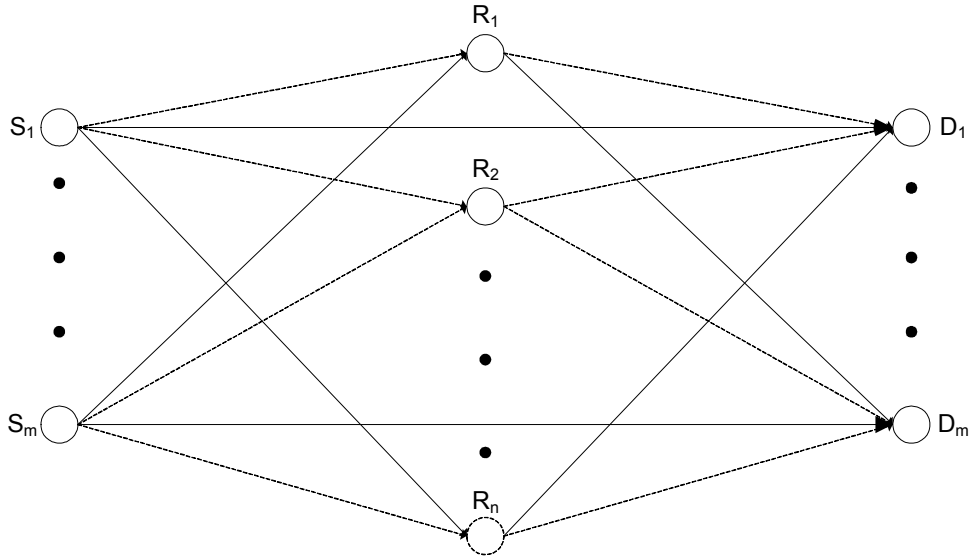


Figure 5.1: A cooperative network with m communication pairs and n relays.

5.2 System Model

We consider the system model shown in Fig. 5.1, in which the network consists of m pairs and n relays where $n \geq m$.¹ Each of the nodes is equipped with a single antenna and operates in a half-duplex mode. In the first time slot, the source of each pair transmits its signal, i.e., m nodes transmit simultaneously in the first time slot using frequency division multiple access (FDMA) [30]. In the second time slot, the selected relays transmit. Note that only one relay is assigned to each pair, and this assignment is done before actual transmission takes place. As such, each relay will have to decode only the signal coming from the pair it is assigned to. We assume there is no direct path between the sources and the destinations.

Let $h_{S_i R_j}$ and $h_{R_j D_i}$ (for $i = 1, \dots, m$, $j = 1, \dots, n$) denote the fading coefficient between the i th source– j th relay and j th relay– i th destination, respectively. Let $y_{S_i R_j}$ denote the received signal at the relay from the i th source, which is expressed as $y_{S_i R_j} = \sqrt{\rho} h_{S_i R_j} x_{S_i} + n_{S_i R_j}$, where

¹In this chapter, we assume that a single relay is assigned to a single pair at any given time, suggesting that the number of relays should be at least as many as the number of pairs. This is a realistic assumption because any node in the network can serve as a relay.

x_{S_i} is the signal transmitted from the i th source and $n_{S_i R_j}$ is an AWGN sample corresponding to the i th source- j th relay link, with zero mean and unit variance and $\rho = \frac{E_b}{N_0}$ is the per-bit SNR. The relay forwards the detected signal to the destination. The signal received from the selected relay at the i th destination is expressed as $y_{R_j D_i} = \sqrt{\rho} h_{R_j D_i} \hat{x}_{S_i R_j} + n_{R_j D_i}$, where $\hat{x}_{S_i R_j}$ is a hard decision made based on $y_{S_i R_j} h_{S_i R_j}^*$.

The channels are assumed to experience independent, slow and frequency-nonselctive Rayleigh fading. Let $\gamma_{S_i R_j}$ and $\gamma_{R_j D_i}$ denote the instantaneous SNRs for the links $S_i \rightarrow R_j$ and $R_j \rightarrow D_i$, respectively. For DF relaying, the E2E instantaneous SNR is well approximated as $\gamma_{ij} = \min(\gamma_{S_i R_j}, \gamma_{R_j D_i})$ [73], and its pdf is expressed as

$$f_\gamma(\gamma) = \frac{1}{\bar{\gamma}} e^{-\frac{1}{\bar{\gamma}}\gamma}, \quad (5.1)$$

where $\bar{\gamma} = \frac{\bar{\gamma}_{SR}\bar{\gamma}_{RD}}{\bar{\gamma}_{SR} + \bar{\gamma}_{RD}}$ and $\bar{\gamma}_{SR} = \rho E[|h_{SR}|^2]$ and $\bar{\gamma}_{RD} = \rho E[|h_{RD}|^2]$ are the average SNRs for the links $S_i \rightarrow R_j$ and $R_j \rightarrow D_i$, respectively. We drop the index here since the average SNRs are assumed to be the same for the source to relay links and relay to destination links, respectively. This corresponds to a network with clustered sources, clustered relays and clustered destinations. Thus the E2E instantaneous SNR in this chapter refers to $\gamma_{ij} = \min(\gamma_{S_i R_j}, \gamma_{R_j D_i})$.

5.3 Relay Assignment with Limited Feedback

In this section, we elaborate on the limited feedback quantization strategy and the corresponding relay assignment schemes. In order to illustrate our relay assignment scheme in conjunction with quantized CSI, as an example, consider the case in which $m = 2$ and $n = 3$. Consequently, there are six possible relay assignment permutations, which are illustrated in the Table 5.1.

In the table, the first entry of each row indicates the relay assigned to the first pair, the second is the relay assigned to the second pair. As we can see, there is correlation between certain rows of the table. For instance, rows one and four are correlated since in both cases, R_1 is assigned to

Table 5.1: Possible relay assignments based on the full CSI.

	Pair 1	Pair 2
Subset 1	R_1	R_2
	R_2	R_3
	R_3	R_1
Subset 2	R_1	R_3
	R_2	R_1
	R_3	R_2

the first pair. To eliminate the correlation, the six relay assignment permutations can be divided into two subsets as shown in the table. The objective is to divide the entire set of permutations into subsets such that no two or more permutations within a subset have the same relay assigned to the same pair. As a consequence, the rows are mutually independent in each subset. More details of the steps to construct subsets can be found in [24].

Let γ_{ij} denote the E2E instantaneous SNR of pair i when the j th relay helps it. Then γ_{ij}^q represents the corresponding quantized E2E SNR. As such, the corresponding E2E SNR with limited feedback is shown in the Table 5.2.

Table 5.2: Quantized CSI based E2E SNR matrix for all possible relay assignments.

	Pair 1	Pair 2
Subset 1	γ_{11}^q	γ_{22}^q
	γ_{12}^q	γ_{23}^q
	γ_{13}^q	γ_{21}^q
Subset 2	γ_{11}^q	γ_{23}^q
	γ_{12}^q	γ_{21}^q
	γ_{13}^q	γ_{22}^q

Note that for relay assignment with full CSI, the corresponding entries in the table are the exact value of the instantaneous E2E SNR, i.e., γ_{ij} . Let $\gamma_{k,\min}$ denote the worst E2E SNR of the k th assignment choice. Thus, the index of the selected assignment choice for fullset selection is obtained as

$$k^* = \arg \max_k \left\{ \gamma_{k,\min}, k = 1, 2, \dots, \frac{n!}{(n-m)!} \right\}. \quad (5.2)$$

We remark that the above selection criterion is for both full CSI and quantized CSI depending on the form of the E2E SNR table. While for subset selection, the best choice is selected within a subset with only n permutations instead of all permutations. We should emphasize that the relay assignment choice may not be unique, especially for the case of quantized CSI. In such a case, the target performance measure of our relay assignment schemes, i.e., the worst E2E SNR among all pairs, cannot be improved no matter which permutation is selected. So when there are more than two available choices, we just select the one with the smallest index k .

In the following, we outline the steps for the limited feedback quantization strategy and the corresponding relay assignment schemes.

1) At the end of the training period, each destination will have acquired the CSI for all source-relay links, as well as the links between all the relays and its own receiving channels.² Possible ways for the destination to obtain the CSI are illustrated in [63] and [71].³

2) The instantaneous SNR range $[0, \infty]$ is divided by $N - 1$ thresholds, γ_{thl} ($l = 1, 2, \dots, N - 1$), into N quantization levels. Then the destination uses $\log_2 N$ bits to feedback the quantization level. Therefore, each destination sends $n \log_2 N$ feedback bits for each channel coherence time. The feedback channels between each destination to the relays are assumed to be error free.

3) Upon receiving the feedbacks from all the destinations, the relays construct the E2E SNR table for fullset selection or subset selection. Then the relays calculate $\gamma_{k,\min}$ and determine the relay assignment choice according to the assignment criterion in (5.2). Since the feedback channels are assumed to be error free, the relays will have the same E2E SNR table and make the same relay

²Note that each destination can only acquire the CSI of the source-relay links and its own receiving channel, and each relay can only obtain the CSI of all the sources to itself by training. Therefore, it is impossible for the destinations to perform relay assignment without CSI feedback. Furthermore, it is not sufficient to ask the destinations to feedback the relay-destination CSI to the relays.

³The destination can acquire the CSI of the links between the relays and itself via training. The relays can acquire the CSI of the source-relay link by training. The relays can amplify and forward the received training signals from the sources to the destination, so that the destination can estimate the product of the source-relay and relay-destination links. Since the CSI of the relay-destination links is known by the destination, the CSI of the source-relay links can be estimated.

assignment decision independently. So there is no need for the relays to communicate with each other.⁴

5.4 The End-to-End Bit Error Rate

5.4.1 Preliminaries

As shown in the previous section, the worst E2E SNR, $\gamma_{k^*,\min}$, of the selected assignment choice is critical in the process of relay assignment. Therefore, in this section, we derive the exact E2E BER performance with N quantization levels in terms of $\gamma_{k^*,\min}$ for both subset selection and fullset selection. We consider a general modulation scheme for which the conditional error probability takes the form of $d \cdot \text{erfc} \sqrt{a\gamma}$ [81], where γ is the instantaneous SNR, and (d, a) are constants depending on the modulation scheme (e.g. for binary phase shift keying (BPSK) $d = 1$ and $a = 2$). Therefore, tailoring the BER expressions for M-ary phase shift keying (M-PSK) and M-QAM modulations is straightforward. For example, in Appendix C. 1, we adapt the obtained expression to M-QAM.

Let γ_{thl} ($l = 1, 2, \dots, N - 1$) denote the thresholds separating different quantization levels and the value of γ_{thl} increases with l . Thus $\gamma_{k^*,\min}$ can be either less than γ_{th1} , greater than γ_{thN-1} or belong to the interval $[\gamma_{thl}, \gamma_{th(l+1)}]$. To simplify the presentation of the derivation in this part, we assume that $\gamma_{th0} = 0$ and $\gamma_{thN} = \infty$. According to the value of $\gamma_{k^*,\min}$ of the selected assignment permutation, we divide the calculation of P_e to N separate parts as

$$P_e = \sum_{l=0}^{N-1} P_{el}, \quad (5.3)$$

⁴We can design the feedback strategy in such a way that one node collects all the quantized CSI and makes the decision. However, there will be additional overheads since this node needs to notify the relays to help which pairs. While for the proposed scheme, the relays make decisions by themselves in a distributed manner and without a need for additional overheads.

where P_{el} represents the BER that $\gamma_{k^*,\min}$ belongs to the interval $[\gamma_{thl}, \gamma_{th(l+1)}]$, which is given by

$$P_{el} = P_r(\gamma_{thl} < \gamma_{k^*,\min} < \gamma_{th(l+1)})P(\varepsilon | \gamma_{thl} < \gamma_{k^*,\min} < \gamma_{th(l+1)}), \quad (5.4)$$

where $P_r(\gamma_{thl} < \gamma_{k^*,\min} < \gamma_{th(l+1)})$ represents the probability that $\gamma_{thl} < \gamma_{k^*,\min} < \gamma_{th(l+1)}$ and $P(\varepsilon | \gamma_{thl} < \gamma_{k^*,\min} < \gamma_{th(l+1)})$ is the BER conditioned on $\gamma_{thl} < \gamma_{k^*,\min} < \gamma_{th(l+1)}$.

5.4.2 Subset Selection

Lemma 5.1 *For a network with m source-destination pairs and n relays, using $N-1$ quantization thresholds and subset selection results in*

$$\begin{aligned} P_e &= \left(1 - e^{-\frac{\gamma_{th1}}{\bar{\gamma}_{\min}}}\right)^n d \cdot I(a, \bar{\gamma}_{\min}, 0, \gamma_{th1}) \\ &+ \sum_{l=1}^{N-1} \sum_{j=1}^n \frac{n!}{j!(n-j)!} \left(e^{-\frac{\gamma_{thl}}{\bar{\gamma}_{\min}}} - e^{-\frac{\gamma_{th(l+1)}}{\bar{\gamma}_{\min}}}\right)^j \left(1 - e^{-\frac{\gamma_{thl}}{\bar{\gamma}_{\min}}}\right)^{n-j} \\ &\cdot d \cdot I(a, \bar{\gamma}_{\min}, \gamma_{thl}, \gamma_{th(l+1)}), \end{aligned} \quad (5.5)$$

where

$$\begin{aligned} I(a, b, \gamma_{thl}, \gamma_{th(l+1)}) &= \int_{\gamma_{thl}}^{\gamma_{th(l+1)}} \operatorname{erfc} \sqrt{a\gamma} \frac{1}{b} e^{-\frac{1}{b}\gamma} d\gamma \\ &= e^{-\frac{1}{b}\gamma_{thl}} \operatorname{erfc} \sqrt{a\gamma_{thl}} - \sqrt{\frac{ab}{1+ab}} \operatorname{erfc} \sqrt{\gamma_{thl} \left(a + \frac{1}{b}\right)} \\ &\quad - e^{-\frac{1}{b}\gamma_{th(l+1)}} \operatorname{erfc} \sqrt{a\gamma_{th(l+1)}} + \sqrt{\frac{ab}{1+ab}} \operatorname{erfc} \sqrt{\gamma_{th(l+1)} \left(a + \frac{1}{b}\right)}. \end{aligned}$$

$$\text{and } \bar{\gamma}_{\min} = \frac{1}{m} \frac{\bar{\gamma}_{SR}\bar{\gamma}_{RD}}{\bar{\gamma}_{SR} + \bar{\gamma}_{RD}}.$$

Proof. See Appendix C. 1. ■

5.4.3 Fullset Selection

Lemma 5.2 *For a network with two source-destination pairs and n relays, using $N - 1$ quantization thresholds and fullset selection results in*

$$P_e = \sum_{l=0}^{N-1} [1 - P_r(\gamma_{k^*,\min} > \gamma_{th(l+1)}) - P_r(\gamma_{k^*,\min} < \gamma_{thl})] d \cdot I(a, \bar{\gamma}, \gamma_{thl}, \gamma_{th(l+1)})$$

where the probability that $\gamma_{k^*,\min}$ is greater than a particular threshold, $\gamma_{th(l+1)}$, is derived as

$$\begin{aligned} P_r(\gamma_{k^*,\min} > \gamma_{th(l+1)}) &= \frac{n!}{(n-2)!} e^{-\frac{2\gamma_{th(l+1)}}{\bar{\gamma}}} \left(1 - e^{-\frac{\gamma_{th(l+1)}}{\bar{\gamma}}}\right)^{2n-2} \\ &+ \sum_{t=3}^n \left(\frac{2n!}{t!(2n-t)!} - 2\frac{n!}{t!(n-t)!}\right) e^{-\frac{t\gamma_{th(l+1)}}{\bar{\gamma}}} \left(1 - e^{-\frac{\gamma_{th(l+1)}}{\bar{\gamma}}}\right)^{2n-t} \\ &+ \sum_{t=n+1}^{2n} \frac{2n!}{t!(2n-t)!} e^{-\frac{t\gamma_{th(l+1)}}{\bar{\gamma}}} \left(1 - e^{-\frac{\gamma_{th(l+1)}}{\bar{\gamma}}}\right)^{2n-t} \end{aligned} \quad (5.6)$$

and the probability that $\gamma_{k^*,\min}$ is less than a particular threshold, γ_{thl} , is derived as

$$\begin{aligned} P_r(\gamma_{k^*,\min} < \gamma_{thl}) &= \left(1 - e^{-\frac{\gamma_{thl}}{\bar{\gamma}}}\right)^{2n} + 2ne^{-\frac{\gamma_{thl}}{\bar{\gamma}}} \left(1 - e^{-\frac{\gamma_{thl}}{\bar{\gamma}}}\right)^{2n-1} \\ &+ \left(\frac{2n!}{2(2n-2)!} - \frac{n!}{(n-2)!}\right) e^{-\frac{2\gamma_{thl}}{\bar{\gamma}}} \left(1 - e^{-\frac{\gamma_{thl}}{\bar{\gamma}}}\right)^{2n-2} \\ &+ \sum_{t=3}^n \left(2\frac{n!}{t!(n-t)!}\right) e^{-\frac{t\gamma_{thl}}{\bar{\gamma}}} \left(1 - e^{-\frac{\gamma_{thl}}{\bar{\gamma}}}\right)^{2n-t} \end{aligned} \quad (5.7)$$

Proof. See Appendix C. 2. ■

So far, we have obtained closed-form expressions for the E2E BER for both subset and fullset selection. As expected, these expressions are functions of the average E2E SNR and thresholds. Since the E2E BER expressions for both subset and fullset selection are not invertible, the exact optimal thresholds can only be obtained by numerically minimizing the E2E BER with exhaustive grid search, and this is the approach followed in this chapter. That is, we have used our mathematical derivation to obtain the exact optimal thresholds numerically

5.5 Asymptotic E2E BER Performance

Since the final expressions derived above are exact and the optimal thresholds are obtained numerically, they do not give much insight about the diversity order achieved and the form of the optimal thresholds. So in this section, we analyze the behavior of the E2E BER at high SNR while using the optimal thresholds for relay assignment with limited feedback. Since the BER performance of one threshold is an upper bound on the BER performance of multiple thresholds, we focus on the asymptotic analysis for one threshold, which is denoted as γ_{th} .

5.5.1 Asymptotic E2E BER

Lemma 5.3 *The E2E BER for subset selection can be upper bounded as*

$$P_e^{asy} \leq \frac{\gamma_{th}^{n-1}}{4\rho^n} + \frac{e^{-\gamma_{th}}}{4\rho}. \quad (5.8)$$

Proof. See Appendix C. 3. ■

5.5.2 The Asymptotic Optimal Threshold

To find the asymptotic optimal threshold, γ_{opt} , that minimizes (5.8), we differentiate (5.8) with respect to γ_{th} , which yields

$$\frac{\partial P_e^{asy}}{\partial \gamma_{th}} = \frac{(n-1)\gamma_{th}^{n-2}}{4\rho^n} - \frac{e^{-\gamma_{th}}}{4\rho} = 0. \quad (5.9)$$

It is not tractable to solve the optimal threshold γ_{opt} for any n directly from this equation. While for $n = 2$, we have

$$\frac{1}{4\rho^2} - \frac{e^{-\gamma_{th}}}{4\rho} = 0. \quad (5.10)$$

By solving (5.10), we have

$$\gamma_{opt} = \log \rho.$$

Note that $\gamma_{opt} = \log \rho = (2 - 1) \log \rho$, where 2 is the number of relays. Therefore, based on the insight from the asymptotic optimal threshold derived above for $n = 2$, we extrapolate that the optimal threshold function could be in the form of

$$\gamma_{opt} = (n - 1) \log c\rho, \quad (5.11)$$

where c is a constant which is independent of ρ . To validate our observation, we plug $\gamma_{th} = (n - 1) \log c\rho$ into (5.9), which yields

$$\frac{\partial P_e^{asy}}{\partial \gamma_{th}} = \frac{(n - 1)^{n-1} (\log c\rho)^{n-2}}{4\rho^n} - \frac{1}{4c^{n-1}\rho^n}. \quad (5.12)$$

For sufficiently large ρ , it is obvious that

$$\frac{\partial P_e^{asy}}{\partial \gamma_{th}} \Big|_{\gamma_{th}=(n-1)\log c\rho} > 0. \quad (5.13)$$

Then we plug $\gamma_{th} = (n - 1) \log \left(\frac{c\rho}{\log c\rho} \right)$ into (5.9), then we have

$$\frac{\partial P_e^{asy}}{\partial \gamma_{th}} = \frac{(n - 1)^{n-1} (\log c\rho - \log(\log c\rho))^{n-2}}{4\rho^n} - \frac{(\log c\rho)^{n-1}}{4c^{n-1}\rho^n}. \quad (5.14)$$

For sufficiently large ρ , we have

$$\frac{\partial P_e^{asy}}{\partial \gamma_{th}} \Big|_{\gamma_{th}=(n-1)\log\left(\frac{c\rho}{\log c\rho}\right)} < 0. \quad (5.15)$$

Since $\frac{\partial P_e^{asy}}{\partial \gamma_{th}}$ is a monotonically increasing function with γ_{th} , we have

$$(n - 1) \log \left(\frac{c\rho}{\log c\rho} \right) < \gamma_{opt} < (n - 1) \log c\rho. \quad (5.16)$$

Then we conclude that $\gamma_{opt} = (n - 1) \log c\rho - o(\log c\rho)$. This validates our observation. This result is also confirmed by simulations in Section 5.6.

5.5.3 Achievable Diversity

In this part, we analyze the diversity order achieved by relay assignment with quantized CSI based on the asymptotic E2E BER and the optimal threshold function derived in subsections A and

B. For comparison purposes, we also include the diversity analysis of relay assignment with full CSI.

We adopt the following generalized measure of diversity defined in [71] $d = (d_1, d_2)$, where d_1 and d_2 are the first-order diversity and second-order diversity, respectively. They are given as

$$d_1 = -\lim_{\rho \rightarrow \infty} \frac{\log(BER)}{\log(\rho)}, \quad (5.17)$$

and

$$d_2 = -\lim_{\rho \rightarrow \infty} \frac{\log(BER) + d_1 \log(\rho)}{\log \log(\rho)}. \quad (5.18)$$

As we can see from the definition, the generalized diversity measure not only encapsulates the conventional one as the first-order diversity but also incorporates the second-order diversity which captures the $\log \rho^{d_1}$ term in the error rate expression and its effect on the performance.

Proposition 5.1 *Subset selection with quantized CSI can achieve diversity order of $(n, -(n-1))$.*

Proof. From (5.8), we have

$$P_e^{asy} = P_{e1}^{asy} + P_{e2}^{asy}, \quad (5.19)$$

where $P_{e1}^{asy} = \frac{\gamma_{th}^{n-1}}{4\rho^n}$ and $P_{e2}^{asy} = \frac{e^{-\gamma_{th}}}{4\rho}$. Plugging $\gamma_{opt} = (n-1) \log c\rho$ into P_{e1}^{asy} and P_{e2}^{asy} , respectively, we have

$$P_{e1}^{asy} = \frac{((n-1) \log c\rho)^{n-1}}{4\rho^n}, \quad (5.20)$$

and

$$P_{e2}^{asy} = \frac{1}{4c^{n-1}\rho^n}. \quad (5.21)$$

Plugging (5.20) into (5.17) and (5.18) and after some simple algebraic manipulations, we can obtain the diversity achieved by P_{e1}^{asy} , which is $(n, -(n-1))$. Similarly, plugging (5.21) into (5.17) and (5.18), we obtain the diversity for P_{e2}^{asy} , which is $(n, 0)$. Since the performance of P_e^{asy} in (5.19) is dominated by the term with the lower diversity order, we conclude that subset selection with quantized CSI and one threshold can achieve a diversity order of $(n, -(n-1))$. Since the BER

performance of one threshold is an upper bound on the BER performance of multiple thresholds, we can also conclude that the subset selection with quantized CSI can achieve diversity order of $(n, -(n-1))$ which is stated in Proposition 5. 1. Therefore, the diversity order of subset selection with quantized CSI is at least $(n, -(n-1))$ for any number of quantization levels. ■

Till now, we have analyzed the asymptotic performance of subset selection. Since the BER performance of subset selection is an upper bound on that of fullset selection, we conclude that fullset selection can also achieve the same asymptotic performance.

Proposition 5.2 *Subset selection with full CSI can achieve diversity order of $(n, 0)$.*

Proof. *The E2E BER in terms of the worst E2E SNR for subset selection with full CSI can be expressed as*

$$P_e = \int_0^\infty \frac{1}{2} \operatorname{erfc} \sqrt{\rho h} f_{h_{k^*, \min}}(h) dh, \quad (5.22)$$

where $f_{h_{k^*, \min}}(h)$ is the pdf of the worst E2E channel gain corresponding to the selected assignment choice, which can be expressed as [31]

$$f_{h_{k^*, \min}}(h) = n e^{-2mh} (1 - e^{-2mh})^{n-1}. \quad (5.23)$$

Then plugging (5.23) into (5.22), we have

$$\begin{aligned} P_e &= \int_0^\infty \frac{1}{2} \operatorname{erfc} \sqrt{\rho h} [n e^{-2mh} (1 - e^{-2mh})^{n-1}] dh \\ &\leq \int_0^\infty \frac{1}{4} [n e^{-(\rho+2m)h} (1 - e^{-2mh})^{n-1}] dh \end{aligned} \quad (5.24)$$

$$= \frac{n!}{8m} \left(\prod_{i=1}^n \left(\frac{\rho}{2m} + i + 1 \right) \right)^{-1} \quad (5.25)$$

$$\leq \frac{n! (2m)^n}{8m} \frac{1}{\rho^n}, \quad (5.26)$$

where (5.24) follows from $\operatorname{erfc} \sqrt{x} \leq \frac{1}{2} e^{-x}$ and (5.25) follows from Equation B.1 in [77]. Plugging (5.26) into (5.17) and (5.18), we obtain $d_1 = n$ and $d_2 = 0$. As such, subset selection with full CSI

can achieve diversity order of $(n, 0)$. Since the BER performance of subset selection is an upper bound on that of fullset selection, we conclude that fullset selection can also achieve diversity $(n, 0)$. ■

Therefore, relay assignment with limited feedback suffers from a second-order diversity loss compared to relay assignment with full CSI. This fact is also confirmed by simulations in the next section.

5.6 Simulation Results

We present in this section numerical examples that aim at validating the E2E BER expressions derived for fullset and subset selection. The performance of relay assignment with quantized CSI and full CSI are also compared. Throughout the simulations, we assume all channel variances are set to 0.25 and all nodes use BPSK.⁵ The curves in this part are generated by using the exact optimal thresholds, which are obtained by minimizing the E2E BER expressions.

In Fig. 5.2, we show the performance results for a network with $m = 2$ and $n = 3$ for subset selection. We also include the curves obtained by using $\frac{1}{\rho^3}$ and $\frac{(\log \rho)^2}{\rho^3}$. They are used as references since these two curves achieve diversity $(3, 0)$ and $(3, -2)$, respectively. By comparing the slopes of the curves, subset selection with full CSI and limited feedback achieve the achievable diversity gains $(3, 0)$ and $(3, -2)$, respectively, which is expected. This confirms our analysis of diversity. In addition, we can see the degradation in SNR due to using only quantized CSI, which is about 3 dB at BER 10^{-4} for one threshold. This degradation diminishes as the number of thresholds increases from 1 to 3. Finally, we can also see the perfect match between theory and simulations, which validates the derived BER expression for subset selection.

The BER performance for fullset selection with $m = 2$ and $n = 3$ is shown in Fig. 5.3, with

⁵We remark that these assumptions are used merely to demonstrate the efficacy of the proposed schemes. That is, the proposed schemes and the conclusions do not depend on the modulation scheme adopted.

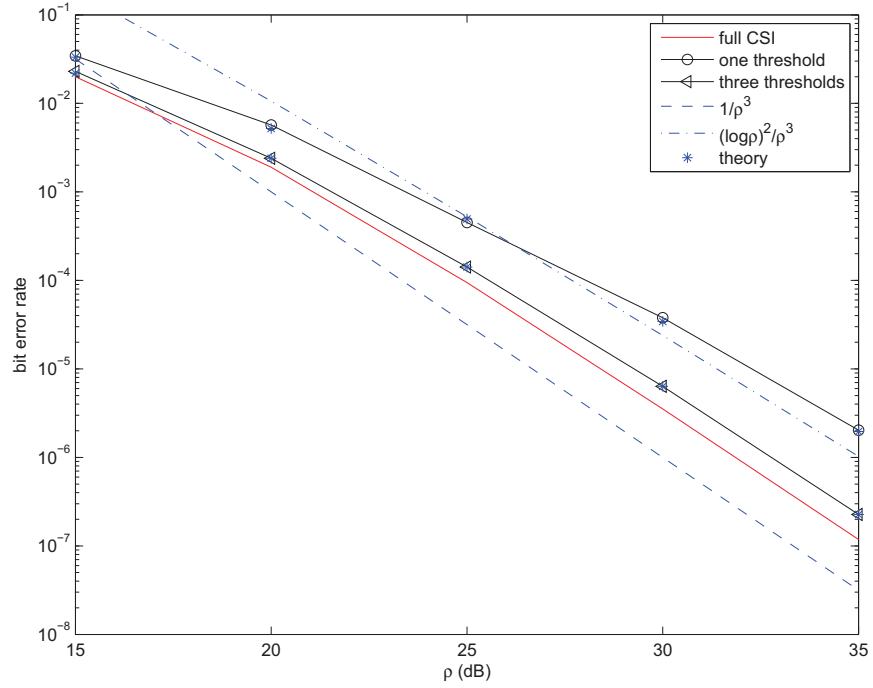


Figure 5.2: Bit error rate performance (theory and simulation) of subset selection with different number of thresholds.

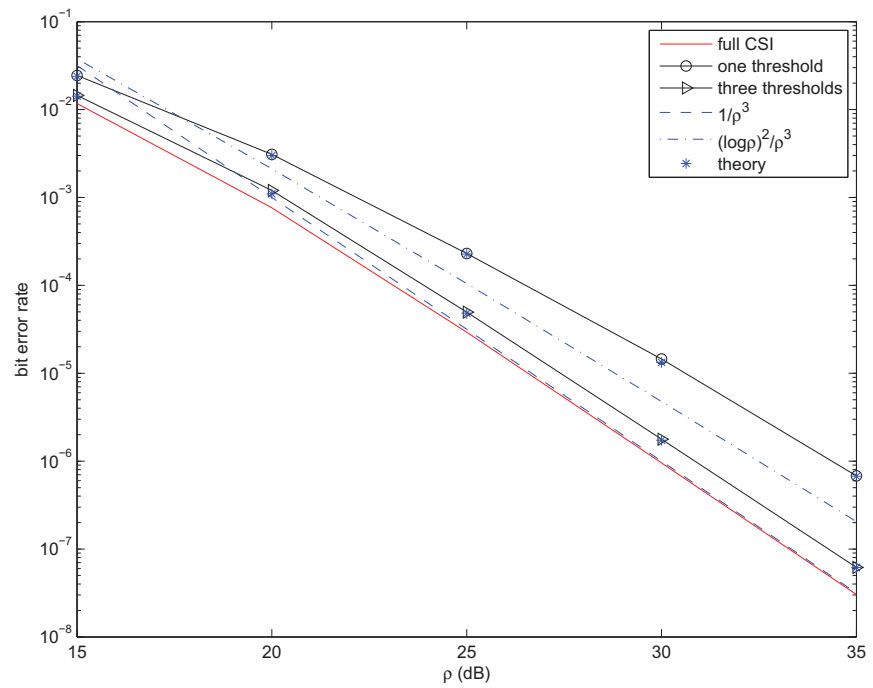


Figure 5.3: Bit error rate performance (theory and simulation) of fullset selection with different number of thresholds.

similar observations. We observe fullset selection with limited feedback also achieves diversity gain $(3, -2)$. As expected, the performance improves as the number of thresholds increases. In addition, the simulation results match the theoretical results, which validates the derived BER expression for fullset selection.

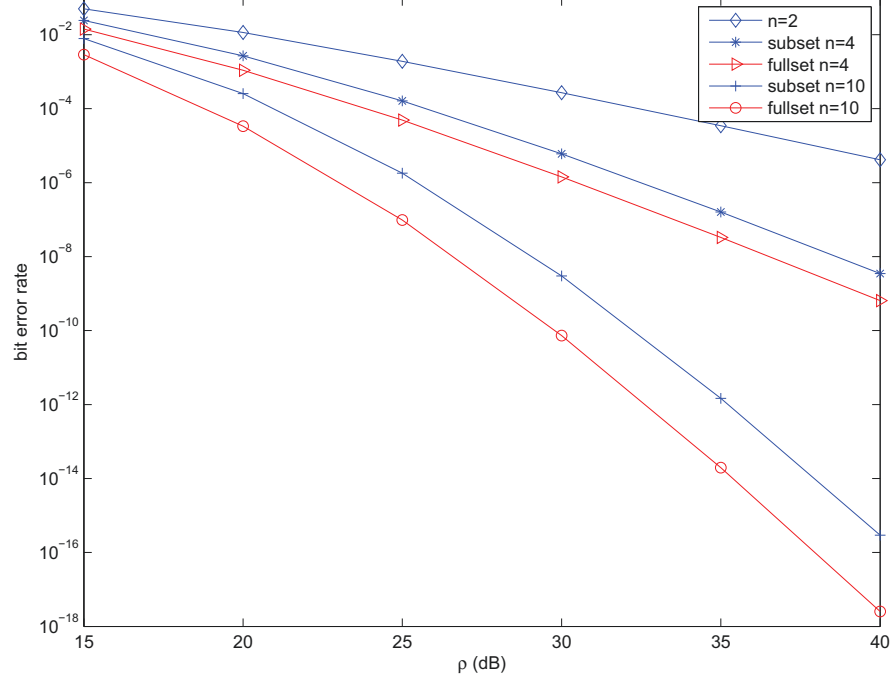


Figure 5.4: Theoretical bit error rate performance comparison between the fullset selection and subset selection.

In Fig. 5.4, we present the theoretical BER performance for the following cases: $m = 2$ and $n = 2, 4, 10$. We consider both fullset selection and subset selection. As shown in the figure, fullset selection achieves the same diversity as subset selection. We can also see the degradation in SNR due to the subset selection scheme, which is about 2 dB at BER 10^{-5} for $n = 4$.

In Fig. 5.5, we demonstrate the optimal threshold values and their corresponding asymptotic values as a function of ρ for the following cases: $m = 2$ and $n = 2, 3, 4$. For all cases, we consider the case of one threshold. For the asymptotic optimal thresholds, we use the function $(n - 1)\log\left(\frac{c\rho}{\log c\rho}\right)$ by setting $c = 0.22$, $c = 0.058$ and $c = 0.0336$ for $n = 2, 3$ and 4 , respectively.

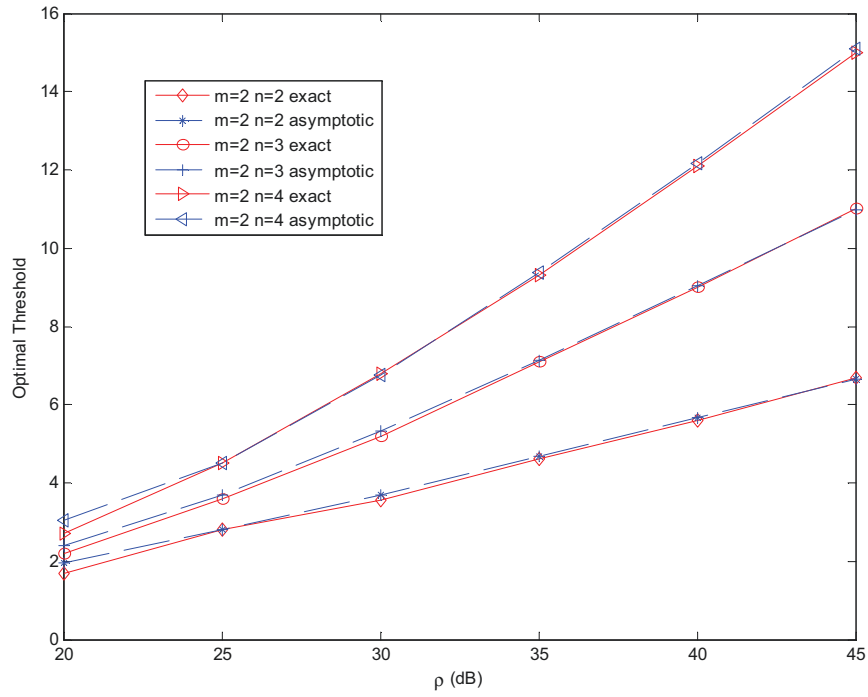


Figure 5.5: The optimal threshold values (exact and asymptotic) as a function of ρ for subset selection.

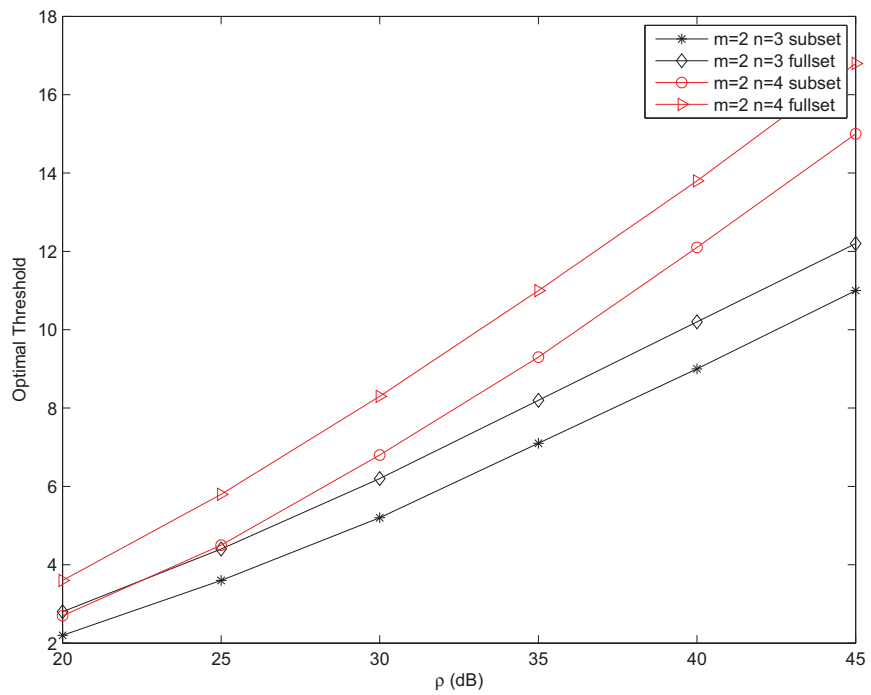


Figure 5.6: Comparison of the optimal threshold values as a function of ρ for subset selection and fullset selection.

It shows that the asymptotic values perfectly match the exact ones, which validates our observation for the form of the optimal threshold in Section 5.5. We also notice that the optimal thresholds increase as ρ and n increase.

In Fig. 5.6, we compare the values of the optimal thresholds for fullset selection and subset selection with $m = 2$, and $n = 3, 4$. We consider the case when there is one threshold. As can be seen in the figure, the curves for fullset selection and subset selection are parallel. It indicates that they have the same asymptotic optimal threshold function. In addition, the threshold value of fullset selection is greater than that of subset selection for the same n .

5.7 Conclusions

In this chapter, we presented a limited feedback quantization strategy and the corresponding relay assignment schemes for relay networks comprising multiple source-destination pairs. We examined two assignment schemes, fullset selection, which is based on searching over all possible assignment permutations, and subset selection, which is based on searching over only a subset on the possible permutations. We have derived BER expressions for both selection schemes based on the worst E2E SNR. By studying the asymptotic performance at high SNR, we found that the asymptotic optimal threshold function is in the form of $(n - 1) \log c\rho$. We also compared the performance of relay assignment with limited feedback and full CSI in terms of the achievable diversity order and resulting E2E BER. For the diversity analysis, we adopted a generalized measure of diversity and showed that they can achieve diversity gains $(n, -(n - 1))$ and $(n, 0)$, respectively. So there is a second-order diversity loss if only quantized CSI is available. As for the E2E BER, we observed that little loss in performance was experienced as compared to that of full CSI.

Chapter 6

Conclusions and Future Work

6.1 Conclusions

Cooperative communications has proven to be an effective way to combat wireless fading by allowing mobile nodes to share their antennas to achieve spatial diversity. However, for practical reasons, cooperative nodes should operate in a half-duplex mode, implying a loss in spectral efficiency. In this thesis, we focused on proposing relaying strategies to mitigate the spectral efficiency loss and achieve the diversity potential of cooperative communications. We considered two-way relay channels and addressed the challenge of coping with asymmetric data rates in two-way relaying. In addition, we studied the impact of quantized CSI on the performance of relay assignment.

Specifically, several relaying strategies for two-way relaying with asymmetric data rates have been proposed and their performance has been analyzed and compared. Moreover, a practical limited feedback strategy in conjunction with relay assignment has been designed and the impacted of limited feedback on the performance of relay assignment has been evaluated.

In Chapter 3, a HZPNC scheme has been designed for two-way relaying with asymmetric data rates. This involves employing hierarchical modulation by the user with the higher data rate and at

the relay, while padding zeros at specific positions of the shorter bit sequence at the relay. A OUS scheme, which exploits the inherent multiuser nature of two-way relaying has also been studied. For this scheme, only one user with the best E2E instantaneous SNR transmits at a time. The BER, access probability and throughput of the HZPNC and OUS schemes have been evaluated analytically.

In Chapter 4, a HNCOUS scheme has been proposed for two-way relaying with an effort to exploit both spectral efficiency and multiuser diversity. It is a combination of HZPNC scheme and OUS scheme. In particular, for a given threshold γ_{th} , if both instantaneous E2E SNRs are above γ_{th} , both users transmit and HZPNC is used; otherwise, OUS is employed. The BER, access probability and throughput of the HNCOUS scheme has been evaluated analytically. It has been shown that our proposed HNCOUS scheme have the better E2E BER performance than that of HZPNC and OUS. In addition, its throughput approach that of HZPNC at high SNR. The asymptotic E2E BER performance of HNCOUS at high SNR for both users is also examined. It is shown that the proposed scheme achieves full diversity, which is the number of available users

In Chapter 5, a limited feedback quantization strategy and the corresponding relay assignment schemes have been presented. In this strategy, each destination acquires its SNR, quantizes it, and feeds it back to the relays. The relays then construct the E2E SNR table and select the relay assignment permutation from all possible relay assignment permutations or only a subset of these permutations. The asymptotic BER performance at high SNR in terms of the worst E2E SNR among all pairs has been analyzed. The optimal threshold values that minimize the E2E BER under quantized CSI assumptions at the relays have been derived analytically. It has been observed that the optimal threshold increases logarithmically with the average link SNRs. The BER performance of relay assignment with quantized CSI have also been evaluated and it has been shown that the optimal quantized levels can improve BER significantly. It has been proven that relay assignment with quantized CSI can achieve the same first-order diversity as that of the full CSI case, but there

is a second-order diversity loss.

6.2 Future Work

6.2.1 Extending the Performance Analysis of Our Proposed Schemes to Other Scenarios

In Chapters 3 and 4, we proposed the HZPNC, OUS and HNCOUS schemes for two-way relaying with asymmetric data rates. We examined the proposed schemes in terms of BER, access probability and throughput for cooperative networks with two users communicating with each other via a relay, i.e., two-way communication. For simplicity, we assumed that there is no direct path between the two users. In addition, the CSI is assumed to be perfectly known. As we can see, there are several assumptions. Therefore, investigating our proposed schemes without these assumptions can be another topic for future studies.

When the direct path is considered, the challenge would be how to control error propagation at the destination. Another challenge is when one considers multiple hops. In our analysis, we only derived E2E BER expressions, the performance of outage probability can also be investigated. Also, the analysis of HZPNC, OUS and HNCOUS can be extended to networks that have multiple relays. Specifically, the performance with relay selection can be analyzed. Finally, the performance of the proposed schemes with imperfect CSI estimation can be investigated. The BER analysis performed in Chapter 5 are based on the worst E2E SNR among all pairs. Deriving the exact E2E BER of each pair can be another topic for future studies.

6.2.2 Investigation of the Proposed Schemes in the Context of Variable Rate Transmission

Adaptive modulation refers to the scenario when the transmitter adjusts the modulation scheme according to the quality of the channel. As a practical way to improve the spectral efficiency [82], one may combine cooperative diversity and adaptive modulation.

The performance of repetition-based cooperative relaying with adaptive modulation is studied in [85]. In order to reduce the spectral loss caused by orthogonal channels for relaying transmission, the authors in [86] investigated opportunistic incremental cooperative relaying in conjunction with adaptive modulation. But in [86], since the source-to-destination link is used as long as it can support the minimum data rate, the spectral efficiency is not maximized. In contrast, the authors studied an adaptive modulation scheme to maximize the spectral efficiency for an AF cooperative system with multiple relays. Adaptive modulation combined with best relay selection for AF relaying and DF relaying are investigated in [87] and [88], respectively. In [89], the authors studied the two-way AF relaying with adaptive modulation and analyze its performance in terms of the average spectral efficiency.

As we can see, there is no work for two-way DF relaying with adaptive modulation. Therefore, extending our proposed schemes to use adaptive modulation can be one topic for future studies. That is, when each user adapts its transmission rate depending on the channel quality and bandwidth availability.

6.2.3 Design Spatial Modulation (SM)-based Asymmetric Two-way Relaying Schemes

Spatial modulation (SM) is a new modulation scheme proposed recently for multiple-input multiple-output (MIMO) systems [90]-[93]. In SM, the antenna indices are employed to convey

information. SM-based MIMO has advantages over the convention MIMO systems in the aspects of inter-channel interference (ICI), inter-antenna synchronization, number of radio frequency (RF) chains and energy consumption.

Due to its promising application, SM has received lots of investigations recently. Most of the work done focused on point-to-point and one-way relaying [94]-[101]. Therefore, SM for two-way relaying can be considered as future work. In light of the high energy efficiency potential of SM, we believe that it is promising to achieve both spectral efficiency and energy efficiency for SM-based asymmetric two-way relaying schemes.

Appendix A Derivations for Chapter 3

A.1 Proof of Equation (3.24)

The pdf of γ_{im} given $\gamma_i > \gamma_j$ can be expressed as

$$f_{\gamma_{im}|\gamma_i>\gamma_j}(\gamma_{im}) = \int_0^{\infty} f_{\gamma_{im}|\gamma_i=\gamma}(\gamma_{im}) f_{\gamma_i|\gamma_i>\gamma_j}(\gamma) d\gamma, \quad (\text{A.1})$$

where $\gamma_i = \min(\gamma_{im}, \gamma_{in})$ for $i, j, n, m = 1, 2$ where $i \neq j$, and $m \neq n$. The pdf of γ_{im} and γ_i is given in (3.1) and (3.2). Thus (A.1) can be further expressed as [82]

$$f_{\gamma_{im}|\gamma_i>\gamma_j}(\gamma_{im}) = \int_0^{\infty} \frac{\frac{1}{\bar{\gamma}_{im}} e^{-\frac{\gamma_{im}}{\bar{\gamma}_{im}}} \frac{1}{\bar{\gamma}_{in}} e^{-\frac{\gamma_{in}}{\bar{\gamma}_{in}}}}{\frac{1}{\bar{\gamma}_i} e^{-\frac{\gamma_i}{\bar{\gamma}_i}}} f_{\gamma_i|\gamma_i>\gamma_j}(\gamma) d\gamma + \frac{\frac{1}{\bar{\gamma}_{im}} e^{-\frac{\gamma_{im}}{\bar{\gamma}_{im}}} e^{-\frac{\gamma_{in}}{\bar{\gamma}_{in}}}}{\frac{1}{\bar{\gamma}_i} e^{-\frac{\gamma_{im}}{\bar{\gamma}_i}}} f_{\gamma_i|\gamma_i>\gamma_j}(\gamma_{im}), \quad (\text{A.2})$$

where $i, j, n, m = 1, 2$, and $i \neq j, m \neq n$. The conditional cumulative distribution function (CDF) $F(\gamma_i | \gamma_i > \gamma_j)$ can be expressed as

$$F_{\gamma_i|\gamma_i>\gamma_j}(\gamma) = \frac{P_r(\gamma_i < \gamma, \gamma_i > \gamma_j)}{P_r(\gamma_i > \gamma_j)} \quad (\text{A.3})$$

By using the law of total probability, the numerator in (A.3) is given by

$$P_r(\gamma_i < \gamma, \gamma_i > \gamma_j) = \int_0^{\gamma} \frac{1}{\bar{\gamma}_i} e^{-\frac{\gamma_i}{\bar{\gamma}_i}} d\gamma_i \int_0^{\gamma_i} \frac{1}{\bar{\gamma}_j} e^{-\frac{\gamma_j}{\bar{\gamma}_j}} d\gamma_j = 1 - e^{-\frac{\gamma}{\bar{\gamma}_i}} - \frac{1}{\bar{\gamma}_i} \frac{1}{\frac{1}{\bar{\gamma}_i} + \frac{1}{\bar{\gamma}_j}} \left(1 - e^{-\left(\frac{1}{\bar{\gamma}_i} + \frac{1}{\bar{\gamma}_j}\right)\gamma}\right), \quad (\text{A.4})$$

and the denominator is given by

$$P_r(\gamma_i > \gamma_j) = \int_0^{\infty} \frac{1}{\bar{\gamma}_j} e^{-\frac{\gamma_j}{\bar{\gamma}_j}} dz_j \int_{\gamma_j}^{\infty} \frac{1}{\bar{\gamma}_i} e^{-\frac{\gamma_i}{\bar{\gamma}_i}} d\gamma_1 = \frac{\bar{\gamma}_i}{\bar{\gamma}_i + \bar{\gamma}_j}. \quad (\text{A.5})$$

Plugging (A.4) and (A.5) into (A.3), we can derive the conditional CDF $F_{\gamma_i|\gamma_i>\gamma_j}(\gamma)$. The conditional pdf $f_{\gamma_i|\gamma_i>\gamma_j}(\gamma)$ is obtained by taking the derivative of $F_{\gamma_i|\gamma_i>\gamma_j}(\gamma)$ as

$$f_{\gamma_i|\gamma_i>\gamma_j}(\gamma) = \frac{\bar{\gamma}_i + \bar{\gamma}_j}{\bar{\gamma}_i} \left(\frac{1}{\bar{\gamma}_i} e^{-\frac{\gamma}{\bar{\gamma}_i}} - \frac{1}{\bar{\gamma}_i} e^{-(\frac{1}{\bar{\gamma}_i} + \frac{1}{\bar{\gamma}_j})\gamma} \right) \quad (\text{A.6})$$

Plugging (A.6) into (A.2) and carrying out the integration, we can get

$$f_{\gamma_{im}|\gamma_i>\gamma_j}(\gamma_{im}) = \frac{\bar{\gamma}_{in}(\bar{\gamma}_i + \bar{\gamma}_j)}{\bar{\gamma}_{im}\bar{\gamma}_i(\bar{\gamma}_{in} + \bar{\gamma}_j)} (e^{-\frac{1}{\bar{\gamma}_{im}}\gamma_{im}} - e^{-(\frac{1}{\bar{\gamma}_i} + \frac{1}{\bar{\gamma}_j})\gamma_{im}}), \quad (\text{A.7})$$

where $i, j, n, m = 1, 2$ where $i \neq j, m \neq n$.

Appendix B Derivations for Chapter 4

B.1 Proof of Lemma 4.1

According to the proposed scheme, if both instantaneous E2E SNRs of the two users are above γ_{th} , both users transmit using HZPNC. In this case, three time-slots are needed for two new transmissions. In contrast, if either instantaneous E2E SNRs of the two users is below a threshold γ_{th} , only the better user transmits. Then two time-slots are needed per transmission. To elaborate, let us assume, without loss of generality, that the coherence time is six time slots (of course the coherence time is normally much larger than this; this is used merely for illustration purposes.) When HZPNC is used, two new transmissions are completed per coherence time, whereas three new transmissions are completed for the same duration for the OUS case.

Given the hybrid nature of our proposed scheme, errors can occur when HZPNC or OUS is used. Let N_{OUS}^e and N_{OUS}^b represent the number of decoded errors and number of transmitted bits when OUS is used, respectively. Similarly, let N_{NC}^e and N_{NC}^b represent the number of decoded errors and number of transmitted bits when HZPNC is used, respectively. As such, the E2E BER corresponding to user S_i can be expressed as

$$\begin{aligned} P_i &= \frac{N_{OUS}^e + N_{NC}^e}{N_{OUS}^b + N_{NC}^b} \\ &= \frac{N_{NC}^b \times P(\varepsilon_i \mid \min(\gamma_i, \gamma_j) > \gamma_{th}) + N_{OUS}^b \times P(\varepsilon_i \mid \gamma_i > \gamma_j, \gamma_j < \gamma_{th})}{N_{OUS}^b + N_{NC}^b}, \end{aligned} \quad (\text{B.1})$$

where $P(\varepsilon_i | \min(\gamma_i, \gamma_j) > \gamma_{th})$ is the BER corresponding to S_i , conditioned on $\min(\gamma_i, \gamma_j) > \gamma_{th}$, and $P(\varepsilon_i | \gamma_i > \gamma_j, \gamma_j < \gamma_{th})$ is the BER corresponding to S_i , conditioned on $\gamma_i > \gamma_j, \gamma_j < \gamma_{th}$.

Let us assume that the number of coherent time-slots is A and the number of bits transmitted during this coherence time is B_i per transmission for S_i . Thus, N_{NC}^b and N_{OUS}^b for S_i can be written as

$$N_{NC}^b = 2AB_i P_r(\min(\gamma_i, \gamma_j) > \gamma_{th}), \quad (\text{B.2})$$

and

$$N_{OUS}^b = 3AB_i P_r(\gamma_i > \gamma_j, \gamma_j < \gamma_{th}), \quad (\text{B.3})$$

respectively. $P_r(\min(\gamma_i, \gamma_j) > \gamma_{th})$ and $P_r(\gamma_i > \gamma_j, \gamma_j < \gamma_{th})$ are the probabilities of using NC and OUS, respectively, which are derived as

$$P_r(\min(\gamma_i, \gamma_j) > \gamma_{th}) = \int_{\gamma_{th}}^{\infty} \frac{1}{\bar{\gamma}_i} e^{-\frac{\gamma_i}{\bar{\gamma}_i}} d\gamma_i \int_{\gamma_{th}}^{\infty} \frac{1}{\bar{\gamma}_j} e^{-\frac{\gamma_j}{\bar{\gamma}_j}} d\gamma_j = e^{-(\frac{1}{\bar{\gamma}_i} + \frac{1}{\bar{\gamma}_j})\gamma_{th}}, \quad (\text{B.4})$$

and

$$P_r(\gamma_i > \gamma_j, \gamma_j < \gamma_{th}) = \int_0^{\gamma_{th}} \frac{1}{\bar{\gamma}_j} e^{-\frac{\gamma_j}{\bar{\gamma}_j}} d\gamma_j \int_{\gamma_j}^{\infty} \frac{1}{\bar{\gamma}_i} e^{-\frac{\gamma_i}{\bar{\gamma}_i}} d\gamma_i = \frac{\bar{\gamma}_i}{\bar{\gamma}_i + \bar{\gamma}_j} \left(1 - e^{-(\frac{1}{\bar{\gamma}_i} + \frac{1}{\bar{\gamma}_j})\gamma_{th}}\right). \quad (\text{B.5})$$

Plugging (B.2), (B.3) into (B.1), we obtain (4.3).

B.2 Proof of Lemma 4.2

The BER over any of the links can be expressed as

$$P(\varepsilon_{im} | \gamma_{im} > \gamma_{th}) = \int_0^{\infty} P_e^{4\text{-QAM}}(\gamma_{im}) f_{\gamma_{im} | \gamma_{im} > \gamma_{th}}(\gamma_{im}) d\gamma_{im}, \quad (\text{B.6})$$

and

$$P(\varepsilon_{im}^{hp} | \gamma_{im} > \gamma_{th}) = \int_0^{\infty} P_{e, hp}^{4/16\text{-QAM}}(\gamma_{im}) f_{\gamma_{im} | \gamma_{im} > \gamma_{th}}(\gamma_{im}) d\gamma_{im}, \quad (\text{B.7})$$

where $P_e^{4\text{-QAM}}(\gamma_{im})$ and $P_{e,hp}^{4/16\text{-QAM}}(\gamma_{im})$ are the exact conditional BER for 4-QAM and the HP bits of 4/16-QAM, conditioned on the instantaneous SNR, and are given by [83]

$$P_e^{4\text{-QAM}}(\gamma_{im}) = \frac{1}{2} \operatorname{erfc} \sqrt{\gamma_{im}}, \quad (\text{B.8})$$

and [43]

$$P_{e,hp}^{4/16\text{-QAM}}(\gamma_{im}) = \frac{1}{2} \left[\frac{1}{2} \operatorname{erfc} \sqrt{\frac{2(d^2 - 2d + 1)}{1 + d^2} \gamma_{im}} + \frac{1}{2} \operatorname{erfc} \sqrt{\frac{2(d^2 + 2d + 1)}{1 + d^2} \gamma_{im}} \right], \quad (\text{B.9})$$

respectively, where d is the constellation priority parameter and $f_{\gamma_{im}|\gamma_{im} > \gamma_{th}}(\gamma_{im})$ is the conditional pdf of γ_{im} conditioned on $\gamma_{im} > \gamma_{th}$, which is derived as

$$f_{\gamma_{im}|\gamma_{im} > \gamma_{th}}(\gamma_{im}) = e^{\frac{1}{\bar{\gamma}_{im}} \gamma_{th}} \frac{1}{\bar{\gamma}_{im}} e^{-\frac{1}{\bar{\gamma}_{im}} \gamma_{im}}. \quad (\text{B.10})$$

Plugging (B.8) and (B.10) into (B.6), we obtain (4.5). Similarly, plugging (B.9) and (B.10) into (B.7) and integrating by parts, we obtain (4.6).

B.3 Proof of Lemma 4.3

The BER over any of the links for the LP bits can be expressed as

$$P(\varepsilon_{im}^{lp} | \gamma_{im} > \gamma_{th}) = \int_0^{\infty} P_{e,lp}^{4/16\text{-QAM}}(\gamma_{im}) f_{\gamma_{im}|\gamma_{im} > \gamma_{th}}(\gamma_{im}) d\gamma_{im}, \quad (\text{B.11})$$

where $P_{e,lp}^{4/16\text{-QAM}}(\gamma_{im})$ is the exact conditional BER for the LP bits, conditioned on the instantaneous SNR, for the 4/16-QAM modulation, and is given by [43]

$$\begin{aligned} P_{e,lp}^{4/16\text{-QAM}}(\gamma_{im}) &= \frac{1}{2} \operatorname{erfc} \sqrt{\frac{2}{1 + d^2} \gamma_{im}} + \frac{1}{4} \operatorname{erfc} \sqrt{\frac{2(4d^2 - 4d + 1)}{1 + d^2} \gamma_{im}} \\ &\quad - \frac{1}{2} \operatorname{erfc} \sqrt{\frac{2(4d^2 + 4d + 1)}{1 + d^2} \gamma_{im}}. \end{aligned} \quad (\text{B.12})$$

Then plugging (B.10) and (B.12) into (B.11) and carrying out the integration, we obtain (4.10).

B.4 Proof of Lemma 4.4

For the M -QAM modulation, the BER over any of the links can be expressed as

$$P(\varepsilon_{im} | \gamma_i > \gamma_j, \gamma_j < \gamma_{th}) = \int_0^{\infty} P_e^{M\text{-QAM}}(\gamma_{im}) f_{\gamma_{im} | \gamma_i > \gamma_j, \gamma_j < \gamma_{th}}(\gamma_{im}) d\gamma_{im}, \quad (\text{B.13})$$

where $i, j, n, m = 1, 2$, and $i \neq j, m \neq n$, $P_e^{M\text{-QAM}}(\gamma_{im})$ is the exact conditional BER, conditioned on the instantaneous SNR, and is given by [83]

$$P_e^{M\text{-QAM}}(\gamma_{im}) = \frac{1}{\sqrt{M} \log_2(\sqrt{M})} \sum_{k=1}^{\log_2(\sqrt{M})} \sum_{i=0}^{(1-2^{-k})\sqrt{M}-1} \left[(-1)^{\lfloor \frac{i \cdot 2^{k-1}}{\sqrt{M}} \rfloor} \times \left(2^{k-1} - \left\lfloor \frac{i \cdot 2^{k-1}}{\sqrt{M}} + \frac{1}{2} \right\rfloor \right) \right] \cdot \text{erfc} \left((2i+1) \sqrt{\frac{3 \log_2(\sqrt{M}) \gamma_{im}}{2(M-1)}} \right), \quad (\text{B.14})$$

and $f_{\gamma_{im} | \gamma_{im} > \gamma_{th}}(\gamma_{im})$ is the conditional pdf of γ_{im} conditioned on $\gamma_{im} > \gamma_{th}$, which is derived in (B.25) and (B.26) in Lemma 4.5. Note that the pdfs $f_{\gamma_{im} | \gamma_i > \gamma_j, \gamma_j < \gamma_{th}}(\gamma_{im})$ have different expressions for $\gamma_{im} < \gamma_{th}$ and $\gamma_{im} > \gamma_{th}$. Therefore, (B.13) can be rewritten as

$$P(\varepsilon_{im} | \gamma_i > \gamma_j, \gamma_j < \gamma_{th}) = \int_0^{\gamma_{th}} P_e^{M\text{-QAM}}(\gamma_{im}) f_{\gamma_{im} | \gamma_i > \gamma_j, \gamma_j < \gamma_{th}}(\gamma_{im}) d\gamma_{im} + \int_{\gamma_{th}}^{\infty} P_e^{M\text{-QAM}}(\gamma_{im}) f_{\gamma_{im} | \gamma_i > \gamma_j, \gamma_j < \gamma_{th}}(\gamma_{im}) d\gamma_{im}. \quad (\text{B.15})$$

Plugging (B.14), (B.25) and (B.26) into (B.15) and carrying out the integration, we obtain (4.12).

B.5 Proof of Lemma 4.5

The pdf of γ_{im} , given $\gamma_i > \gamma_j, \gamma_j < \gamma_{th}$, can be expressed as

$$f_{\gamma_{im} | \gamma_i > \gamma_j, \gamma_j < \gamma_{th}}(\gamma_{im}) = \int_0^{\infty} f_{\gamma_{im} | \gamma_i = \gamma}(\gamma_{im}) f_{\gamma_i | \gamma_i > \gamma_j, \gamma_j < \gamma_{th}}(\gamma) d\gamma, \quad (\text{B.16})$$

where $\gamma_i = \min(\gamma_{im}, \gamma_{in})$ for $i, j, n, m = 1, 2$ and $i \neq j, m \neq n$. The pdfs of γ_{im} and γ_i are given in (4.1) and (4.2), respectively. Then (B.16) can be further expressed as [82]

$$f_{\gamma_{im}|\gamma_i > \gamma_j, \gamma_j < \gamma_{th}}(\gamma_{im}) = \int_0^\infty \frac{\frac{1}{\bar{\gamma}_{im}} e^{-\frac{\gamma_{im}}{\bar{\gamma}_{im}}} \frac{1}{\bar{\gamma}_{in}} e^{-\frac{\gamma_{in}}{\bar{\gamma}_{in}}}}{\frac{1}{\bar{\gamma}_i} e^{-\frac{\gamma_i}{\bar{\gamma}_i}}} f_{\gamma_i|\gamma_i > \gamma_j, \gamma_j < \gamma_{th}}(\gamma) d\gamma + \frac{\frac{1}{\bar{\gamma}_{im}} e^{-\frac{\gamma_{im}}{\bar{\gamma}_{im}}} e^{-\frac{\gamma_{in}}{\bar{\gamma}_{in}}}}{\frac{1}{\bar{\gamma}_i} e^{-\frac{\gamma_{im}}{\bar{\gamma}_i}}} f_{\gamma_i|\gamma_i > \gamma_j, \gamma_j < \gamma_{th}}(\gamma_{im}). \quad (\text{B.17})$$

The conditional CDF of γ_i , conditioned on $\gamma_i > \gamma_j$ and $\gamma_j < \gamma_{th}$, is defined as

$$F_{\gamma_i|\gamma_i > \gamma_j, \gamma_j < \gamma_{th}}(\gamma) = \frac{Pr(\gamma_i < \gamma, \gamma_i > \gamma_j, \gamma_j < \gamma_{th})}{Pr(\gamma_i > \gamma_j, \gamma_j < \gamma_{th})}. \quad (\text{B.18})$$

By using the law of total probability, the numerator in (B.18) is given by

$$\begin{aligned} & Pr(\gamma_i < \gamma, \gamma_i > \gamma_j, \gamma_j < \gamma_{th}) \\ &= Pr(\gamma_i < \gamma, \gamma_i > \gamma_j, \gamma_i < \gamma_{th}) + Pr(\gamma_i < \gamma, \gamma_{th} > \gamma_j, \gamma_i > \gamma_{th}) \\ &= \begin{cases} Pr(\gamma_i < \gamma, \gamma_i > \gamma_j), & \gamma < \gamma_{th} \\ Pr(\gamma_i < \gamma_{th}, \gamma_i > \gamma_j) + Pr(\gamma_i < \gamma, \gamma_i > \gamma_{th}, \gamma_j < \gamma_{th}), & \gamma > \gamma_{th} \end{cases} \end{aligned} \quad (\text{B.19})$$

where

$$\begin{aligned} Pr(\gamma_i < \gamma, \gamma_i > \gamma_j) &= \int_0^\gamma \frac{1}{\bar{\gamma}_i} e^{-\frac{\gamma_i}{\bar{\gamma}_i}} d\gamma_i \int_0^{\gamma_i} \frac{1}{\bar{\gamma}_j} e^{-\frac{\gamma_j}{\bar{\gamma}_j}} d\gamma_j \\ &= 1 - e^{-\frac{1}{\bar{\gamma}_i} \gamma} - \frac{\bar{\gamma}_j}{\bar{\gamma}_i + \bar{\gamma}_j} \left(1 - e^{-(\frac{1}{\bar{\gamma}_i} + \frac{1}{\bar{\gamma}_j}) \gamma} \right), \end{aligned} \quad (\text{B.20})$$

and

$$\begin{aligned} Pr(\gamma_i < \gamma_{th}, \gamma_i > \gamma_j) &= \int_0^{\gamma_{th}} \frac{1}{\bar{\gamma}_i} e^{-\frac{\gamma_i}{\bar{\gamma}_i}} d\gamma_i \int_0^{\gamma_i} \frac{1}{\bar{\gamma}_j} e^{-\frac{\gamma_j}{\bar{\gamma}_j}} d\gamma_j \\ &= 1 - e^{-\frac{1}{\bar{\gamma}_i} \gamma_{th}} - \frac{\bar{\gamma}_j}{\bar{\gamma}_i + \bar{\gamma}_j} \left(1 - e^{-(\frac{1}{\bar{\gamma}_i} + \frac{1}{\bar{\gamma}_j}) \gamma_{th}} \right), \end{aligned} \quad (\text{B.21})$$

and

$$\begin{aligned} Pr(\gamma_i < \gamma, \gamma_i > \gamma_{th}, \gamma_j < \gamma_{th}) &= \int_{\gamma_{th}}^\gamma \frac{1}{\bar{\gamma}_i} e^{-\frac{\gamma_i}{\bar{\gamma}_i}} d\gamma_i \int_0^{\gamma_{th}} \frac{1}{\bar{\gamma}_j} e^{-\frac{\gamma_j}{\bar{\gamma}_j}} d\gamma_j \\ &= \left(e^{-\frac{1}{\bar{\gamma}_i} \gamma_{th}} - e^{-\frac{1}{\bar{\gamma}_i} \gamma} \right) \left(1 - e^{-\frac{1}{\bar{\gamma}_j} \gamma_{th}} \right). \end{aligned} \quad (\text{B.22})$$

The denominator in (B.18) is given by

$$\begin{aligned} P_r(\gamma_i > \gamma_j, \gamma_j < \gamma_{th}) &= \int_0^{\gamma_{th}} \frac{1}{\bar{\gamma}_j} e^{-\frac{\gamma_j}{\bar{\gamma}_j}} d\gamma_j \int_{r_j}^{\infty} \frac{1}{\bar{\gamma}_i} e^{-\frac{\gamma_i}{\bar{\gamma}_i}} d\gamma_i \\ &= \frac{\bar{\gamma}_i}{\bar{\gamma}_i + \bar{\gamma}_j} \left(1 - e^{-\left(\frac{1}{\bar{\gamma}_i} + \frac{1}{\bar{\gamma}_j}\right)\gamma_{th}} \right). \end{aligned} \quad (\text{B.23})$$

Plugging (B.20), (B.21), (B.22) and (B.23) into (B.18), we can derive the conditional CDF $F_{\gamma_i|\gamma_i > \gamma_j, \gamma_j < \gamma_{th}}(\gamma)$.

The conditional pdf $f_{\gamma_i|\gamma_i > \gamma_j, \gamma_j < \gamma_{th}}(\gamma)$ is given by taking derivative of $F_{\gamma_i|\gamma_i > \gamma_j, \gamma_j < \gamma_{th}}(\gamma)$ as

$$f_{\gamma_i|\gamma_i > \gamma_j, \gamma_j < \gamma_{th}}(\gamma) = \begin{cases} \frac{\frac{\bar{\gamma}_i + \bar{\gamma}_j}{\bar{\gamma}_i^2} \left(e^{-\frac{1}{\bar{\gamma}_i}\gamma} - e^{-\left(\frac{1}{\bar{\gamma}_i} + \frac{1}{\bar{\gamma}_j}\right)\gamma} \right)}{1 - e^{-\left(\frac{1}{\bar{\gamma}_i} + \frac{1}{\bar{\gamma}_j}\right)\gamma_{th}}}, & \gamma_i < \gamma_{th} \\ \frac{\frac{\bar{\gamma}_i + \bar{\gamma}_j}{\bar{\gamma}_i^2} e^{-\frac{1}{\bar{\gamma}_i}\gamma} \left(1 - e^{-\frac{1}{\bar{\gamma}_j}\gamma_{th}} \right)}{1 - e^{-\left(\frac{1}{\bar{\gamma}_i} + \frac{1}{\bar{\gamma}_j}\right)\gamma_{th}}}, & \gamma_i > \gamma_{th} \end{cases}. \quad (\text{B.24})$$

Then for $\gamma_{im} > \gamma_{th}$, (B.17) can be further expressed as

$$\begin{aligned} f_{\gamma_{im}|\gamma_i > \gamma_j, \gamma_j < \gamma_{th}}(\gamma_{im}) &= \int_0^{\gamma_{th}} \frac{\frac{1}{\bar{\gamma}_{im}} e^{-\frac{\gamma_{im}}{\bar{\gamma}_{im}}} \frac{1}{\bar{\gamma}_{in}} e^{-\frac{\gamma_{in}}{\bar{\gamma}_{in}}} \frac{\bar{\gamma}_i + \bar{\gamma}_j}{\bar{\gamma}_i^2} \left(e^{-\frac{1}{\bar{\gamma}_i}\gamma} - e^{-\left(\frac{1}{\bar{\gamma}_i} + \frac{1}{\bar{\gamma}_j}\right)\gamma} \right)}{\frac{1}{\bar{\gamma}_i} e^{-\frac{\gamma_i}{\bar{\gamma}_i}} \left(1 - e^{-\left(\frac{1}{\bar{\gamma}_i} + \frac{1}{\bar{\gamma}_j}\right)\gamma_{th}} \right)} d\gamma \\ &+ \int_{\gamma_{th}}^{\gamma_{im}} \frac{\frac{1}{\bar{\gamma}_{im}} e^{-\frac{\gamma_{im}}{\bar{\gamma}_{im}}} \frac{1}{\bar{\gamma}_{in}} e^{-\frac{\gamma_{in}}{\bar{\gamma}_{in}}} \frac{\bar{\gamma}_i + \bar{\gamma}_j}{\bar{\gamma}_i^2} e^{-\frac{1}{\bar{\gamma}_i}\gamma} \left(1 - e^{-\frac{1}{\bar{\gamma}_j}\gamma_{th}} \right)}{\frac{1}{\bar{\gamma}_i} e^{-\frac{\gamma_i}{\bar{\gamma}_i}} \left(1 - e^{-\left(\frac{1}{\bar{\gamma}_i} + \frac{1}{\bar{\gamma}_j}\right)\gamma_{th}} \right)} d\gamma \\ &+ \frac{\frac{1}{\bar{\gamma}_{im}} e^{-\frac{\gamma_{im}}{\bar{\gamma}_{im}}} e^{-\frac{\gamma_{in}}{\bar{\gamma}_{in}}} \frac{\bar{\gamma}_i + \bar{\gamma}_j}{\bar{\gamma}_i^2} e^{-\frac{1}{\bar{\gamma}_i}\gamma_{im}} \left(1 - e^{-\frac{1}{\bar{\gamma}_j}\gamma_{th}} \right)}{\frac{1}{\bar{\gamma}_i} e^{-\frac{\gamma_i}{\bar{\gamma}_i}} \left(1 - e^{-\left(\frac{1}{\bar{\gamma}_i} + \frac{1}{\bar{\gamma}_j}\right)\gamma_{th}} \right)} \\ &= \frac{\bar{\gamma}_{in} (\bar{\gamma}_i + \bar{\gamma}_j) \left(1 - e^{-\left(\frac{1}{\bar{\gamma}_{in}} + \frac{1}{\bar{\gamma}_j}\right)\gamma_{th}} \right)}{\bar{\gamma}_{im} \bar{\gamma}_i (\bar{\gamma}_{in} + \bar{\gamma}_j) \left(1 - e^{-\left(\frac{1}{\bar{\gamma}_i} + \frac{1}{\bar{\gamma}_j}\right)\gamma_{th}} \right)} e^{-\frac{1}{\bar{\gamma}_{im}}\gamma_{im}}, \end{aligned} \quad (\text{B.25})$$

and for $\gamma_{im} < \gamma_{th}$, (B.17) can be further expressed as

$$\begin{aligned} f_{\gamma_{im}|\gamma_i > \gamma_j, \gamma_j < \gamma_{th}}(\gamma_{im}) &= \int_0^{\gamma_{th}} \frac{\frac{1}{\bar{\gamma}_{im}} e^{-\frac{\gamma_{im}}{\bar{\gamma}_{im}}} \frac{1}{\bar{\gamma}_{in}} e^{-\frac{\gamma_{in}}{\bar{\gamma}_{in}}} \frac{\bar{\gamma}_i + \bar{\gamma}_j}{\bar{\gamma}_i^2} \left(e^{-\frac{1}{\bar{\gamma}_i}\gamma} - e^{-\left(\frac{1}{\bar{\gamma}_i} + \frac{1}{\bar{\gamma}_j}\right)\gamma} \right)}{\frac{1}{\bar{\gamma}_i} e^{-\frac{\gamma_i}{\bar{\gamma}_i}} \left(1 - e^{-\left(\frac{1}{\bar{\gamma}_i} + \frac{1}{\bar{\gamma}_j}\right)\gamma_{th}} \right)} d\gamma \\ &+ \frac{\frac{1}{\bar{\gamma}_{im}} e^{-\frac{\gamma_{im}}{\bar{\gamma}_{im}}} e^{-\frac{\gamma_{in}}{\bar{\gamma}_{in}}} \frac{\bar{\gamma}_i + \bar{\gamma}_j}{\bar{\gamma}_i^2} \left(e^{-\frac{1}{\bar{\gamma}_i}\gamma_{im}} - e^{-\left(\frac{1}{\bar{\gamma}_i} + \frac{1}{\bar{\gamma}_j}\right)\gamma_{im}} \right)}{\frac{1}{\bar{\gamma}_i} e^{-\frac{\gamma_i}{\bar{\gamma}_i}} \left(1 - e^{-\left(\frac{1}{\bar{\gamma}_i} + \frac{1}{\bar{\gamma}_j}\right)\gamma_{th}} \right)} \\ &= \frac{\bar{\gamma}_{in} (\bar{\gamma}_i + \bar{\gamma}_j) \left[e^{-\frac{1}{\bar{\gamma}_{im}}\gamma_{im}} - e^{-\left(\frac{1}{\bar{\gamma}_i} + \frac{1}{\bar{\gamma}_j}\right)\gamma_{im}} \right]}{\bar{\gamma}_{im} \bar{\gamma}_i (\bar{\gamma}_{in} + \bar{\gamma}_j) \left(1 - e^{-\left(\frac{1}{\bar{\gamma}_i} + \frac{1}{\bar{\gamma}_j}\right)\gamma_{th}} \right)}, \end{aligned} \quad (\text{B.26})$$

where $i, j, n, m = 1, 2$ and $i \neq j, m \neq n$.

Appendix C Derivations for Chapter 5

C.1 Proof of Lemma 5.1

For subset selection, $\gamma_{k,\min}$ varies identically and independently and its pdf for a network with m pairs and n relays can be expressed as [31]

$$f_{\gamma_{\min}}(\gamma_{\min}) = \frac{1}{\bar{\gamma}_{\min}} e^{-\frac{\gamma_{\min}}{\bar{\gamma}_{\min}}}, \quad (\text{C.1})$$

where $\bar{\gamma}_{\min} = \frac{1}{m} \frac{\bar{\gamma}_{SR}\bar{\gamma}_{RD}}{\bar{\gamma}_{SR} + \bar{\gamma}_{RD}}$. Since the instantaneous SNR range $[0, \infty]$ is divided by $N - 1$ thresholds, γ_{thl} ($l = 1, 2, \dots, N - 1$), there are N quantization levels. If the worst E2E SNR of the selected choice, $\gamma_{k^*,\min}$, belongs to the quantization level $[\gamma_{thl}, \gamma_{th(l+1)})$, it means that at least one of $\gamma_{k,\min}$ belongs to this quantization level and no $\gamma_{k,\min}$ are greater than $\gamma_{th(l+1)}$. For the probability term in (5.4) when $l = 0$, i.e., $\gamma_{k^*,\min}$ is less than γ_{th1} , it means that all $\gamma_{k,\min}$ are less than γ_{th1} . Then we have

$$\begin{aligned} P_r(\gamma_{k^*,\min} < \gamma_{th1}) &= (P_r(\gamma_{\min} < \gamma_{th1}))^n \\ &= \left(\int_0^{\gamma_{th1}} \frac{1}{\bar{\gamma}_{\min}} e^{-\frac{\gamma_{\min}}{\bar{\gamma}_{\min}}} d\gamma_{\min} \right)^n \\ &= \left(1 - e^{-\frac{\gamma_{th1}}{\bar{\gamma}_{\min}}} \right)^n. \end{aligned} \quad (\text{C.2})$$

When $l \geq 1$, the probability terms in (5.4) can be expressed as

$$\begin{aligned}
P_r(\gamma_{thl} < \gamma_{k^*,\min} < \gamma_{th(l+1)}) &= \sum_{j=1}^n \frac{n!}{j!(n-j)!} (P_r(\gamma_{thl} < \gamma_{\min} < \gamma_{th(l+1)}))^j (P_r(\gamma_{\min} < \gamma_{thl}))^{n-j} \\
&= \sum_{j=1}^n \frac{n!}{j!(n-j)!} \left(\int_{\gamma_{thl}}^{\gamma_{th(l+1)}} \frac{1}{\bar{\gamma}_{\min}} e^{-\frac{\gamma_{\min}}{\bar{\gamma}_{\min}}} d\gamma_{\min} \right)^j \left(\int_0^{\gamma_{thl}} \frac{1}{\bar{\gamma}_{\min}} e^{-\frac{\gamma_{\min}}{\bar{\gamma}_{\min}}} d\gamma_{\min} \right)^{n-j} \\
&= \sum_{j=1}^n \frac{n!}{j!(n-j)!} \left(e^{-\frac{\gamma_{thl}}{\bar{\gamma}_{\min}}} - e^{-\frac{\gamma_{th(l+1)}}{\bar{\gamma}_{\min}}} \right)^j \left(1 - e^{-\frac{\gamma_{thl}}{\bar{\gamma}_{\min}}} \right)^{n-j}. \tag{C.3}
\end{aligned}$$

The BER conditioned on $\gamma_{thl} < \gamma_{k^*,\min} < \gamma_{th(l+1)}$ can be expressed as

$$P(\varepsilon | \gamma_{thl} < \gamma_{k^*,\min} < \gamma_{th(l+1)}) = \int_0^{\infty} d \cdot \operatorname{erfc} \sqrt{a\gamma_{\min}} f_{\gamma_{\min} | \gamma_{thl} < \gamma_{\min} < \gamma_{th(l+1)}}(\gamma_{\min}) d\gamma_{\min}, \tag{C.4}$$

where $f_{\gamma_{\min} | \gamma_{thl} < \gamma_{\min} < \gamma_{th(l+1)}}(\gamma_{\min})$ is the conditional pdf of γ_{\min} conditioned on $\gamma_{thl} < \gamma_{\min} < \gamma_{th(l+1)}$, which is derived as

$$f_{\gamma_{\min} | \gamma_{thl} < \gamma_{\min} < \gamma_{th(l+1)}}(\gamma_{\min}) = \frac{1}{e^{-\frac{1}{\bar{\gamma}_{\min}} \gamma_{thl}} - e^{-\frac{1}{\bar{\gamma}_{\min}} \gamma_{th(l+1)}}} \frac{1}{\bar{\gamma}_{\min}} e^{-\frac{1}{\bar{\gamma}_{\min}} \gamma_{\min}}. \tag{C.5}$$

Plugging (C.5) into (C.4) and carrying out the integration, we obtain

$$P(\varepsilon | \gamma_{thl} < \gamma_{k^*,\min} < \gamma_{th(l+1)}) = \frac{d}{e^{-\frac{1}{\bar{\gamma}_{\min}} \gamma_{thl}} - e^{-\frac{1}{\bar{\gamma}_{\min}} \gamma_{th(l+1)}}} I(a, \bar{\gamma}_{\min}, \gamma_{thl}, \gamma_{th(l+1)}). \tag{C.6}$$

Plugging (C.2), (C.3) and (C.6) into (5.4) and then into (5.3) yields (5.5), which completes the proof.

Note that the obtained results can be adapted to other modulation schemes. For instance, for M-QAM, the exact BER, conditioned on the instantaneous SNR, γ , is given by [83]

$$\begin{aligned}
P_e^{M\text{-QAM}}(\gamma) &= \frac{1}{\sqrt{M} \log_2(\sqrt{M})} \sum_{k=1}^{\log_2(\sqrt{M})} \sum_{i=0}^{(1-2^{-k})\sqrt{M}-1} \left[(-1)^{\lfloor \frac{i \cdot 2^{k-1}}{\sqrt{M}} \rfloor} \times \left(2^{k-1} - \left\lfloor \frac{i \cdot 2^{k-1}}{\sqrt{M}} + \frac{1}{2} \right\rfloor \right) \right] \\
&\quad \cdot \operatorname{erfc} \left((2i+1) \sqrt{\frac{3 \log_2(\sqrt{M}) \gamma}{2(M-1)}} \right).
\end{aligned}$$

Therefore, the analysis in this work can be directly extended to M-QAM by setting $a = (2i + 1)^{2\frac{3\log_2(\sqrt{M})}{2(M-1)}}$ and $d = \frac{1}{\sqrt{M}\log_2(\sqrt{M})} \sum_{k=1}^{\log_2(\sqrt{M})} \sum_{i=0}^{(1-2^{-k})\sqrt{M}-1} (-1)^{\lfloor \frac{i \cdot 2^{k-1}}{\sqrt{M}} \rfloor} \times \left(2^{k-1} - \left\lfloor \frac{i \cdot 2^{k-1}}{\sqrt{M}} + \frac{1}{2} \right\rfloor \right)$.

C.2 Proof of Lemma 5.2

Since there are correlations among $\gamma_{k,\min}$ for different k , the calculation of the selected worst E2E BER cannot be done in the same way as that of subset selection. Alternatively, we can calculate the probability terms in Equation (5.4) in the following way. We first derive the probability terms for the case when there is only one threshold, γ_{thl} ($l = 1, 2, \dots, N - 1$). Then we generalize it to multiple thresholds. In the case of one threshold, the quantized CSIs are only distinguished by whether they are greater or less than γ_{thl} . As a consequence, the selected worst E2E SNR, i.e., $\gamma_{k^*,\min}$, can only be either greater or less than γ_{thl} . Let T denote the number of γ_{ij}^q that are greater than γ_{thl} . Note that T is an integer. Since the total number of items in the E2E SNR matrix for a network with two pairs and n relays is $2n$, the probability terms for this case can be written as

$$P_r(\gamma_{k^*,\min} > \gamma_{thl}) = \sum_{t=0}^{2n} P_r(\gamma_{k^*,\min} > \gamma_{thl} | T = t) P_r(T = t), \quad (\text{C.7})$$

and

$$P_r(\gamma_{k^*,\min} < \gamma_{thl}) = \sum_{t=0}^{2n} P_r(\gamma_{k^*,\min} < \gamma_{thl} | T = t) P_r(T = t), \quad (\text{C.8})$$

where $P_r(T = t)$ represents the probability of having exactly t items greater than γ_{thl} , and $P_r(\gamma_{k^*,\min} > \gamma_{thl} | T = t)$ is the probability that $\gamma_{k^*,\min}$ is greater than γ_{thl} given that there are t items greater than γ_{thl} . Note that the pdf of the E2E SNR is given in (5.1). The term $P_r(T = t)$ in (C.7) and (C.8) can be derived as

$$\begin{aligned} P_r(T = t) &= \frac{2n!}{t!(2n-t)!} \left(\int_{\gamma_{thl}}^{\infty} \frac{1}{\gamma} e^{-\frac{\gamma}{\gamma}} d\gamma \right)^t \left(\int_0^{\gamma_{thl}} \frac{1}{\gamma} e^{-\frac{\gamma}{\gamma}} d\gamma \right)^{2n-t} \\ &= \frac{2n!}{t!(2n-t)!} e^{-\frac{t\gamma_{thl}}{\gamma}} \left(1 - e^{-\frac{\gamma_{thl}}{\gamma}} \right)^{2n-t}. \end{aligned} \quad (\text{C.9})$$

For $0 \leq T \leq 1$, since $\gamma_{k^*,\min}$ is always less than γ_{thl} in this case, we have

$$P_r(\gamma_{k^*,\min} > \gamma_{thl} | 0 \leq T \leq 1) = 0, \quad (\text{C.10})$$

and

$$P_r(\gamma_{k^*,\min} < \gamma_{thl} | 0 \leq T \leq 1) = 1. \quad (\text{C.11})$$

For $T = 2$, we find that $\gamma_{k^*,\min}$ will be greater than γ_{thl} once the two items that are greater than γ_{thl} are on the same row in the E2E SNR matrix. Since there are a total of $\frac{n!}{(n-2)!}$ rows in the fullset E2E SNR matrix, we have

$$P_r(\gamma_{k^*,\min} > \gamma_{thl} | T = 2) = \frac{\frac{n!}{(n-2)!}}{\frac{2n!}{2(2n-2)!}}, \quad (\text{C.12})$$

and

$$P_r(\gamma_{k^*,\min} < \gamma_{thl} | T = 2) = \frac{\frac{2n!}{2(2n-2)!} - \frac{n!}{(n-2)!}}{\frac{2n!}{2(2n-2)!}}. \quad (\text{C.13})$$

For $2 < T \leq n$, we observe that $\gamma_{k^*,\min}$ will be less than γ_{thl} if the items that are greater than γ_{thl} are in the same column of the E2E SNR matrix. Otherwise, $\gamma_{k^*,\min}$ will be greater than γ_{thl} in this case. Since the total number of non identical items in one column is n and there are two columns in the matrix, we have

$$P_r(\gamma_{k^*,\min} > \gamma_{thl} | 2 < T \leq n) = \frac{\frac{2n!}{t!(2n-t)!} - 2\frac{n!}{t!(n-t)!}}{\frac{2n!}{t!(2n-t)!}}, \quad (\text{C.14})$$

and

$$P_r(\gamma_{k^*,\min} < \gamma_{thl} | 2 < T \leq n) = \frac{2\frac{n!}{t!(n-t)!}}{\frac{2n!}{t!(2n-t)!}}. \quad (\text{C.15})$$

For $n < T \leq 2n$, $\gamma_{k^*,\min}$ will always be greater than γ_{thl} in this case. Then we have

$$P_r(\gamma_{k^*,\min} > \gamma_{thl} | n < T \leq 2n) = 1, \quad (\text{C.16})$$

and

$$P_r(\gamma_{k^*,\min} < \gamma_{thl} | n < T \leq 2n) = 0. \quad (\text{C.17})$$

Then plugging (C.9)-(C.17) into C.7) and C.8), we obtain the expressions for $P_r(\gamma_{k^*,\min} < \gamma_{thl})$, which is given in (5.7) and $P_r(\gamma_{k^*,\min} > \gamma_{thl})$. By replacing γ_{thl} with $\gamma_{th(l+1)}$, we obtain $P_r(\gamma_{k^*,\min} > \gamma_{th(l+1)})$ as expressed in (5.6). Now we generalize the results of one threshold to multiple thresholds. By observing that

$$P_r(\gamma_{thl} < \gamma_{k^*,\min} < \gamma_{th(l+1)}) = 1 - P_r(\gamma_{k^*,\min} > \gamma_{th(l+1)}) - P_r(\gamma_{k^*,\min} < \gamma_{thl}), \quad (\text{C.18})$$

we can indirectly calculate the probability term in (5.4) from (C.18). Note that we can also use $P_r(\gamma_{thl} < \gamma_{k^*,\min} < \gamma_{th(l+1)}) = P_r(\gamma_{k^*,\min} > \gamma_{thl}) - P_r(\gamma_{k^*,\min} > \gamma_{th(l+1)})$ or $P_r(\gamma_{thl} < \gamma_{k^*,\min} < \gamma_{th(l+1)}) = P_r(\gamma_{k^*,\min} < \gamma_{th(l+1)}) - P_r(\gamma_{k^*,\min} < \gamma_{thl})$. Then we obtain a closed-form expression for P_e as expressed in Lemma 5. 2.

C.3 Proof of Lemma 5.3

According to the E2E BER given in (5.3) for subset selection, the E2E BER with one threshold is given as

$$P_e = P_{e0} + P_{e1},$$

where P_{e0} and P_{e1} are the BERs that $\gamma_{k^*,\min}$ is less and greater than γ_{th} , respectively. According to (5.4), (C.2), (C.4) and (C.5), P_{e0} can be expressed as

$$\begin{aligned} P_{e0} &= \left(1 - e^{-\frac{\gamma_{th}}{\rho}}\right)^n \frac{1}{1 - e^{-\frac{\gamma_{th}}{\rho}}} \int_0^{\gamma_{th}} \frac{1}{2} \operatorname{erfc} \sqrt{\gamma} \frac{1}{\rho} e^{-\frac{\gamma}{\rho}} d\gamma \\ &\leq \left(1 - e^{-\frac{\gamma_{th}}{\rho}}\right)^{n-1} \int_0^{\infty} \frac{1}{2} \operatorname{erfc} \sqrt{\gamma} \frac{1}{\rho} e^{-\frac{\gamma}{\rho}} d\gamma \\ &\leq \frac{\gamma_{th}^{n-1}}{\rho^{n-1}} \times \int_0^{\infty} \frac{1}{4} e^{-\gamma} \frac{1}{\rho} e^{-\frac{\gamma}{\rho}} d\gamma \end{aligned} \quad (\text{C.19})$$

$$\leq \frac{\gamma_{th}^{n-1}}{4\rho^n}, \quad (\text{C.20})$$

where (C.19) follows from the fact that $1 - e^{-x} \leq x$ and $\operatorname{erfc} \sqrt{x} \leq \frac{1}{2}e^{-x}$. Since the asymptotic behavior will not be changed by the assumption of the symmetric channels and modulation scheme

[77], we simply assume $\bar{\gamma}_{\min} = \rho$ by assuming that the equivalent worst E2E channel gains are modeled as zero mean, unit variance complex Gaussian random variables. We also assume BPSK in this part. According to (5.4), (C.4) and (C.5), P_{e1} can be expressed as

$$\begin{aligned}
P_{e1} &= P_r(\gamma_{k^*,\min} > \gamma_{th}) e^{\frac{1}{\rho}\gamma_{th}} \int_{\gamma_{th}}^{\infty} \frac{1}{2} \operatorname{erfc}\sqrt{\gamma} \frac{1}{\rho} e^{-\frac{\gamma}{\rho}} d\gamma \\
&\leq e^{\frac{1}{\rho}\gamma_{th}} \int_{\gamma_{th}}^{\infty} \frac{1}{2} \operatorname{erfc}\sqrt{\gamma} \frac{1}{\rho} e^{-\frac{\gamma}{\rho}} d\gamma \tag{C.21}
\end{aligned}$$

$$\begin{aligned}
&\leq e^{\frac{1}{\rho}\gamma_{th}} \int_{\gamma_{th}}^{\infty} \frac{1}{4} e^{-\gamma} \frac{1}{\rho} e^{-\frac{\gamma}{\rho}} d\gamma \tag{C.22}
\end{aligned}$$

$$\begin{aligned}
&= \frac{1}{4(1+\rho)} e^{-\gamma_{th}} \\
&\leq \frac{1}{4\rho} e^{-\gamma_{th}}, \tag{C.23}
\end{aligned}$$

where (C.21) follows from knowing that the probability that $\gamma_{k^*,\min} > \gamma_{th}$ is less than one and (C.22) follows from $\operatorname{erfc}\sqrt{x} \leq \frac{1}{2}e^{-x}$. Then plugging (C.23) and (C.20) into (5.3), yields the asymptotic E2E BER for subset selection, which is given by (5.8). This completes the proof.

Bibliography

- [1] A. Sendonaris, E. Erkip and B. Aazhang, “User cooperation diversity part I: system description,” *IEEE Trans. Commun.*, vol. 51, pp. 1927-1938, Nov. 2003.
- [2] A. Sendonaris, E. Erkip and B. Aazhang, “User cooperation diversity part II: implementation aspects and performance analysis,” *IEEE Trans. Commun.*, vol. 51, pp.1927-1938, Nov. 2003.
- [3] J. N. Laneman, D. N. C. Tse, and G. W. Wornell, “Cooperative diversity in wireless networks: Efficient protocols and outage behavior,” *IEEE Trans. Inf. Theory*, vol. 50, pp. 3062-3080, Dec. 2004.
- [4] Z. Yi and I.-M. Kim, “An opportunistic-based protocol for bidirectional cooperative networks,” *IEEE Trans. Wireless Commun.*, vol. 8, no. 9, pp. 4836–4847, Sep. 2009.
- [5] Y. Shi, S. Sharma and Y.-T. Hou, “Optimal relay assignment for cooperative communications,” *Proceedings of the 9th ACM International Symposium on Mobile ad hoc Networking and Computing*, 2008.
- [6] B. Rankov and A. Wittneben, “Spectral efficient protocols for half-duplex fading relay channel,” *IEEE J. Select. Area Commun.*, vol. 25, pp. 379-389, Feb. 2007.
- [7] Y. Wu, P. A. Chou, and S.-Y. Kung, “Information exchange in wireless networks with net-

- work coding and physical-layer broadcast,” in *Proc. CISS*, Baltimore, MD, USA, March. 2005.
- [8] R. Ahlswede, N. Cai, S.-Y. R. Li and R. W. Yeung, “Network information flow,” *IEEE Trans. Inform. Theory*, vol. IT-46, pp. 1204-1216, July 2000.
- [9] P. Larsson, N. Johansson, and K.-E. Sunell, “Coded bi-directional relaying,” *ADHOC05*, Stockholm, Sweden, May 2005.
- [10] T. Wang and G. B. Giannakis, “Complex field network coding for multiuser cooperative communications,” *IEEE J. Sel. Areas Commun.*, vol. 26, no. 3, pp. 561-571, Apr. 2008.
- [11] Hung Viet Nguyen; Chao Xu; Soon Xin Ng; Hanzo, L., “Non-Coherent Near-Capacity Network Coding for Cooperative Multi-User Communications,” *IEEE Trans. Commun.*, vol. 60, no. 10, pp. 3059-3070, Oct. 2012.
- [12] C. Peng, Q. Zhang, M. Zhao, and Y. Yao, “SNCC: A selective network coded cooperation scheme in wireless networks,” in *Proc. IEEE ICC 2007*.
- [13] C. E. Shannon, “Two-way communication channels,” in *Proc. 4th Berkeley Symp. Math. Stat. and Prob.*, vol. 1, pp. 611-644, 1961.
- [14] S. Katti, S. S. Gollakota, and D. Katabi, “Embracing wireless interference: Analog network coding,” *MIT Tech. Report*, Cambridge, Ma, February, 2007.
- [15] K.-S. Hwang, Y.-C. Ko and M.-S. Alouini, “Performance bounds for two-way amplify-and-forward relaying based on relay path selection,” in *Proc. IEEE VTC Spring 2009*.
- [16] K.-S. Hwang, Y.-C. Ko and M.-S. Alouini, “Performance Analysis of Two-Way Amplify and Forward Relaying with Adaptive Modulation,” in *Proc. IEEE PIMRC Spring 2009*.

- [17] S. Zhang, S. C. Liew, P. P. Lam, “Hot Topic: Physical-layer Network Coding,” *ACM Mobi-Com’06*, pp. 358-365, Sept. 2006.
- [18] T. Koike-Akino, P. Popovski, and V. Tarokh, “Optimized constellations for two-way wireless relaying with physical network coding,” *IEEE J. Sel. Areas Commun.*, vol. 27, no. 5, pp. 773-787, 2009.
- [19] H. J. Yang, Y. Choi, and J. Chun, “Modified high-order pams for binary coded physical-layer network coding,” *IEEE Commun. Lett.*, vol. 14, no. 8, pp. 689–691, 2010.
- [20] M. Noori and M. Ardakani, “On symbol mapping for binary physical layer network coding with PSK modulation,” *IEEE Trans. Wireless Commun.*, vol. 11, no. 1, pp. 21–26, Jan. 2012.
- [21] S. Nguyen, A. Ghrayeb, G. Al-Habian and M. Hasna, “Mitigating error propagation in two-way relay channels with network coding,” *IEEE Trans. Wireless Commun.*, vol. 9, no. 11, pp. 3380–3390, Nov. 2010.
- [22] G. Al-Habian, A. Ghrayeb, M. Hasna and A. Abu-Dayya, “Threshold-based relaying in coded cooperative networks,” *IEEE Trans. Veh. Technol.*, vol. 60, no. 1, pp. 123–135, Jan. 2011
- [23] X. Zeng, A. Ghrayeb and M. Hasna, “Joint optimal threshold-based relaying and ML detection in network-coded two-way relay channels,” *IEEE Trans. Commun.*, vol. 60, no. 9, pp. 2657-2667, Sept. 2012.
- [24] X. Zhang, A. Ghrayeb, and M. Hasna, “On relay assignment in network coded cooperative systems,” *IEEE Trans. Wireless Commun.*, vol. 10, no. 3, pp. 868–876, Mar. 2011.
- [25] Y. Li, R. H. Y. Louie, and B. Vucetic, “Relay selection with network coding in two-way relay channels,” *IEEE Trans. Veh. Technol.*, vol. 59, no. 9, pp. 4489–4499, Nov. 2010.

- [26] P. Popovski, and H. Yomo, "The anti-packets can increase the achievable throughput of a wireless multi-hop networks," *IEEE Proc. ICC2006*, 2006.
- [27] Y. Zhao, R. Adve, and T. J. Lim, "Symbol error rate of selection amplify-and-forward relay systems," *IEEE Commun. Lett.*, vol. 10, pp. 757-759, Nov. 2006.
- [28] A. Bletsas, A. Khisti, D. P. Reed, and A. Lippman, "A simple cooperative diversity method based on network path selection," *IEEE J. Sel. Areas Commun.*, vol. 24, no. 3, pp. 659-672, 2006.
- [29] A. Bletsas, H. Shin and M. Z. Win, "Outage-optimal cooperative communications with regenerative relays," in *Proc. CISS 2006*, Mar. 2006.
- [30] J. N. Laneman and G. W. Wornell, "Distributed space-time coded protocols for exploiting cooperative diversity in wireless networks," *IEEE Trans. Inform. Theory*, vol. 59, pp. 2415-2525, Oct. 2003.
- [31] Y. Jing and H. Jafarkhani, "Single and multiple relay selection schemes and their achievable diversity orders," *IEEE Trans. Wireless Commun.*, vol. 8, no. 3, pp. 1414 -1423, Mar. 2009.
- [32] E. Beres and R. S. Adve, "Selection cooperation in multi source cooperative networks," *IEEE Trans. Wireless Commun.*, vol. 7, no. 1, pp. 118-127, 2008.
- [33] S. S. Ikki and M. H. Ahmed, "Performance of multiple-relay cooperative diversity systems with best selection over rayleigh fading channels," *EURASIP J. Advances Signal Processing*, vol. 2008, Article ID 580368.
- [34] A. Adinoyi, Y. Fan, H. Yanikomeroglu, and H. V. Poor, "On the performance of selection relaying," in *Proc. IEEE VTC-Fall*, 2008.

- [35] D. S. Michalopoulos and G. K. Karagiannidis, "Performance analysis of single relay selection in rayleigh fading," *IEEE Trans. Wireless Commun.*, vol. 7, no. 10, pp. 3718 -3724, Oct 2008.
- [36] S. Ikki and M. H. Ahmed, "Performance analysis of adaptive decode-and-forward cooperative diversity networks with the best relay selection scheme," *IEEE Transactions on Communications*, vol. 8, no. 2, pp. 68-72, Feb., 2009.
- [37] X. Zhang, A. Ghrayeb and M. Hasna, "On hierarchical network coding versus opportunistic user selection for two-way relay channels with asymmetric data rates". *IEEE Trans. Commun.*, vol. 61, no. 7, pp. 2900-2910, July 2013.
- [38] X. Zhang, M. Hasna and A. Ghrayeb, "An adaptive transmission scheme for two-way relaying with asymmetric data rates". *Submitted to IEEE Trans. Veh. Technol.*
- [39] X. Zhang, H. Jafarkhani, A. Ghrayeb and M. Hasna, "Relay assignment in multiple source-destination cooperative networks with limited feedback". in *Proc. of IEEE ICC*, Jun. 2014.
- [40] X. Zhang, H. Jafarkhani, A. Ghrayeb and M. Hasna, "Relay assignment in multiple source-destination cooperative networks with limited feedback". *IEEE Trans. Wireless Commun.*, 2014.
- [41] S. Tang, H. Yomo, T. Ueda, R. Miura, and S. Obana, "Full rate network coding via nesting modulation constellations," *EURASIP Journal on WCN*, 2011.
- [42] Y. Hu, K. H. Li, and K. C. Teh, "Performance analysis of two-user multiple access systems with DF relaying and superposition modulation," *IEEE Trans. Veh. Technol.*, vol. 60, pp. 3118–3126, Sep. 2011.

- [43] P.K. Vitthaladevuni and M.-S. Alouini, "A recursive algorithm for the exact BER computation of generalized hierarchical QAM constellations" *IEEE Trans. Inf. theory.*, vol. 49, no. 1, pp. 297-307, Jan. 2003.
- [44] T. Wang, A. Cano, G. B. Giannakis, and F. Ramos, "Multi-tier cooperative broadcasting with hierarchical modulations," *IEEE Trans. Wireless Commun.*, vol. 6, pp. 3047-3057, Aug. 2007.
- [45] M. Chang and S. Lee, "Performance analysis of cooperative communication system with hierarchical modulation over Rayleigh fading channel," *IEEE Trans. Wireless Commun.*, vol. 8, no. 6, pp. 2848-2852, Jun. 2009.
- [46] C. Hausl and J. Hagenauer, "Relaying communication with hierarchical modulation," *IEEE Commun. Lett.*, vol. 11, pp. 64-66, Jan. 2007.
- [47] R. Whang, H. Liu and E. Hong, "Multiuser cooperative relay communication employing hierarchical modulation," *VTC Spring, 2010*, pp. 1-5.
- [48] R. Knopp and P. Humblet, "Information capacity and power control in single-cell multiuser communications," in *Proc. ICC*, Seattle, WA, Jun. 1995, vol. 1, pp. 331-335.
- [49] D. N. C. Tse, "Optimal power allocation over parallel Gaussian channels," in *Proc. ISIT*, Ulm, Germany, Jun. 1997, p. 27.
- [50] P. Viswanath, D. Tse, and R. Laroia, "Opportunistic beamforming using dumb antennas," *IEEE Trans. Inf. theory.*, vol. 48, no. 6, pp. 1277-1294, Jun. 2002.
- [51] L. Yang and M.-S. Alouini, "Performance analysis of multiuser selection diversity," *IEEE Trans. Veh. Technol.*, vol. 55, pp. 1003-1018, May 2006.

- [52] D. Piazza and L. Milstein, "Multiuser diversity-mobility tradeoff: Modeling and performance analysis of a proportional fair scheduling," in *Proc. IEEE Globecom*, Taipei, Taiwan, Nov. 2002, vol. 1, pp. 906–910.
- [53] X. Zhang, W. Wang, and X. Ji, "Multiuser diversity in multiuser two hop cooperative relay wireless networks: System model and performance analysis," *IEEE Trans. Veh. Technol.*, vol. 58, no. 2, pp. 1031–1036, Feb. 2009.
- [54] S. Chen, W. Wang, and X. Zhang, "Performance analysis of multiuser diversity in cooperative multi-relay networks under Rayleigh-fading channels," *IEEE Trans. Wireless Commun.*, vol. 8, no. 7, pp. 3415–3419, Jul. 2009.
- [55] L. Sun, T. Zhang, L. Lu, and H. Niu, "On the combination of cooperative diversity and multiuser diversity in multi-source multi-relay wireless networks," *IEEE Signal Process. Lett.*, vol. 17, no. 6, pp. 535–538, Jun. 2010.
- [56] J. Kim, D. S. Michalopoulos, and R. Schober, "Diversity analysis of multi-user multi-relay networks," *IEEE Trans. Wireless Commun.*, vol. 10, no. 7, pp. 2380–2389, Jul. 2011.
- [57] M. Ju and I.-M. Kim, "Joint relay selection and opportunistic source selection in bidirectional cooperative diversity networks," *IEEE Trans. Veh. Technol.*, vol. 59, no. 6, pp. 2885–2897, Jul. 2010.
- [58] X. Zhang, A. Ghrayeb, and M. Hasna, "Performance analysis of relay assignment schemes for cooperative networks with multiple source-destination pairs," *IEEE Trans. Wireless Commun.*, vol. 11, no. 1, pp. 166–177, Jan. 2012.
- [59] X. Zhang, A. Ghrayeb, and M. Hasna, "Network coding and relay assignment schemes for systems with multiple two-way relay channels," in *Proc. of IEEE ICC*, May. 2010.

- [60] X. Zhang, A. Ghrayeb, and M. Hasna, "Relay assignment schemes for multiple source-destination cooperative networks," in *Proc. of IEEE ICT*, Apr. 2010.
- [61] X. Zhang, A. Ghrayeb, and M. Hasna, "Relay assignment in network-coded cooperative systems with M-PSK modulation over asymmetric channels," in *Proc. of IEEE PIMRC*, Sept. 2010, 470-475.
- [62] Y. Shi, S. Sharma and Y.-T. Hou, "Optimal relay assignment for cooperative communications," in *Proc. the 9th ACM International Symposium on Mobile ad hoc Networking and Computing*, 2008.
- [63] S. Atapattu, Y. Jing, H. Jiang, and C. Tellambura, "Relay selection and performance analysis in multiple-user networks," *IEEE J. Sel. Areas Commun.*, vol. 31, no. 8, pp. 1–13, Aug. 2013.
- [64] A. Minayi-Jalil, V. Meghdadi, A. Ghrayeb, and J.-P. Cances, "A simple optimal solution for relay assignment in cooperative systems based on the max-min criterion," in *Proc. of IEEE PIMRC*, Sept. 2011, 1768-1772.
- [65] A. Minayi-Jalil, V. Meghdadi and J.-P. Cances, "Diversity analysis of relay assignement in cooperative networks based on sum-rate criterion," *IEEE Trans. Veh. Technol.*, vol. 62, no. 7, pp. 3469–3474, Sept. 2013.
- [66] N. Ahmed, M. A. Khojastepour, A. Sabharwal, and B. Aazhang, "Outage minmization with limited feedback for the fading relay channel," *IEEE Trans. Commun.*, vol. 54, no. 4, pp. 659–666, Apr. 2006.
- [67] T. T. Kim and M. Skoglund, "Decode-and-forward relay channels with quantized channel state feedback: An outage exponent analysis," *IEEE Trans. Inf. Theory*, vol. 54, no. 10, pp. 4548–4564, Oct. 2008.

- [68] Z. Fang, X. Zho, X. Bao, and Z. Wang, "Outage minimized relay selection with partial channel information," in *Proc. IEEE Int. Conf. Acoust., Speech, Signal Process. (ICASSP)*, Taipei, Taiwan, Apr. 19-24, 2009, pp. 2617-2620.
- [69] Y. Zhao, R. S. Adve, and T. J. Lim, "Beamforming with limited feedback in amplify-and-forward cooperative networks," in *IEEE Global Telecommun. Conf.*, Nov. 2007.
- [70] E. Koyuncu, Y. Jing, and H. Jafarkhani, "Beamforming in wireless relay networks with quantized feedback," *IEEE J. Selected Areas Commun.*, vol. 26, pp. 1429-1439, Oct. 2008.
- [71] E. Koyuncu and H. Jafarkhani, "Distributed beamforming in wireless multiuser relay-interference networks with quantized feedback," *IEEE Trans. Inf. Theory*, vol. 58, no. 7, pp. 4538-4576, July 2012.
- [72] Park, J. M., Kim, S.-L.; and Choi, J., "Hierarchically modulated network coding for asymmetric two-way relay systems," *IEEE Trans. Veh. Technology.*, vol. 59, June 2010.
- [73] D. Chen and J. N. Laneman, "Modulation and demodulation for cooperative diversity in wireless systems," *IEEE Trans. Wireless Commun.*, vol. 5, pp. 1785-1794, Jul. 2006.
- [74] J. Proakis, *Digital Communication*, Fourth ed., McGraw-Hill, 2001.
- [75] Z. B. Zabinsky, *Stochastic Adaptive Search for Global Optimization*. Springer, 2003.
- [76] P. Herhold, E. Zimmermann, and G. Fettweis, "A simple cooperative extension to wireless relaying," in *Proceedings of International Zurich Seminar on Communications*, 2004.
- [77] Z. Yi and I.-M. Kim, "Diversity order analysis of the decode-and-forward cooperative networks with relay selection," *IEEE Trans. Wireless Commun.*, vol. 7, no. 5, pp. 1792-1799, May 2008.

- [78] F. Floren, O. Edfors, and B-A Molin, "The effect of feedback quantization on the throughput of a multiuser diversity scheme," in *Proc. IEEE Global Telecommunications Conference*, Sanfrancisco, CA, Dec. 2003.
- [79] D. J. Love, R. W. Heath Jr., V. K. N. Lau, D. Gesbert, B. D. Rao, and M. Andrews, "An overview of limited feedback in wireless communication systems," *IEEE J. Sel. Areas Commun.*, vol. 26, pp. 1341–1365, Oct. 2008.
- [80] J. Lee and J. H. Lee, "Relay assignment schemes for multiuser DF-AF cooperative wireless networks," in *Proc. IEEE VTC-Fall'11*, Sept. 2011.
- [81] S. Ikki and M. H. Ahmed, "Exact error probability and channel capacity of the best-relay cooperative-diversity networks," *IEEE Signal Processing Letters*, vol. 16, no. 12, pp. 1051-1054, Dec. 2009.
- [82] K. Tourki, H.-C. Yang and M.-S. Alouini, "Accurate outage analysis of incremental decode-and-forward opportunistic relaying.," *IEEE Trans. Wireless Commun.*, vol. 8, no. 9, pp. 4836–4847, Sep. 2009.
- [83] K. Cho and D. Yoon, "On the general BER expression of one and two dimensional amplitude modulations," *IEEE Trans. Commun.*, vol. 50, pp. 1074–1080, July 2002.
- [84] M. S. Alounini and A. J. Goldsmith, "Adaptive modulation over nakagami fading channels," *Wireless personal Communications*, vol. 13, no. 1, pp. 119-143, 2000.
- [85] T. Nechiporenko, P. Kalansuriya, and C. Tellambura, "Performance of optimum switching adaptive mqam for amplify-and-forward relays," *IEEE Trans. Veh. Technol.*, vol. 58, no. 5, pp. 2258–2268, 2009.

- [86] K. S. Hwang, Y. C. Ko, and M. S. Alouini, "Performance analysis of incremental opportunistic relaying over identically and non-identically distributed cooperative paths," *IEEE Trans. Wireless Commun.*, vol. 8, no. 4, pp. 1953-1961, April 2009.
- [87] E. S. Altubaishi and X. Shen, "Spectrally efficient variable-rate best-relay selection scheme for adaptive cooperative system," in *Proc. IEEE Globecom 2011*.
- [88] E. S. Altubaishi and X. Shen, "Variable-rate based relay selection scheme for decode-and-forward cooperative networks," in *Proc. IEEE WCNC'11*. Cancun, Mexico, March 28-31, 2011.
- [89] J. W. Kwon, K. Young-Chai, and H. C. Yang, "Maximum spectral efficiency of amplify-and-forward cooperative transmission with multiple relays," *IEEE Trans. Wireless Commun.*, vol. 10, no. 1, pp. 49-54, 2011.
- [90] R. Y. Mesleh, H. Haas, S. Sinanović, C. W. Ahn and S. Yun, "Spatial Modulation," *IEEE Trans. Veh. Technol.*, vol. 57, no. 4, pp. 2228-41, July 2008.
- [91] Y. A. Chau and S.-H. Yu, "Space modulation on wireless fading channels," in *Proc. IEEE 54th VTC' 01 (Fall)*, vol. 3, pp. 1668-1671, 2001.
- [92] J. Jeganathan, A. Ghayeb and L. Szczecinski, "Spatial modulation: Optimal detection and performance analysis," *IEEE Commun. Lett.*, vol. 12, no. 8, pp. 545-547, Aug. 2008
- [93] J. Jeganathan, A. Ghayeb, L. Szczecinski and A. Ceron, "Space shift keying modulation for MIMO channels," *IEEE Trans. Wireless Commun.*, vol. 8, no. 7, pp. 4836-4847, Sep. 2009.
- [94] M. Di Renzo and H. Haas, "Performance comparison of different spatial modulation schemes in correlated fading channels," *IEEE ICC, May 2010*, Cape Town, South Africa.

- [95] M. Di Renzo and H. Haas, "A general framework for performance analysis of space shift keying (SSK) modulation for MISO correlated Nakagami- m fading channels", *IEEE Trans. Commun.*, vol. 59, no. 9, pp. 2590–2603, Sep. 2010.
- [96] M. Di Renzo and H. Haas, "Space shift keying (SSK) MIMO over correlated Rician fading channels: performance analysis and a new method for transmit-diversity", *IEEE Trans. Commun.*, vol. 59, no. 1, pp. 116–129, Jan. 2011.
- [97] M. Di Renzo, H. Haas, A. Ghayeb, S. Sugiura, L. Hanzo: Spatial Modulation for Generalized MIMO: Challenges, Opportunities, and Implementation. *Proceedings of the IEEE.*, vol. 102, no. 1, pp. 56–103, Jan. 2014.
- [98] M. Di Renzo, H. Haas and P. M. Grant, "Spatial modulation for multiple-antenna wireless systems: a survey", *IEEE Commun. Mag.*, vol. 49, no. 12, pp. 182–191, Dec. 2011.
- [99] M. Di Renzo and H. Haas, "Bit error probability of SM-MIMO over generalized fading channels," *IEEE Trans. Veh. Technol.*, vol. 61, no. 3, pp. 1124–1144, Mar. 2012.
- [100] M. Di Renzo, D. De Leonardis, F. Graziosi, and H. Haas, "Space shift keying (SSK) MIMO with practical channel estimates", *IEEE Trans. Commun.*, vol. 60, no. 4, pp. 998–1012, Apr. 2012.
- [101] Mesleh R, Ikki S, Alwakeel M, "Performance analysis of space shift keying with amplify and forward relaying", *IEEE Commun. Lett.* 2011,15(99):1–3.